INSTITUTE OF GEOPHYSICS
POLISH ACADEMY OF SCIENCES

PUBLICATIONS OF THE INSTITUTE OF GEOPHYSICS POLISH ACADEMY OF SCIENCES

MONOGRAPHIC VOLUME

E-6 (390)

ENVIRONMENTAL HYDRAULICS

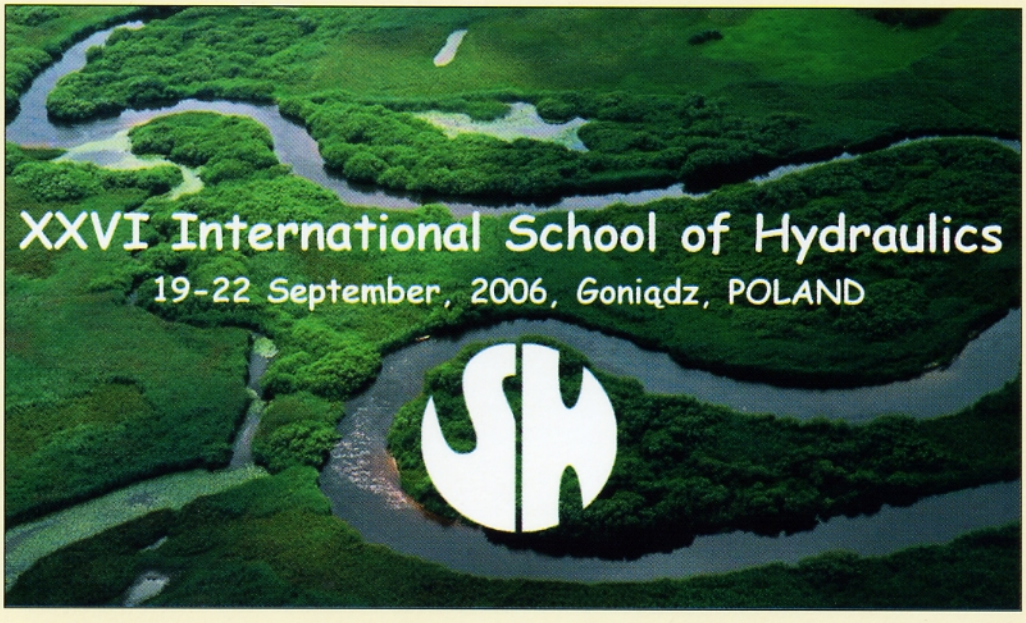

WARSZAWA 2006

INSTITUTE OF GEOPHYSICS
POLISH ACADEMY OF SCIENCES

PUBLICATIONS OF THE INSTITUTE OF GEOPHYSICS POLISH ACADEMY OF SCIENCES

MONOGRAPHIC VOLUME

E-6 (390)

ENVIRONMENTAL HYDRAULICS

Editor:
Paweł M. Rowiński

WARSZAWA 2006

Editorial Office

Instytut Geofizyki Polskiej Akademii Nauk
ul. Księcia Janusza 64, 01-452 Warszawa, Poland

SUBSCRIPTION
Subscription orders should be addressed directly to the Editorial Office.
The list of issues to be published in 2006 is on the inside back cover.

The front cover was prepared with the use of photo made by Wiktor Wołkow

Circulation: 200 copies

ISBN-83-88765-62-0 ISSN-0138-0133

Camera ready copy prepared by:
Dział Infromacji i Wydawnictw Naukowych
Instytutu Geofizyki PAN

Printed and bound by:
PPH Remigraf sp. z o.o.
Ratuszowa 11, 03-450 Warszawa

PUBLS. INST. GEOPHYS. POL. ACAD. SC., E-6 (390), 2006

Environmental Hydraulics
Preface

Paweł M. ROWIŃSKI

Institute of Geophysics, Polish Academy of Sciences

This Volume arose from XXVI International School of Hydraulics held at *Bartlowizna Leisure and Training Center* at Goniądz, Poland, in the period of 19-22 September 2006. The meeting attracted a group of both – top researchers mostly from around Europe, and young scientists. Conference venue was located in the heart of Biebrza National Park, unique in Europe for its marshes and peatlands, as well as its highly diversified fauna, especially birds – the Park was designated as a wetland site of global significance and is under protection of the RAMSAR Convention.

The International School of Hydraulics (till 2003 a national event) has a very long tradition; it was initiated in 1981 and took place without interruption each year. Throughout all that long, 25-year period it was successfully chaired by Prof. Wojciech Majewski and organized by the Institute of Hydro-Engineering of the Polish Academy of Sciences. The School has been organized under the auspices of the Committee for Water Resources Management of the Polish Academy of Sciences. This year it has been decided that the XXVI School of Hydraulics would be organized by the Institute of Geophysics of the Polish Academy of Sciences.

The overall theme of the XXVI School of Hydraulics was ENVIRONMENTAL HYDRAULICS. Environmental Hydraulics is claimed as a domain of research and investigation of the physical, chemical and biological attributes of flowing water, with the objective of protecting and enhancing the quality of the environment, including public welfare. It is a cross-disciplinary field of study, combining, among others, technological, human-sociological and more general environmental interests. One of its aims is to equip managers, geophysicists and engineers working in water-related arenas, with available information and technology, to make rapid and robust decisions as they address the increasing challenges of ensuring a sustainable water environment and adequate water resources for generations to come. Using sophisticated numerical models, in some cases physical models and field experiments, spe-

cialists in Environmental Hydraulics examine the nature of environmental hydraulics problems and develop potential solutions.

A great success behind hydraulics engineers in modelling of flows in a variety of engineering objects imposes the view that a similar success is easy in analogous river flows. There are, however, great differences between environmental flows and their engineered counterparts and they are revealed in terms of length scales, levels of turbulence and geometrical complexities. Environmental flows usually cannot be designed (as in traditional hydraulics), they are rather observed and the interest is centred on understanding their role in environmental quality.

The XXVI School of Hydraulics was intended to provide a forum for scientists and engineers working in the field of broadly understood hydraulics. By bringing together experts (academics and practitioners) as well as young scientists, we aimed to create a very good atmosphere for scientific debate and learning, and also to make this occasion an enjoyable experience for the participants. An important part of the School constituted lectures delivered by renowned scientists from different countries:

- Prof. Vladimir Nikora, **keynote speaker**, from Engineering Department, University of Aberdeen, UK: "Hydrodynamics of aquatic ecosystems"
- Prof. Andreas Dittrich from Technical University of Braunschweig, Germany: "Morphodynamic development of river course and flood plains"
- Prof. Ian Guymer from the School of Engineering, University of Warwick, UK: "Employing Tracer Techniques to Parameterize Mixing Processes"
- Prof. Wojciech Majewski from the Institute of Meteorology and Water Management, Gdynia, Poland: "Flow in open channels under the influence of ice cover"
- Prof. Andrea Marion from University of Padova, Italy: "Recent model developments on hyporheic flows in rivers: laboratory and field applications"
- Assoc. Prof. Tomasz Okruszko from Warsaw Agriculture University: "Presentation of Biebrza Valley and Its Problems"
- Dr. Steve Wallis from School of the Built Environment, Heriot-Watt University, Edinburgh, UK: "The Numerical Solution of the Advection-Dispersion Equation: A review of some basic principles"
- Prof. Anders Wörman from Department of Biometry and Engineering, Swedish University of Agricultural Sciences, Uppsala, Sweden: "Impact of groundwater discharge depth on residence times for leaking radionuclides in land-based surface water"

Fifty-four researchers from eight countries (Poland, Germany, Great Britain, Sweden, Italy, Russia, Ukraine and Iran) participated in the School. All presentations were reviewed by the following Scientific Committee:

- Assoc. Prof. Paweł M. Rowiński – Chairman, Institute of Geophysics, Polish Academy of Sciences, Warsaw
- Prof. Włodzimierz Czernuszenko – Institute of Geophysics, Polish Academy of Sciences, Warsaw
- Prof. Janusz Kubrak – Warsaw Agriculture University
- Prof. Wojciech Majewski – Institute of Meteorology and Water Management, Gdynia
- Prof. Marek Mitosek – Warsaw Technical University
- Prof. Jarosław Napiórkowski – Institute of Geophysics, Polish Academy of Sciences, Warsaw
- Prof. Romuald Szymkiewicz – Gdańsk University of Technology

I would like to express my appreciation to all the members of the Scientific Committee for their hard work in reviewing the papers.

This Volume is based on the presentations given during the School. Remaining, selected articles, are included in the Special Issue of Acta Geophysica (Vol. 55 No. 1). Abstracts of those papers are included in this volume for completeness.

A number of colleagues from the Institute of Geophysics of the Polish Academy of Sciences provided their time and skills to ensure the meeting went smoothly. I am specially indebted to Anna Łukanowska and Monika Kalinowska who spent many long days and nights ensuring the meeting and the publications were professionally organized. We are also grateful to Robert Bialik, Agata Mazurczyk, Marzena Osuch, and Adam Piotrowski. I am also thankful to the Director and employees of Biebrza National Park for their hospitality, kindness, and organization of fascinating trip within the park. They also offered interesting materials to the School participants.

The event and relevant publications would not be possible without financial support of the Committee for Water Resources Management of the Polish Academy of Sciences, Institute of Geophysics of the Polish Academy of Sciences and also German company *G.U.N.T. Gerätebau GmbH* from Hamburg. Additionally, this company presented a variety of educational equipment used for hydraulic training at universities and prepared a small exhibition.

PUBLS. INST. GEOPHYS. POL. ACAD. SC., E-6 (390), 2006

Measurements of Armour Layer Roughness Geometry Function and Porosity

Jochen ABERLE

Leichtweiss-Institute for Hydraulic Engineering,
Technical University of Braunschweig
Beethovenstr. 51, 38106 Braunschweig, Germany;
e-mail: j.aberle@tu-bs.de

Abstract

The roughness geometry function of the interfacial sublayer of a gravel-bed armour layer was measured directly by filling water stepwise into a laboratory flume and indirectly from a digital elevation model (DEM) of the surface. The results of both methods are compared and show that the DEM can be used to reliably estimate the roughness density function for a wide range of the interfacial sublayer. The direct measurements revealed an absolute minimum of porosity at the level of the roughness trough which is significantly smaller than porosity in the undisturbed subsurface and porosity estimates obtained from relationships found in the literature. The significance of the results for hydraulic engineering and ecological applications is highlighted.

Key words: Armour Layer, porosity, digital elevation model, flume study.

Full text was published in *Acta Geophysica*, Vol. 55, No. 1, p. 23-32.

PUBLS. INST. GEOPHYS. POL. ACAD. SC., E-6 (390), 2006

Expanded Transport Models of both Conservative and Organic Contaminants in Groundwater

Andrzej ANISZEWSKI

Szczecin University of Technology
Piastów 50a, 70 -310 Szczecin, Poland
email: andrzej.aniszewski@ps.pl

Abstract

The paper addresses the expanded mathematical models (equations) of both conservative and organic (reactive) contaminant transport in a groundwater stream. These models include, except the advection and dispersion processes, both the source (negative) term of reversible sorption and the term of radioactive decay or biodegradation. The term of reversible sorption can be described by linear or non-linear adsorption (desorption) isotherms in relation to statics of this process, whereas the term of radioactive decay or biodegradation can be described by the first-order irreversible rate reactions for the reactive solutes flowing in ground medium.

1. Introduction

For description of contaminant concentration fields in a groundwater stream, the practical expanded 2D-models of contaminant transport were worked out in this paper, combining advection, dispersion, adsorption and radioactive decay or biodegradation processes.

For description of the adsorption process, the Henry linear isotherm, as well as the Freundlich and Langmuir non-linear isotherms were accepted, which are widely applied to practice in relation to statics of this process.

However, for description of the term of radioactive decay or biodegradation, the first-order irreversible rate reactions were accepted for the dissolved and sorbed phases of the organic (reactive) contaminants spreading in a groundwater stream (Anderson 1979, Chiang 2001).

2. Approach and methods

Concern over the potential for migration of wastes in the subsurface has generated a great deal of interest in the mechanisms responsible for contaminant transport through groundwater systems.

To prevent the deterioration of groundwater quality, it has become necessary to develop a methodology for description, analyzing, monitoring and predicting (in the form of mathematical models) the movement of contaminants through the saturated zones (Anderson 1979, Chiang 2001).

2.1 Description of contaminant transport in groundwater

For description of conservative and organic contaminant transport incorporating both the reversible sorption and radioactive decay (biodegradation) terms, the expanded well-known 2D-advection-diffusion equation was used, resulting from the transport continuity equation (Anderson 1979, Chiang 2001):

$$\frac{\partial C}{\partial t} + u_x \frac{\partial C}{\partial x} = D_x \frac{\partial^2 C}{\partial x^2} + D_y \frac{\partial^2 C}{\partial y^2} - \frac{\rho}{m}\frac{\partial S}{\partial t} - \lambda_1 C - \frac{\lambda_2 \rho\, S}{m} \tag{1}$$

where: C = the solute concentration in flowing groundwater in aqueous phase (in the local equilibrium conditions); S = the mass of the solute species adsorbed on the grounds per unit bulk dry mass of the porous medium (in the local equilibrium conditions); u_x = component of the average (real) seepage velocity in pore space along the x axis (as pore velocity of groundwater); D_x = component of the longitudinal dispersion coefficient along the x axis; D_y = component of the transverse dispersion coefficient along the y axis; λ_1 = the first-order rate constant for the dissolved (aqueous) phase; λ_2 = the first-order rate constant for the sorbed (solid) phase; ρ = the bulk density of the porous medium; m = the effective porosity of the porous medium; t = co-ordinate of time; (x, y) = Cartesian co-ordinates of the assumed reference system.

Equation (1) assumes one-dimensional flow of groundwater along the x axis, hence, both the components of the average (real) seepage velocities in pore space ($u_y = u_z = 0$) and the advection terms ($u_y \partial C/\partial y = u_z \partial C/\partial z = 0$) can be neglected in the other axes, y and z.

Assuming also in Eq. (1) the 2D-contaminant transport along the x and y axes, the dispersion term ($D_z \partial^2 C/\partial z^2 = 0$) along the vertical z axis can be treated as negligible, simulating in further analysis the longitudinal ($D_x \partial^2 C/\partial x^2$) and transverse ($D_y \partial^2 C/\partial y^2$) dispersion of flowing contaminant mass in the aquifer.

The longitudinal and transverse dispersion coefficients (D_x and D_y) which are being considered in Eq. (1), called also as the hydrodynamic dispersion coefficients, consist of both the terms representing mechanical dispersion coefficients ($\alpha_L u_x$ and $\alpha_T u_x$) and the effective (modified) molecular diffusion ($\tau\ D_M$) (Kleczkowski 1984, Chiang 2001).

Thus, the values of hydrodynamic dispersion coefficients take the form:

$$\begin{aligned} D_x &= \alpha_L u_x + \tau D_M \\ D_y &= \alpha_T u_x + \tau D_M \end{aligned} \tag{2}$$

where: (α_L , α_T) = the constants of the longitudinal and the transverse dispersivity along the *x* and *y* axes; D_M = the molecular (effective) diffusion coefficient; τ = the dimensionless tortuosity parameter of the porous medium.

The constants of dispersivity (α_L) and (α_T) depend on the scale (length) of contaminant region spreading in the aquifer. Detailed description of the dispersivity (α_L) and (α_T) (as macro-dispersion process) is given in (Anderson 1979, Kleczkowski 1984, Gelhar et al. 1992, Kleczkowski 1997, Chiang 2001).

The values of molecular (effective) coefficients (D_M) are generally very low, basing on laboratory and site surveys for the various graining (porosity) of the ground media being considered. Thus, in most cases they can be negligible in Eq. (2) for calculations of the hydrodynamic dispersion coefficients (Anderson 1979, Chiang 2001).

The tortuosity parameter (τ), which expresses the solute mass flow along longer available pathways through the pore space is described in (Kleczkowski 1984, Chiang 2001).

The $\partial S / \partial t$ term in Eq. (1) represents generally the negative source term of the reversible sorption (as the adsorption-desorption system) connected with the mass exchange phenomenon, which expresses general relationship $\partial S / \partial t = f(C,S)$, between the mass of the solute species adsorbed on the grounds per unit bulk dry mass of the porous medium (S) and the solute concentration in flowing groundwater in aqueous phase (C).

Making an assumption of the local equilibrium condition between phases – aqueous (free) and sorption (solid) – function $S = f(C)$ implicates that the sorption term ($\partial S / \partial t$) in Eq. (1) can be replaced by the expression $(\partial S / \partial C) \cdot (\partial C / \partial t)$.

Equation (1) may be written in the following form, taking into account the above remark and by factoring out the term ($\partial C / \partial t$):

$$\frac{\partial C}{\partial t}\left(1+\frac{\rho}{m}\frac{\partial S}{\partial C}\right)+u_x\frac{\partial C}{\partial x}=D_x\frac{\partial^2 C}{\partial x^2}+D_y\frac{\partial^2 C}{\partial y^2}-\lambda_1 C-\frac{\lambda_2\rho\, S}{m} \tag{3}$$

As a result of detailed literature review, in the case of reversible sorption assumption (as negative source term) in Eq. (3) by the ($\partial C/\partial t$) term, the constant expression $R = [1+(\rho/m)(\partial S/\partial C)]$ will always be found, which in literature is known as the retardation factor (Anderson 1979, Chiang 2001).

The term $\lambda_1 C$ in Eq. (1) represents generally the first-order irreversible rate of the reaction for the dissolved (aqueous) phase in relation to the reactive solutes in soil (Travis 1978, Bear 1987, Chiang 2001).

However, the last term ($\lambda_2 \rho\, S/m$) in Eq. (1) represents generally the first-order irreversible rate of the reaction for the sorbed (solid) phase in relation also to the reactive solutes in soil (Travis 1978, Bear 1987, Chiang 2001).

The rates of constants of the free and sorbed solute (λ_1 and λ_2) are usually given in terms of the half-life ($t_{1/2}$). The half-life is the time required for the concentration to decrease to one-half of the original value.

Generally, the decay (biodegradation) rate (λ) is calculated by the equation (Anderson 1979, Travis 1978, Bear 1987, Chiang 2001):

$$\lambda=\frac{\ln 2}{t_{1/2}} \tag{4}$$

Generally, if the reaction is radioactive decay, the λ_2 constant should be set equal to the λ_1 constant. However, for certain types of biodegradation the λ_2 constant may be different from the λ_1 one (Anderson 1979, Travis, 1978, Bear 1987, Chiang 2001).

3. Results

The practical expanded 2-D transport models of both conservative and organic (reactive) contaminants, presented in the paper, include also the previously accepted well-known empirical equations of the Henry, Freundlich and Langmuir adsorption isotherms which are widely applied to practice (Anderson 1979, Travis 1978, Chiang 2001).

The Henry linear isotherm, as the simplest equilibrium relationship, assumes that the sorbed concentration *S* is directly proportional to the dissolved concentration *C*. This type of isotherm can be found in transport problems with relatively low concentrations of flowing contaminants in a groundwater stream (Travis 1978, Anderson 1979, Bear 1987, Chiang 2001).

The Freundlich non-linear isotherm, as a more general equilibrium relationship, assumes that the sorbed concentration *S* is not directly proportional to the dissolved concentration *C*. The proportion between concentrations *S* and *C* is fitted in most cases to the exponential relationships with relatively higher concentrations of flowing contaminants in a groundwater stream (Travis 1978, Anderson 1979, Bear 1987, Chiang 2001).

Also, the Langmuir non-linear isotherm, as a more general equilibrium relationship, assumes that the sorbed concentration *S* is not also directly proportional to the dissolved concentration *C*. This isotherm concerns the condition of the maximal adsorption value just in the moment when the ground grain surface will be adsorbed by mono-molecular layer of flowing contaminant particles. In this case, the adsorption energy is the same in all points of the ground grain surface and the adsorbed particles can not be moved on this surface (Travis 1978, Anderson 1979, Bear 1987, Chiang 2001).

For the equilibrium-controlled state, it can be assumed that the rate of the reversible adsorption process is equal to zero ($\partial S / \partial t = 0$) in relation to the ground medium with the finite sorption capacity (for the constant temperature and negligible value of the irreversible chemical sorption) (Travis 1978, Anderson 1979, Bear 1987, Chiang 2001).

The empirical equations of the chosen adsorption isotherms together with a detailed description of the required parameters accepted for this analysis were given in (Aniszewski 2005).

3.1 The model for the equation of the Henry linear isotherm

For the accepted empirical equation of the Henry linear isotherm, the contaminant transport according to Eq. (3) in a groundwater stream takes the form:

$$\frac{\partial C}{\partial t} + A_1 \frac{\partial C}{\partial x} = B_1 \frac{\partial^2 C}{\partial x^2} + C_1 \frac{\partial^2 C}{\partial y^2} - C\left(D_1 + E_1\right). \tag{5}$$

Taking into account the expression $A_0 = 1 + \rho / m$, it is also possible to write:

$$\frac{u_x}{A_0 K_1} = A_1; \quad \frac{D_x}{A_0 K_1} = B_1; \quad \frac{D_y}{A_0 K_1} = C_1; \quad \frac{\lambda_1}{A_0 K_1} = D_1; \quad \frac{\lambda_2 \rho}{A_0 m} = E_1 \tag{6}$$

where: K_1 = the parameter of the Henry linear isotherm (as the distribution coefficient, that depends on the solute species, the nature of the porous medium and other conditions of the system).

3.2 The model for the equation of the Freundlich non-linear isotherm

For the accepted empirical equation of the Freundlich non-linear isotherm, the contaminant transport according to Eq. (3) in a groundwater stream takes the form:

$$\frac{\partial C}{\partial t} + A_2 \frac{\partial C}{\partial x} = B_2 \frac{\partial^2 C}{\partial x^2} + C_2 \frac{\partial^2 C}{\partial y^2} - C\left(D_2 + E_2\right). \tag{7}$$

Taking into account the expression $A_0 = 1 + \rho / m$, it is also possible to write:

$$\begin{aligned} &\frac{u_x}{A_0 N K_2 C^{(N-1)}} = A_2;\ \frac{D_x}{A_0 N K_2 C^{(N-1)}} = B_2;\ \frac{D_y}{A_0 N K_2 C^{(N-1)}} = C_2 \\ &\frac{\lambda_1}{A_0 N K_2 C^{(N-1)}} = D_2;\quad \frac{\lambda_2 \rho}{A_0 m N} = E_2 \end{aligned} \tag{8}$$

where: K_2, N = the parameters of the Freundlich non-linear isotherm (K_2 = the Freundlich constant; N = the Freundlich exponent, that depend on the solute species, the nature of the porous medium and other conditions of the system).

3.3 The model for the equation of the Langmuir non-linear isotherm

For the accepted empirical equation of the Langmuir non-linear isotherm, the contaminant transport according to Eq. (3) in a groundwater stream takes the form:

$$\frac{\partial C}{\partial t} + A_3 \frac{\partial C}{\partial x} = B_3 \frac{\partial^2 C}{\partial x^2} + C_3 \frac{\partial^2 C}{\partial y^2} - C\left(D_3 + E_3\right) \tag{9}$$

Taking into account the expression $A_0 = 1 + \rho / m$, it is also possible to write:

$$\begin{aligned} &\frac{u_x (1 + K_3 C)^2}{A_0 K_3 \bar{S}} = A_3;\ \frac{D_x (1 + K_3 C)^2}{A_0 K_3 \bar{S}} = B_3;\ \frac{D_y (1 + K_3 C)^2}{A_0 K_3 \bar{S}} = C_3 \\ &\frac{\lambda_1 (1 + K_3 C)^2}{A_0 K_3 \bar{S}} = D_3;\ \frac{\lambda_2 \rho\,(1 + K_3 C)}{A_0 m} = E_3 \end{aligned} \tag{10}$$

where: K_3, $\bar{S}$ = the parameters of the Langmuir non-linear isotherm (K_3 = the Langmuir constant that is named also the constant of the adsorption energy; $\bar{S}$ = the maximum amount of the solute adsorbed by the ground matrix).

4. Discussion

The 2D-transport models (equations) for only the conservative contaminants flowing in a groundwater stream, neglecting at the same time the term of radioactive decay or

biodegradation (as the first-order irreversible rate reactions), were presented in (Aniszewski 2005).

Practical using of the contaminant transport models presented as Eqs. (5)-(10) depends on identification of the required parameters in these equations (Anderson 1979, Kleczkowski 1984, Chiang 2001).

The values of parameters characterizing the ground and hydraulic properties of the ground medium (u_x, m and ρ), the values of the contaminant dispersion coefficients (D_x and D_y) calculated according to Eq. (2), for the previously determined parameters (u_x, α_L and α_T), as well as the values of the first-order rate constants (λ_1 and λ_2) calculated according to Eq. (4) and characterizing processes of radioactive decay or biodegradation should be defined basing on the own or the literature site surveys carried out in the natural aquifers (Anderson 1979, Travis 1978, Kleczkowski 1984, Bear 1987, Gelhar et al. 1992, Kleczkowski 1997, Chiang 2001, Aniszewski 2005).

However, the values of linear and non-linear adsorption isotherm parameters (K_1, K_2, N, K_3, $\overline{S}$) in relation to static of this process should be calculated basing on separate static experiments, the so-called „batch" laboratory experiments (with immobile groundwater) and simultaneously for using in this research both the similar ground media and contaminant indicators to be chosen in the site verifications (Travis 1978, Kleczkowski 1984, Kleczkowski 1997, Chiang 2001).

In such cases, it is fully admissible to use all the parameters (u_x, m, ρ, D_x, D_y, α_L, α_T, λ_1, λ_2, K_1, K_2, N, K_3 and $\overline{S}$) determined in this way for site verification of the transport models presented as Eqs. (5)-(10) in relation also to other similar natural ground media without the necessity of determining geometric scale-dependent similarity (Kleczkowski 1984, Gelhar et al. 1992, Kleczkowski 1997, Chiang 2001, Aniszewski 2005). This similarity greatly depends on the scale (length) of site surveys as macro-dispersion process caused by macroscopic heterogeneities of the natural ground media (Gelhar et al. 1992, Chiang 2001).

5. Conclusion

The practical expanded contaminant transport models presented as Eqs. (5)-(10) combining the advection, dispersion, physical adsorption and radioactive decay or biodegradation processes, can be used for the engineering calculations of the contaminant concentration fields in the natural aquifers.

Practical using of these expanded models for site verifications greatly depends on both the proper mathematical description of all the processes and the proper identification of the all required parameters in these models (equations).

The presented transport models make it possible to use both the conservative and organic contaminants spreading in aquifer, giving simultaneously the calculated concentration values closed to the real values considered in natural ground conditions.

References

Anderson, M.P., 1979, *Using models to simulate the movement of contaminants through groundwater flow systems*, Critical reviews in Environmental Control **9**, 2, 97-156.

Aniszewski, A., 2005, *2D-models of contaminant in ground for the chosen types of sorption isotherms*, XXV International School of Hydraulics, Hydraulic Problems in Environmental Engineering, Debrzyno, 12-16 September, Institute of Hydro-Engineering (IBW PAN), Gdańsk, 177-184.

Bear, J., and A. Veruijt, 1987, *Modeling groundwater flow and pollution*, D. Reidel Publishing, Dordrecht, 385 pp.

Chiang, W.H., and W. Kinzelbach, 2001, *3D-Groundwater modeling with PMWIN. A simulation system for modeling groundwater flow and pollution*, Springer-Verlag, Berlin-Heidelberg, 346 pp.

Gelhar, L.W., C. Welty and K.R. Rehfeldt, 1992, *A critical review of data on field-scale dispersion in aquifers*, Water Resour. Research **28**, 7, 1955-1974.

Kleczkowski, A.S., 1984, *Groundwater protection*, Geological Proceedings, Warsaw, 285 pp. (in Polish).

Kleczkowski, A.S., and A. Różkowski, 1997, *Hydrogeological dictionary*, TRIO Proceedings, Warsaw, 328 pp. (in Polish).

Travis, C.C., 1978, *Mathematical description of adsorption and transport of reactive solutes in soil: A review of selected literature*, Oak Ridge Natl. Lab. ORNL-5403, 176 pp.

Accepted September 12, 2006

PUBLS. INST. GEOPHYS. POL. ACAD. SC., E-6 (390), 2006

Numerical Solution of Two-Dimensional Advection Equation on Curvilinear Grid Using TVD-Schemes

Roman BEZHENAR

Institute of Mathematical Machine and System Problems, Ukrainian Academy of Sciences
Glushkov avenue, 42, 03187 Kiev, Ukraine
email: roman@env.kiev.ua

Abstract

The numerical solution of two-dimensional advection equation on the irregular curvilinear grid is considered. The simple upstream differencing scheme and TVD (Total Variation Diminishing) schemes are compared. The test solution for rotation of two-dimensional scalar field in the Cartesian and curvilinear coordinates is numerically realized. It was concluded that the results of modeling in both coordinate systems are identical.

1. Introduction

The modeling of pollutant transport requires a numerical solution of transport equation on the irregular curvilinear grid. This is important for simulation of different types of pollutants in the rivers, lakes and coastal regions of seas. Using curvilinear grids for building a finite-difference scheme for water bodies with complex form of boundary allows us to describe transport in these areas more accurately.

In the paper, the results of modeling of two-dimensional scalar field rotating in Cartesian and curvilinear coordinates are compared. Initial shape of field is a circle with constant concentration inside and zero concentration outside. Pure advection equation is solved. This problem has an analytical solution; the result of modeling must be equal to initial conditions. The aim of the work was to test a numerical solution of two-dimensional advection equation on irregular curvilinear grid using different TVD (Total Variation Diminishing) schemes.

2. Methods

The two-dimensional advection equation is

$$\frac{\partial u}{\partial t}+\frac{\partial\left(v_x u\right)}{\partial x}+\frac{\partial\left(v_y u\right)}{\partial y}=0\ , \tag{1}$$

where u = concentration of a scalar; t = time; (v_x, v_y) = velocity components in x and y directions.

Equation (1) can be transformed into a system of finite-difference equations in Cartesian and in curvilinear coordinates using simple upstream differencing scheme and TVD schemes.

2.1 Simple upstream differencing scheme (first order of accuracy)

There are four different combinations for characters of velocities (v_x, v_y) on the computational region at the rotating scalar field. For each combination, the finite-difference scheme has its own form:

$$\frac{u_{i,j}^{k+1}-u_{i,j}^{k}}{\Delta t}+\frac{u_{i,j}^{k}v_{xi,j}-u_{i-1,j}^{k}v_{xi-1,j}}{\Delta x_{i,j}}+\frac{u_{i,j}^{k}v_{yi,j}-u_{i,j-1}^{k}v_{yi,j-1}}{\Delta y_{i,j}}=0 \tag{2}$$

for $v_x > 0$ and $v_y > 0$

$$\frac{u_{i,j}^{k+1}-u_{i,j}^{k}}{\Delta t}+\frac{u_{i+1,j}^{k}v_{xi+1,j}-u_{i,j}^{k}v_{xi,j}}{\Delta x_{i,j}}+\frac{u_{i,j}^{k}v_{yi,j}-u_{i,j-1}^{k}v_{yi-1,j}}{\Delta y_{i,j}}=0 \tag{3}$$

for $v_x < 0$ and $v_y > 0$

$$\frac{u_{i,j}^{k+1}-u_{i,j}^{k}}{\Delta t}+\frac{u_{i,j}^{k}v_{xi,j}-u_{i-1,j}^{k}v_{xi-1,j}}{\Delta x_{i,j}}+\frac{u_{i,j+1}^{k}v_{yi,j+1}-u_{i,j}^{k}v_{yi,j}}{\Delta y_{i,j}}=0 \tag{4}$$

for $v_x > 0$ and $v_y < 0$

$$\frac{u_{i,j}^{k+1}-u_{i,j}^{k}}{\Delta t}+\frac{u_{i+1,j}^{k}v_{xi+1,j}-u_{i,j}^{k}v_{xi,j}}{\Delta x_{i,j}}+\frac{u_{i,j+1}^{k}v_{yi,j+1}-u_{i,j}^{k}v_{yi,j}}{\Delta y_{i,j}}=0 \tag{5}$$

for $v_x < 0$ and $v_y < 0$

where i, j = indexes which denote numbers of nodes on spatial grid in the x and y directions, respectively; k = index which denotes the number of time step; Δx, Δy = spatial grid steps in the x and y directions, respectively; Δt = time step.

2.2 TVD schemes

All linear TVD schemes, as simple upstream differencing schemes, are only of first-order accuracy, but due to stability condition they have a property of monotonicity preservation. The total variation of a discrete solution could be defined as a measure of the overall amount oscillations. The principle of TVD approach is to limit the oscillations such as:

$$TV(u^{t+\Delta t}) \le TV(u^{t}) \tag{6}$$

where TV = Total Variation.

Equation (6) means that the amount of oscillations of a solution for a TVD scheme does not increase over one time step for any initial data.

The directional split approach is used in the TVD schemes at the two-dimension modeling.

$$u_{i,j}^{k+1/2} = u_{i,j}^{k} - \frac{\Delta t}{\Delta x_{i,j}}\left(F_{i+1/2,j}^{k} - F_{i-1/2,j}^{k}\right), \tag{7}$$

$$u_{i,j}^{k+1} = u_{i,j}^{k+1/2} - \frac{\Delta t}{\Delta y_{i,j}}\left(F_{i,j+1/2}^{k} - F_{i,j-1/2}^{k}\right). \tag{8}$$

Here

$$F_{i+1/2,j} = v_{xi+1/2,j}\left(u_{i,j} + 1/2\Phi_{i+1/2,j}^{+}\left(1-\left|c_{xi+1/2,j}\right|\right)\left(u_{i+1,j} - u_{i,j}\right)\right) \quad \text{for } v_x > 0, \tag{9}$$

$$F_{i+1/2,j} = v_{xi+1/2,j}\left(u_{i,j} + 1/2\Phi_{i+1/2,j}^{-}\left(1-\left|c_{xi+1/2,j}\right|\right)\left(u_{i,j} - u_{i+1,j}\right)\right) \quad \text{for } v_x < 0, \tag{10}$$

$$F_{i,j+1/2} = v_{yi,j+1/2}\left(u_{i,j} + 1/2\Phi_{i,j+1/2}^{+}\left(1-\left|c_{yi,j+1/2}\right|\right)\left(u_{i,j+1} - u_{i,j}\right)\right) \quad \text{for } v_y > 0, \tag{11}$$

$$F_{i,j+1/2} = v_{yi,j+1/2}\left(u_{i,j} + 1/2\Phi_{i,j+1/2}^{-}\left(1-\left|c_{yi,j+1/2}\right|\right)\left(u_{i,j} - u_{i,j+1}\right)\right) \quad \text{for } v_y < 0, \tag{12}$$

where

$$c_x = \frac{v_x \Delta t}{\Delta x}, \qquad c_y = \frac{v_y \Delta t}{\Delta y}; \tag{13}$$

$$\Phi_{i+1/2,j}^{+} = \alpha_{i+1/2,j} + \beta_{i+1/2,j} r_{i+1/2,j}^{+}; \qquad \Phi_{i+1/2,j}^{-} = \alpha_{i+1/2,j} + \beta_{i+1/2,j} r_{i+1/2,j}^{-}; \tag{14}$$

$$\alpha_{i+1/2,j} = 1/2 + 1/6\left(1 - 2\left|c_{xi+1/2,j}\right|\right); \quad \beta_{i+1/2,j} = 1/2 - 1/6\left(1 - 2\left|c_{xi+1/2,j}\right|\right); \tag{15}$$

$$r_{i+1/2,j}^{+} = \frac{u_{i,j} - u_{i-1,j}}{u_{i+1,j} - u_{i,j}}; \qquad r_{i+1/2,j}^{-} = \frac{u_{i+2,j} - u_{i+1,j}}{u_{i+1,j} - u_{i,j}} \tag{16}$$

$$\Phi^{+}_{i,j+1/2} = \alpha_{i,j+1/2} + \beta_{i,j+1/2} r^{+}_{i,j+1/2}; \qquad \Phi^{-}_{i,j+1/2} = \alpha_{i,j+1/2} + \beta_{i,j+1/2} r^{-}_{i,j+1/2} \tag{17}$$

$$\alpha_{i,j+1/2} = 1/2 + 1/6\left(1 - 2\left|c_{yi,j+1/2}\right|\right); \quad \beta_{i,j+1/2} = 1/2 - 1/6\left(1 - 2\left|c_{yi,j+1/2}\right|\right) \tag{18}$$

$$r^{+}_{i,j+1/2} = \frac{u_{i,j} - u_{i,j-1}}{u_{i,j+1} - u_{i,j}}; \qquad r^{-}_{i,j+1/2} = \frac{u_{i,j+2} - u_{i,j+1}}{u_{i,j+1} - u_{i,j}} \tag{19}$$

There are second-order accuracy TVD schemes, in which additional limiters are used.

a) Leonard limiter (1979)

$$\Phi \to \max\left(0, \min\left(\Phi, \frac{2}{1-|c|}, \frac{2r}{|c|}\right)\right) \tag{20}$$

b) van Leer limiter (1979)

$$\Phi \to \max\left(0, \min\left(2, 2r, \frac{1+r}{2}\right)\right) \tag{21}$$

c) Roe limiter (1985)

$$\Phi \to \max\left(0, \min\left(1, 2r\right), \min\left(r, 2\right)\right) \tag{22}$$

We modeled the rotating scalar circle-shaped field with the following parameters:

$w = 0.2\pi$ (radian/s) – angular velocity of field rotation; $R_0 = 0.25$ – initial radius of field; $h_0 = 1$ – initial concentration inside of circular area; $\Delta t = 0.001$; $\Delta x_{i,j} = \Delta y_{i,j} = 0.01$ – are equal in Cartesian grid; $\Delta x_{i,j}$ and $\Delta y_{i,j}$ – are unequal in curvilinear grid.

Boundaries of the curvilinear grid domain are shown in Fig. 1.

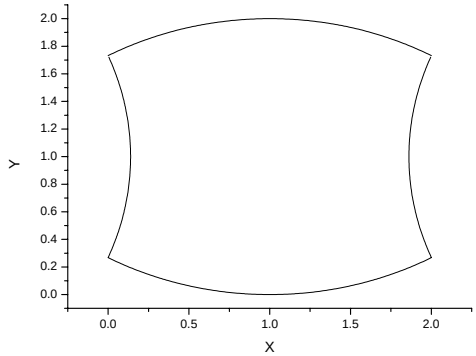

Fig. 1. Boundaries of the curvilinear grid.

3. Results

Initial scalar field and its projection on axis *X* are shown in Fig. 2. The analytical solution has the same form.

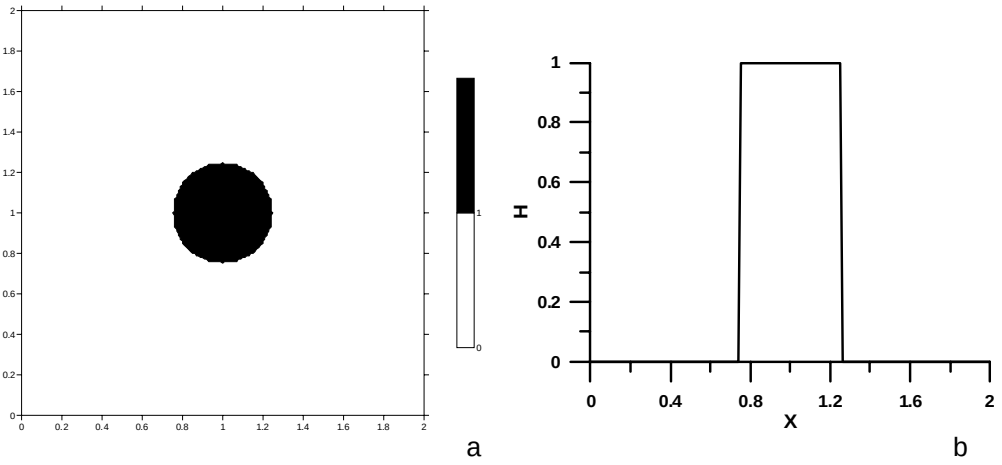

Fig. 2. Initial scalar field (a) and its projection on axis X (b).

Projections of scalar field on axis *X* after modeling the one full turn in Cartesian and curvilinear coordinates, that was realized using simple upstream differencing scheme, are shown in Fig. 3.

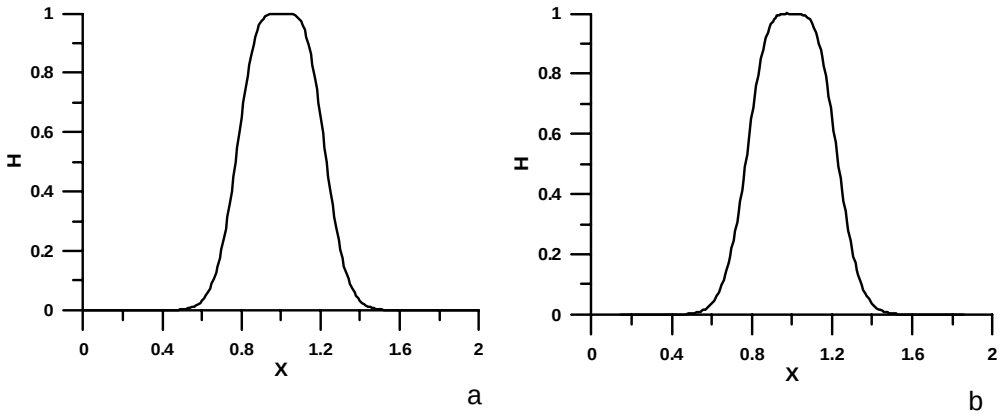

Fig. 3. Result of modeling of scalar field rotation using simple upstream differencing scheme: a) in Cartesian coordinates; b) in curvilinear coordinates.

Results of modeling can be described using the following parameters:

$R_1 = 0.08$ – radius for which $h > 0.99$;

$R_2 = 0.45$ – radius for which $h < 0.01$;

$\Delta R = R_2 - R_0 = 0.2$.

Projections of scalar field on axis X after modeling the one full turn in Cartesian and curvilinear coordinates, that was realized using the TVD scheme, are shown in Fig. 4. Parameters: $R_1 = 0.21$; $R_2 = 0.28$; $\Delta R = R_2 - R_0 = 0.03$.

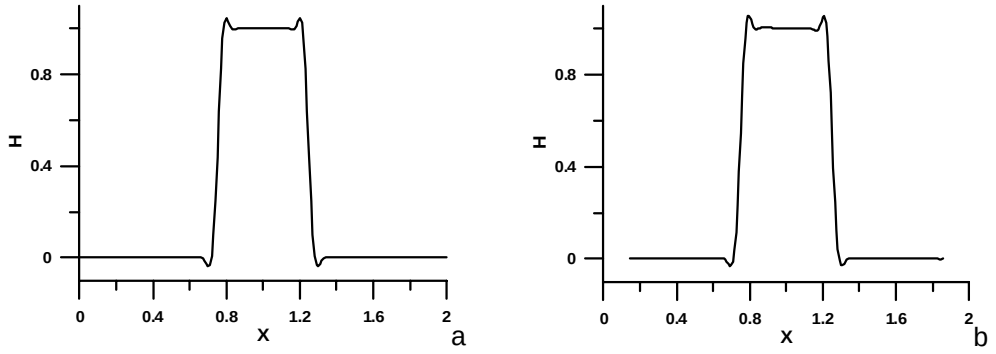

Fig. 4. Result of modeling of scalar field rotating using TVD scheme: a) in Cartesian coordinates; b) in curvilinear coordinates.

Projections of scalar field on axis X after modeling one full turn in Cartesian and curvilinear coordinates that was realized using TVD scheme with Leonard limiter, are shown in Fig. 5. Parameters: $R_1 = 0.21$; $R_2 = 0.28$; $\Delta R = R_2 - R_0 = 0.03$.

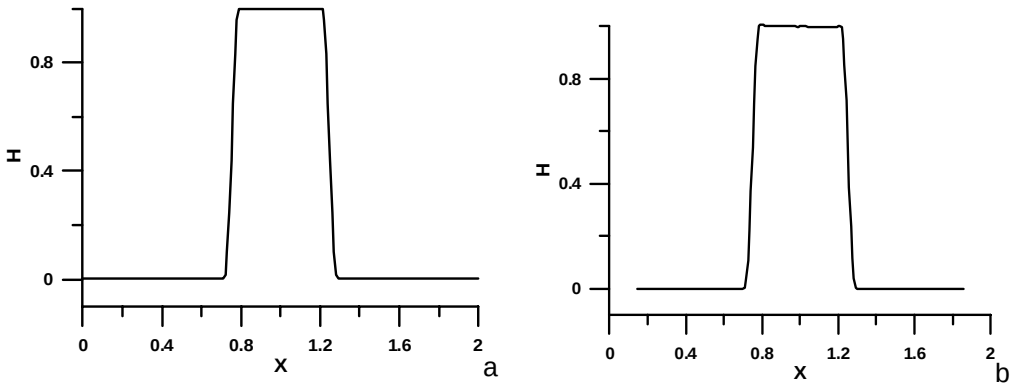

Fig. 5. Result of modeling of scalar field rotating using TVD scheme with Leonard limiter: a) in Cartesian coordinates; b) in curvilinear coordinates.

Projections of scalar field on axis *X* after modeling the one full turn in Cartesian and curvilinear coordinates that was realized using TVD scheme with van Leer limiter, are shown in Fig. 6. Parameters: $R_1 = 0.20$; $R_2 = 0.28$; $\Delta R = R_2 - R_0 = 0.03$.

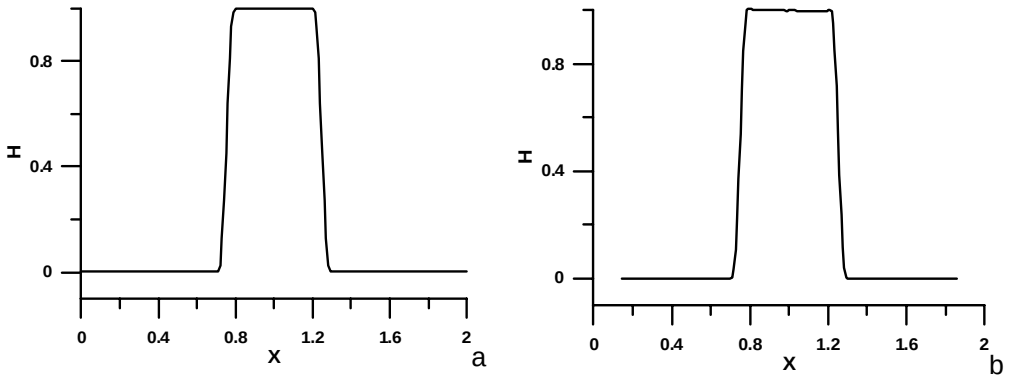

Fig. 6. Result of modeling of scalar field rotating using TVD scheme with van Leer limiter: a) in Cartesian coordinates; b) in curvilinear coordinates.

Projections of scalar field on axis *X* after modeling the one full turn in Cartesian and curvilinear coordinates that was realized using TVD scheme with Roe limiter, are shown in Fig. 7. Parameters: $R_1 = 0.22$; $R_2 = 0.27$; $\Delta R = R_2 - R_0 = 0.02$.

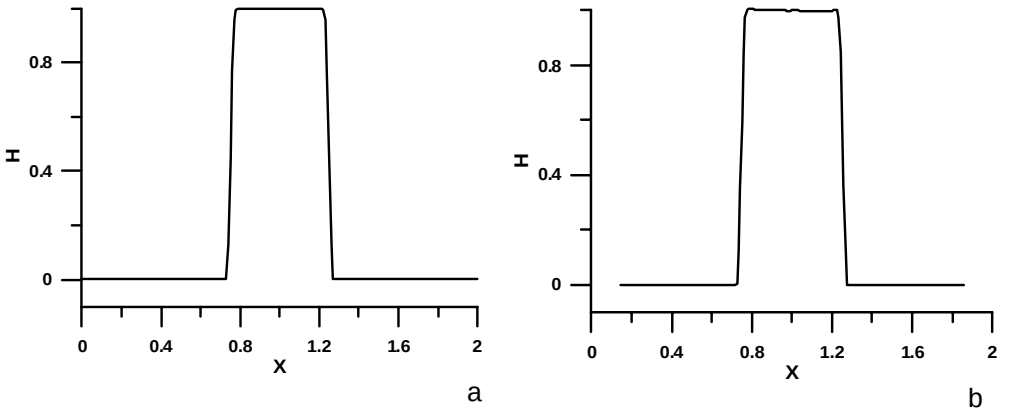

Fig. 7. Result of modeling the scalar field rotating using TVD scheme with Roe limiter: a) in Cartesian coordinates; b) in curvilinear coordinates.

As we can see in Figs. 3-7, the results of modeling the scalar field rotating in Cartesian and curvilinear coordinates are practically identical. It should be noted that the results of modeling are close to the analytical solution when we use any TVD scheme. But using the first-order accuracy TVD scheme reduces the appearance of

oscillations on the field boundaries (see Fig. 4). There are no such oscillations while using additional limiters. Parameters of the modeling results of scalar field rotation are shown in Table 1.

Table 1

Parameters of the modeling results

Parameters	Simple upstream differencing scheme	TVD scheme	TVD scheme with Leonard limiter	TVD scheme with van Leer limiter	TVD scheme with Roe limiter
R_1	0.08	0.21	0.21	0.20	0.22
R_2	0.45	0.28	0.28	0.28	0.27
ΔR	0.20	0.03	0.03	0.03	0.02

4. Conclusion

Using TVD schemes for solving an advection equation gave a result that was close to the analytical solution. So we should use the TVD schemes in curvilinear coordinates for modeling transport of different types of pollution in water bodies with complex coast structure. The best results were obtained for the TVD schemes with van Leer and Roe limiters. The TVD scheme with Roe limiter gives the closest result to the analytical solution, but it allows for negative values at positive initial conditions, whereas the TVD scheme with van Leer limiter prevents them.

References

Leonard, A., 1979, *A stable and accurate convective modeling procedure based on quadratic upstream interpolation*, Comput. Methods Appl. Mech. Eng. **19**, 59-98.

Van Leer, B., 1979, *Towards the ultimate conservative difference scheme. V. A second order sequel to Godunov's method*, J. Compt. Phys. **32**, 101-136.

Roe, P.L., 1985, *Some contributions to the modeling of discontinuous flows*. **In:** B.E. Engquist, S. Osher, and R.C.J. Somerville (eds.), "Large-Scale Computations in Fluid Mechanics", American Mathematical Society, Providence, R.I.

Accepted September 12, 2006

PUBLS. INST. GEOPHYS. POL. ACAD. SC., E-6 (390), 2006

Analysis of Sediment-Laden Flows in Open Channel

Robert J. BIALIK and Włodzimierz CZERNUSZENKO
Institute of Geophysics, Polish Academy of Sciences
Ks. Janusza 64, 01-452 Warsaw, Poland
email: rbialik@igf.edu.pl

Abstract

The transport of suspended sediment in open channel flows is the key issue of the area of fluvial hydraulics. Traditionally, in classical hydraulics, the phenomenon is analyzed as a one-phase composite system. This paper deals with three different models to calculate the vertical distribution of suspended sediment concentration in open channel flows. These models, i.e. the classical one and two new models are briefly presented. The numerical simulations of the vertical sediment transport using these models are presented and main differences are discussed.

1 Introduction

The sediment-laden open-channel flows and the associated sediment transport are the oldest topics in fluvial hydraulics. So far, the traditionally approach basis on the advection diffusion equation has been applied to calculate the vertical concentration distribution. Civil engineers have tried to improve the advection-diffusion equation by introducing some empirical coefficients to correct the fall velocity and the eddy diffusivity for at least 50 years. In effect, the equation has become more empirical with a few empirical coefficients, which are not well defined.

The new analysis based on the two-phase approach indicates that the interaction between the fluid and sediment is the crucial one description in the sediment-laden flows. The interaction between the fluid and sediment is controlled by the distribution of sediment concentration, the turbulence structure and the sediment inertia. Nowadays measurements show that the sediment fall velocity in turbulent flows is always less than the sediment fall in still water and this fact should be taken into an account in presented models. In the paper, two such models are presented and the results of numerical simulations are compared with the classical model.

2 Approach and methods

2.1 Diffusion-Advection Equation

The three-dimensional form of the diffusion-advection equation for suspended sediments is:

$$\frac{\partial C}{\partial t} = \frac{\partial}{\partial x}\left(\eta_p \frac{\partial C}{\partial x}\right) + \frac{\partial}{\partial y}\left(\varepsilon_p \frac{\partial C}{\partial y}\right) + \frac{\partial}{\partial z}\left(\xi_p \frac{\partial C}{\partial z}\right) - U\frac{\partial C}{\partial x} - V\frac{\partial C}{\partial y} - W\frac{\partial C}{\partial z} + \frac{\partial}{\partial y}\left(\omega_s C\right), \quad (1)$$

where C is the time-average concentration of the dissolved substance, U, V, W - the average velocity components in the x (longitudinal), y (vertical with the origin at the bottom channel), z (lateral) directions, respectively, $\eta_p, \varepsilon_p, \xi_p$ are the turbulent diffusion coefficients in the x, y and z directions. The first three terms on the right-hand side represent the diffusion process and the remaining terms the advection process. To consider the classical hydraulics problem, i.e. the distribution of sediment concentration in vertical directions in two-dimensional uniform flow, one can get the most popular one-dimensional form of the eq. (1) as follows:

$$\frac{\partial C}{\partial t} = \frac{\partial}{\partial y}\left(\varepsilon_p \frac{\partial C}{\partial y}\right) - (V - \omega_s)\frac{\partial C}{\partial y}, \quad (2)$$

it was assumed that the fall sediment velocity ω_s is independent of y. For uniform and stationary flows, eq. (1) can be rewritten in the form:

$$\frac{d}{dy}\left[\varepsilon_p \frac{dC}{dy} + (V - \omega_s)C\right] = 0. \quad (3)$$

2.2 The classical approach, the Rouse Formula

The equation for transport of suspended particles in the vertical direction for unidirectional flow is easy to get from eq. (3) by substituting $V = 0$,

$$C\omega_s + \varepsilon_p \frac{dC}{dy} = 0, \quad (4)$$

Eq. (4) is well known as the Rouse formula.

In mixture of high concentrations, the fall velocity is not constant but depends on the concentration because the particles are hindering each other during settling. The falling particles are affected by the return flow of the displaced fluid but also by additional effects such as particle collision, particle-induced turbulence, modified drag coefficient and group effects. The overall effect can be represented by:

$$\omega_s = (1 - C)^{\gamma}\omega \quad (5)$$

in which ω_s is the sediment fall velocity in a mixture, γ ranges from 4 to 5 (for particles of 50 to 500 μm); here $\gamma = 5$. For suspended sand particles in the range $100 - 1000\ \mu m$, the following equation can be used (Van Rijn , 1993):

$$\omega = 10\frac{\nu}{D}\left[\left(1 + \frac{0.01(s-1)gD^3}{\nu^2}\right)^{\frac{1}{2}} - 1\right], \tag{6}$$

in which ν is the kinematic viscosity, D the particle diameter, g the gravity, and s is the density ratio of sediment and water ($s = \varrho_s/\varrho_f$).

Usually the turbulent diffusion coefficient for sediment ε_p in eq. (4) is related to turbulent diffusion coefficient for clear fluid ε_f, as follows:

$$\varepsilon_p = \beta\phi\varepsilon_f. \tag{7}$$

The β factor describes the difference in the diffusion of a fluid particle and a discrete sediment particle. The ϕ factor expresses the influence of the sediment particles on the turbulence structure of the fluid. Given the limited knowledge of the physical processes involved, it is not advisable to use a β factor larger than 2, and the ϕ factor equal 1 (Van Rijn , 1993).

To calculate the particle turbulent diffusion coefficient, the following assumption are made (Czernuszenko , 1999): $\varepsilon_p = \varepsilon_f = \nu_t$. For uniform and unidirectional open-channel flows, the vertical distribution of the eddy viscosity coefficient is:

$$\frac{\nu_t}{u_* y} = \kappa(1 - \zeta) \tag{8}$$

in which $\zeta = y/h$ (y = distance from the bed, h = water depth), κ is the von Karman constant that has been assumed to be 0.4 for both clear-water and suspension flows (Coleman , 1986), u_* is the bed friction velocity that is usually calculated from the Reynolds stress profile near the bed. Thus, the sediment mass concentration along the vertical direction can be derived from eq. (4) in the form (Van Rijn , 1993)

$$C = C(a)\left(\frac{h-y}{y}\frac{a}{h-a}\right)^z, \tag{9}$$

where $C(a)$ is the known sediment concentration at the position $y = a$, and z the suspension coefficient expressed as (Graf , 1984):

$$z = \frac{\varepsilon_p}{\kappa u_*}. \tag{10}$$

2.3 The model of Cao et al.

The new diffusion equation for suspended sediment concentration from a rigorous derivation of the water-sediment mixture's is (Cao , 1995):

$$\varepsilon_p \frac{dC}{dy} = -\omega_s C - \frac{\rho_s - \rho_f}{\rho_f} \omega_s C^2. \tag{11}$$

The difference between this new equation and the well known Rouse formula is:

$$-\frac{\rho_s - \rho_f}{\rho_f} \omega_s C = V, \tag{12}$$

which shows an intrinsic association of the mixture's normal velocity V with sediment concentration C. The model of Cao is easy to get from eq. (3) by substituting for V this new term eq. (12).

Equation (12) implies that a downward mass flux of the water-sediment mixture arises (Cao (1995)). In most previous studies the y component velocity V of the water-sediment mixture is assumed to be zero, $V = 0$, and this new approach of V may not be familiar. As a matter of fact, this mass flux stems from the inequality between the mass of sediment particles and that of water particles in their position exchanging process when the particles fall because of unequal densities of water and sediment. This downward mass flux is balanced by the upward turbulent diffusion flux to reach the steady-state equilibrium (Cao , 1995).

2.4 Czernuszenko Formula

It is assumed that there is an additional mechanism influencing the particle movement in sediment-laden flows, which is called the drift and acts independently of the advection and turbulent diffusion. Based on all three mechanisms, a new equation for the concentration distribution is (Czernuszenko , 1999):

$$(1 - C)^5 C\omega_s + (\varepsilon_p + \varepsilon_{pd}) \frac{dC}{dy} = 0. \tag{13}$$

in which ε_p is the turbulent diffusion coefficient for a single particle in the horizontal and vertical directions, and ε_{pd} is the drift diffusion coefficient. The formula for the drift diffusion coefficient is (Czernuszenko , 1999):

$$\varepsilon_{pd} = \frac{\pi}{2} D \sqrt{\overline{v_p'^2}}. \tag{14}$$

Nezu and Rodi (1986) proposed universal functions for turbulence intensities in this region. These functions were determined by least-square fits to experimental data and expressed in the form:

$$\sqrt{\overline{v_p'^2}} \simeq 1.23 u_* \exp(-0.67\zeta). \tag{15}$$

3 Results of numerical simulations

Equations (4, 11, 13) were solved numerically with the fourth order Runge-Kutta method. Basic data for measurements was taken from Coleman and Lyn (Table 1).

Table 1: Experimental conditions of ((Coleman, 1986) and (Lyn, 1988))

Experiment	Run	U_{max}	u_*	h	D	C(0.1h)	ω_s	ϱ_s
Coleman (1986)	C22	102.4	4.1	17.0	0.21	0.05	1.3	2.65
Coleman (1986)	C25	107.3	4.0	16.7	0.21	0.2	1.3	2.65
Coleman (1986)	C30	109.3	4.1	16.8	0.21	0.5	1.3	2.65
Lyn (1988)	L15	75.7	3.6	6.45	0.15	0.19	2.1	2.65
Lyn (1988)	L19	77.7	3.8	6.51	0.19	0.11	2.5	2.65
Lyn (1988)	L25	85.9	4.3	6.54	0.24	0.072	4.8	2.65

Figs. 1 a,b and 2 a show the vertical concentration distributions of suspended sediment measured by Coleman and Figs. 2 b and 3 a,b measured by Lyn. In the figures: black lines represent the solution of eq. (4), green lines represent the solution of eq. (11), and red lines represent the solution of eq. (13).

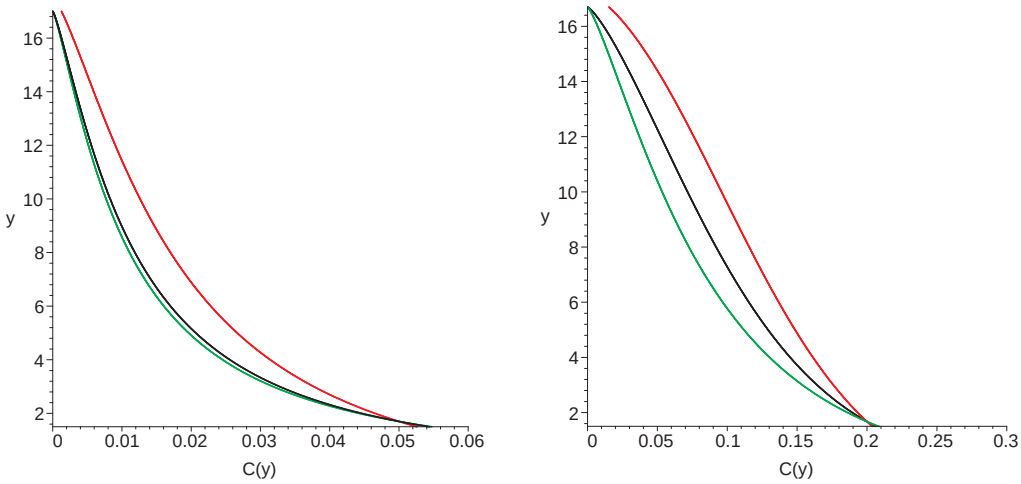

(a) Comparison with Coleman "C22" (b) Comparison with Coleman "C25"

Fig. 1. Vertical distributions of suspended sediment concentration

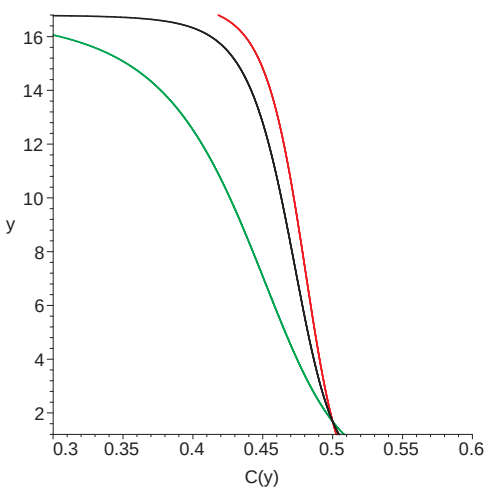

(a) Comparison with Coleman ”C30”

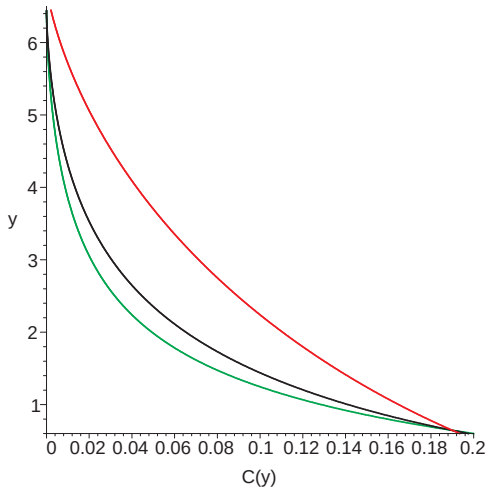

(b) Comparison with Lyn ”L15”

Fig. 2. Vertical distributions of suspended sediment concentration

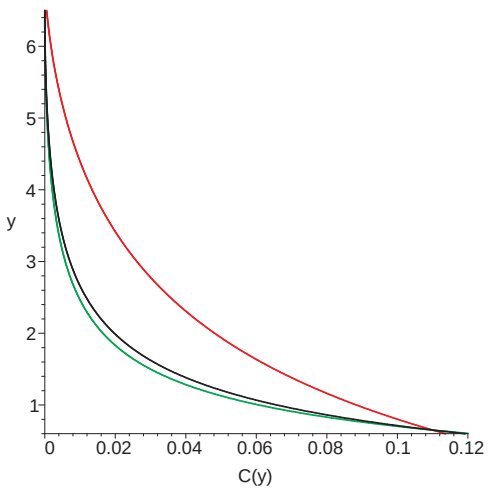

(a) Comparison with Lyn ”L19”

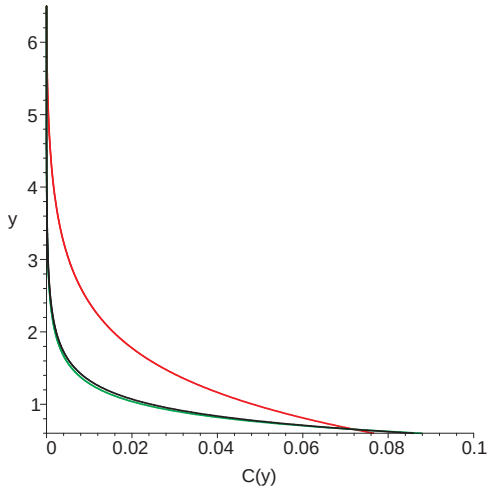

(b) Comparison with Lyn ”L25”

Fig. 3. Vertical distributions of suspended sediment concentration

4 Discussion and Conclusions

1. The classical approach is based on the simplified assumption that the particles follow entirely the mean and turbulent flow velocity. However, this ”passive scalar hypothesis” is valid only under very restrictive assumption. The vertical

component of velocity V in the water-sediment mixture is assumed to be zero, which is acceptable only for very low sediment concentration.

2. The Cao et al. model introduces an additional sediment vertical velocity as a function of differences of densities between sediment and fluid and the sediment concentration. Cao model is the same as Rouse model for $\varrho_s = \varrho_f$.

3. The Czernuszenko model describes the vertical distribution of sediment concentration taking into account an additional mechanism influencing the sediment particle movement in sediment-laden flow. This mechanism created a new, additional vertical flow of sediment called the drift movement.

4. The largest differences between the models appear for higher sediment concentration, i.e. for Lyn's data (run L15) and Coleman's data (run C30). The Models Czernuszenko eq. (13) overstate and that Cao eq. (11) underrate values for higher concentration in comparison with the Rouse formula eq. (4).

Acknowledgments

This work was supported by grant 2 P04D 026 29 from Ministry of Education and Science, Poland. Authors are very grateful to Professor A. Icha from Pomeranian Pedagogical Academy in Słupsk for his help of typesetting this paper in LaTeX.

References

Cao, Z., Wei L. and J. Xie, 1995, Sediment-laden flow in open channels from two-phase flow viewpoint, *Journ. Hydr. Engrg.*, **121**(10), 725-735.

Coleman N.L., 1986, Effects of suspended sediments on the open channel velocity distributon, *Water Resour. Res.*, **22**(10), 1377-1384.

Czernuszenko, W., 1999, Drift velocity concept for sediment-laden flows, *Journ. Hydr. Engrg.*, **124**(10), 1026-1033.

Graf W.H., Hydraulics of sediment transport, *Water Resour. Publ.* Liteon, CO, USA.

Lyn D.A., 1988, A similarity approach to open channel sediment laden flows in open channels, *Journ. Fluid Mech.*, **193**, 1-26.

Nezu I., and W. Rodi, 1986, Open channel flow measurements with a laser-Doppler anemometer, *Journ Hydr. Engrg.*, **112**, 335-355.

Van Rijn, L.C., 1993, *Principles of sediment transport in rivers, estuaries and coastal seas*, Aqua Publ.

Accepted September 12, 2006

PUBLS. INST. GEOPHYS. POL. ACAD. SC., E-6 (390), 2006

3D Non-Hydrostatic Modelling of Bottom Stability Under Impact of the Turbulent Ship Propeller Jet

Igor BROVCHENKO[1], Julia KANARSKA[2], Vladimir MADERICH[1] and Katerina TERLETSKA[1]

[1] Ukrainian Center of Environmental and Water Projects
Glushkova Prospect 42, 03187, Kiev, Ukraine
e-mail: brovchik@env.kiev.ua

[2] Institute of Geophysics and Planetary Physics UCLA
405 Hilgard Ave., Los Angeles, CA 90095, USA

Abstract

New three-dimensional numerical non-hydrostatic model with a free surface that was designed for modelling the bottom and bank stability subjected by ship propeller jets is presented. Unlike all known models, it describes three-dimensional fields of velocities generated by ship propellers, turbulence intensity and length scale in the given domain of arbitrary bottom and coastal topography. Results of simulations are compared with the laboratory experiments.

Key words: non-hydrostatic model, turbulent propeller jet, bottom erosion.

Full text was published in *Acta Geophysica*, Vol. 55, No. 1, p. 47-55.

PUBLS. INST. GEOPHYS. POL. ACAD. SC., E-6 (390), 2006

Coastal Cooling/Heating Events: Laboratory Experiments

Natalia DEMCHENKO and Irina CHUBARENKO

Atlantic Branch of P.P. Shirshov Institute of Oceanology
Russian Academy of Sciences
Prospect Mira 1, 236000 Kaliningrad, Russia
e-mail: ndemchenko@mail.ru

Abstract

We report the results of laboratory experiments on water heating/cooling, performed in 5 m long water channel with a slope. About 63 series of photos were analyzed: for 3 locations, for 3 bottom slopes (3.7, 6.7 and 12 degrees) and for different *Ra* numbers. It was pointed out that there exist two types of mixing characterizing different circulations in the presence of slope: gravity current and undersurface jet; the thermal bar is the region where one type of mixing is replaced by another; the highest speed and flowrate are at the break point; the flow is three-dimensional.

Key words: flowrate, lake's thermal bar, coastal heating event, coastal cooling event.

Full text was published in *Acta Geophysica*, Vol. 55, No. 1, p. 56-64.

PUBLS. INST. GEOPHYS. POL. ACAD. SC., E-6 (390), 2006

Morphological Development of the Retention Basin "Hartheim": A Case Study

Andreas DITTRICH[1], Annette SCHULTE-RENTROP[1], Michael MAREK[1] and Volker SPÄTH[2]

[1] Leichtweiss-Institut of Hydraulic Engineering (LWI), Department of Hydraulic Engineering Beethovenstrasse 51a, 38106 Braunschweig, Germany; e-mail: a.dittrich@tu-bs.de

[2] Institute for Landscape Ecology and Nature Conservation in Buehl (ILN) Sandbachstrasse 2, 77815 Buehl, Germany; e-mail: volker.spaeth@ilnbuehl.de

Abstract

Flow in rivers and on floodplains is complex as it is affected by several interconnected factors such as topography, sediment transport and vegetation characteristics. The resulting processes are explained by the measure "Hartheim" planned for retention purposes at the Upper Rhine river. On the basis of existing formulas and instruments it is demonstrated that a good estimation of the development of the measure is possible. The proposed procedure is a useful tool for estimating morphological developments of restored river sections.

Key words: morphodynamics, resistance of vegetation, 3D-hydrodynamic simulations, stability of armoured river beds.

Full text was published in *Acta Geophysica*, Vol. 55, No. 1, p. 33-46.

PUBLS. INST. GEOPHYS. POL. ACAD. SC., E-6 (390), 2006

Evaluation of the Choghakhor Wetland Status with the Emphasis on Environmental Management Problems

Samaneh EBRAHIMI and Mohammad MOSHARI

Graduate Faculty of Environment, University of Tehran
e-mail: ebrahimi_samaneh@yahoo.com

Abstract

Ecological and eco-touristic importance and the problems of conservation of natural lands around Choghakhor Wetland, located in the Chahar Mahal and Bakhtiari province of Iran, the habitat of many immigrant bird and aquatic creatures, were the main topics of this study; the importance of providing an environmental planning and management plan for this wetland is emphasized. In order to determine priorities according to the status of Choghakhor Wetland, in comparison to the 75 important wetlands of Iran (63 of these have been registered in the Ramsar Convention documents), the five criteria (birds, fish, threatening factors, social-economic problems and conservation status) of the wetland were studied and analyzed, and the macro-invertebrate benthos, including Oligochaeta, Chironomidae and Gammaridae, was surveyed. For Choghakhor Wetland, the result was 80/140, so this wetland got the 8th priority among all other ones. In fact, this classification shows the potential strength of Choghakhor Wetland to have environmental management plan. The results of this study make it clear that construction of a dam is the strongest threatening factor to this habitat and its biodiversity. This clearly shows the necessity of environmental planning and management to assess the impacts in order to establish proper management and wise use of the wetland.

Key words: Choghakhor Wetland, environmental planning and management, Ramsar Convention.

1. Introduction

According to the Ramsar Convention: "Wetlands are areas of marsh, fen, peatland or water, whether natural or artificial, permanent or temporary, with water that is static or flowing, fresh, brackish or salt, including areas of marine water the depth of which

at low tide does not exceed six meters." Benefits of wetlands are their natural riches, tourism and training, wetlands ecology, reduction of flood risks, effects on ground water supply, wetlands as sink (and source) of pollutions, climate change problem, and wetlands as habitat for rich biodiversity.

With the aim of attaining higher levels of social welfare and improving people's quality of life, the government has arranged a specific program for constructing a dam on Choghakhor Wetland which leads to adverse effects on the environment of the wetland.

2. The Case Study Area

Choghakhor Wetland is the largest, unique wetland in Chahar Mahal and Bakhtiari province; it is the habitat of most of the immigrant and endemic species of the province. As a result of human activities (especially the construction of dam on the wetland), it became so fragile and sensitive that during the recent years many valuable species became endangered by extinction and destroying. Some of the land uses of Choghakhor Wetland which cause environmental problems are the water intake for irrigations (and other purposes), the increasing dam's height, boating and incretions; the interaction of these conflicting factors causes disorder in Choghakhor Wetland's bio-system.

Before the dam had been constructed, the extent of water coverage, in the heaviest rainfall season of the year, was 700 to 1000 ha, and most of the edge lands and also the wetland itself were covered with aquatic plants, especially *Junicus*. But since 1999, when the Choghakhor dam was constructed on the exit of the wetland, the water volume increased so that the extent of water coverage, in the heaviest rainfall season of the year, changed to 1500 ha; the volume of water intake is estimated to be around $45*10^6$ m^3, which causes fundamental changes in macro-benthos of the wetland (Document p120 1996).

The Choghakhor Wetland is located 2270 m above sea level and its geographical coordinates are: 31˚54′17″N to 31˚56′31″N and 50˚52′40″E to 50˚56′14″E (Document p120 1996).

Before the dam construction, the deepest part of the wetland in the heaviest rainfall season of the year was 1.5 m, that changed to 6 m or even more afterwards. Water sources of the wetland are mostly the rainfall and high water springs (such as Sibek, Tange Siah, Zoordegan, Oregan, Saki abad, Galoogerd) which are located in the west and south part of the wetland. Surface flow has only a small share in the water supply of Choghakhor Wetland (Document p120 1996).

3. Materials and Methods

In order to survey macro-invertebrates of the wetland, including Oligochaeta, Chironomidae and Gammaridae, six sampling stations selected along the water course from the source to the mouth of Choghakor Wetland were surveyed from October 1995 to September 1996. Each station was sampled 4 times (or more). To obtain quantitative samples of benthic of macro-invertebrate, an Ekman dredge sampler (225 cm^2 opening surface) was selected. This kind of sampler has been widely used both in routine surveys and for detailed benthos sampling programs, as recommended by the Fishing Research Institute of Iran for quantitative sampling of the sites.

In order to sample the benthic species, a very large area of the wetland needs to be sampled, but this was difficult in practice because of unfavorable weather conditions: freezing and local winds. A compromise was therefore sought, and some samples were taken which were considered to provide reliable and representative data. During sampling sessions at the wetland stations, air and water temperature, depth of water, electric conductivity and pH were recorded.

Also, the water samples were being moved to the laboratory for an analysis of macro-benthos species. Preliminary sorting of macro-benthos samples in the laboratory was carried out on the same day the samples were taken. To obtain the biomass of macro-benthos species, first they were dried, and then the macro-benthos species of the same family were weighted separately by using the 0.0001 sensitive weights. Having the total number, average weight of macro-benthos species was obtained to determine biomass weight per m^2.

4. Results

Considering the obtained results of biological and physico-chemical characterization of Choghakhor Wetland and applying the five criteria of birds (18/25) (Evans 1994), fish (17/25) (Coad 1995, 1996), threatening factors (27/50) (Hassanzadeh Kiabi et al. 2004), social-economical problems (18/25) (Department of Environment 2001, Hassanzadeh Kiabi et al. 2004) and conservation (0/15) (Majnoonian 2000, Cosslett 2000), Choghakhor Wetland has 80 scores of the 140 total scores, and got the 8th priority among all the others. In fact, this classification shows the potential strength of Choghakhor Wetland to have environmental management plan. Implementation of environmental management plans needs favorable and desired context, as to both the internal and external conditions of the wetland. Regarding Choghakhor Wetland, the external conditions do not work in the same direction as the internal conditions and factors.

Analyzing the investigations on the five criteria and Choghakhor's score, and then the priority and classification of every of them, we concluded that the dam construction and water intake are the most threatening factors which ruin Choghakhor's

biodiversity and habitat diversity of this resource. The hydrological regime of Choghakhor has been significantly modified through the construction and operation of the dam. The biological and physico-chemical characterization of the wetland is summarized in Table 1.

Table 1

Biological and physico-chemical characterization of the Choghakhor Wetland

	Fall 1995	Winter 1995	Spring 1996	Summer 1996
Air temperature (°C)	13.7	-4.7	20.1	27.5
Water temperature (°C)	10.7	5.2	16.3	23
Water depth (m)	1.9	2.5	3.1	2.5
Electric conductivity (μS)	373	247	233	214
pH	8.6	8	8.27	8.3
Oligochaeta (g/m^2)	2.966	8.78	1.67	0.242
Chironomidae (g/m^2)	0.274	0.593	0.2	0.0027
Gammaridae (g/m^2)	0.248	0	0.106	0.00051

The table shows that different sites of Choghakhor are not the same regarding macro-benthos species abundance and its biomass. This depends on environmental conditions, such as air and water temperature, or water depth. As the table shows, the dominant macro-benthos species of Choghakhor Wetland is Oligochaeta, constituting 90% of the benthos biomass, which lives in places where there is high concentration of organic pollution. The organic pollution of Choghakhor is a result of adding fertilizers and chemicals to water for the needs of fishes introduced to Choghakhor after the dam construction.

Trends of each macro-benthos biomass constituent and biological and physico-chemical factors measured are shown in Figs. 1-3.

The graphs show that the macro-benthos biomass rate decreases significantly in spring which can be a result of increasing temperature and the utilization of macro-invertebrate benthos by the wetland fishes, especially *Cyprinidae*.

According to the graphs, it can be concluded that some factors, such as temperature or a kind of bed, are in a very close relation to the increase in abundance of benthos species, and every change in these factors leads to a change in macro-invertebrate benthos.

We concluded that investigations on wetland, integrated with benthic macro-invertebrate communities, could provide the basis for a robust monitoring of wetlands as a water habitat.

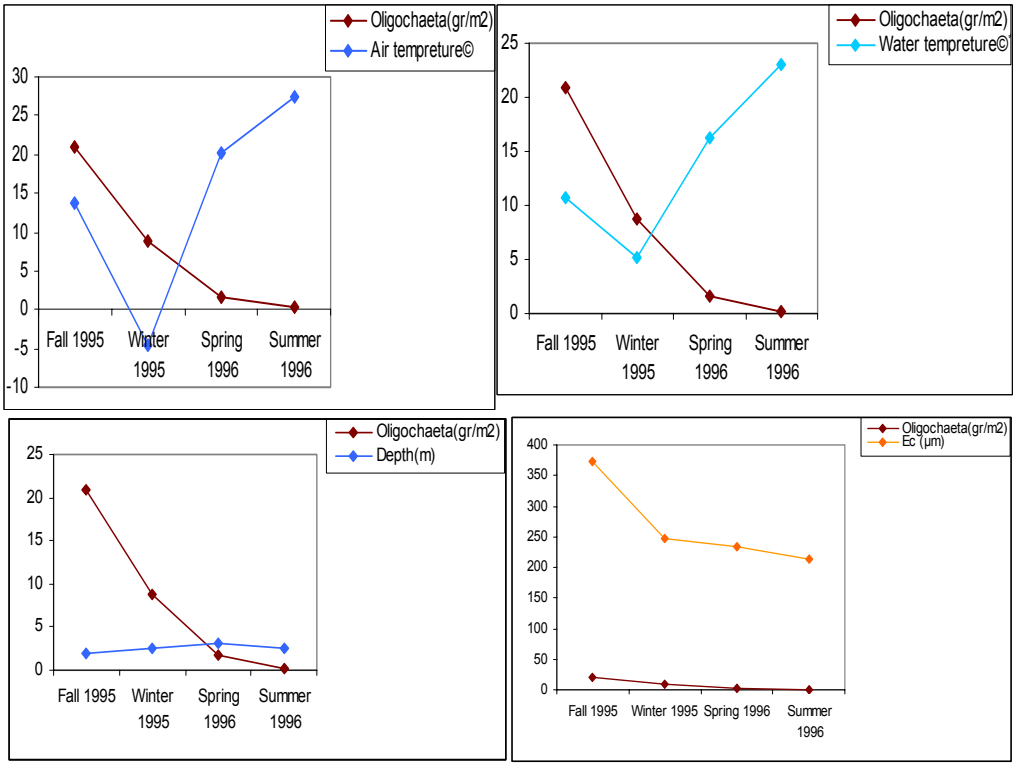

Fig. 1. Trends in Oligochaeta concentration and studied physico-chemical factors.

Biological and physico-chemical characterization and assessments made in this study, using macro-invertebrate benthos and other factors, showed some advantages over chemical analyses that may not overpass analytical limits, and may not identify many potential interactions of substances. Because of these shortcomings, a huge number of contaminants of this wetland have remained undetected and this has to be taken into consideration, at least by assessing their impacts on the aquatic life.

The effects of human's activities on the natural resource such as wetlands have to be considered in a long term, because accurate consideration is impractical in short term. In the wetland there are habitats that are ecologically important and contain many valuable species of flora and fauna, which plays a major role in water life cycles and fisheries resources. In Iran, as well as in many other countries around the world, there is sometimes a lack of basic data and information.

Construction of dams, parallel with other developmental activities and transformations of the natural pattern of the wetland, brought many limitations and points of stress into its natural system. For example, wetlands play a very important role in

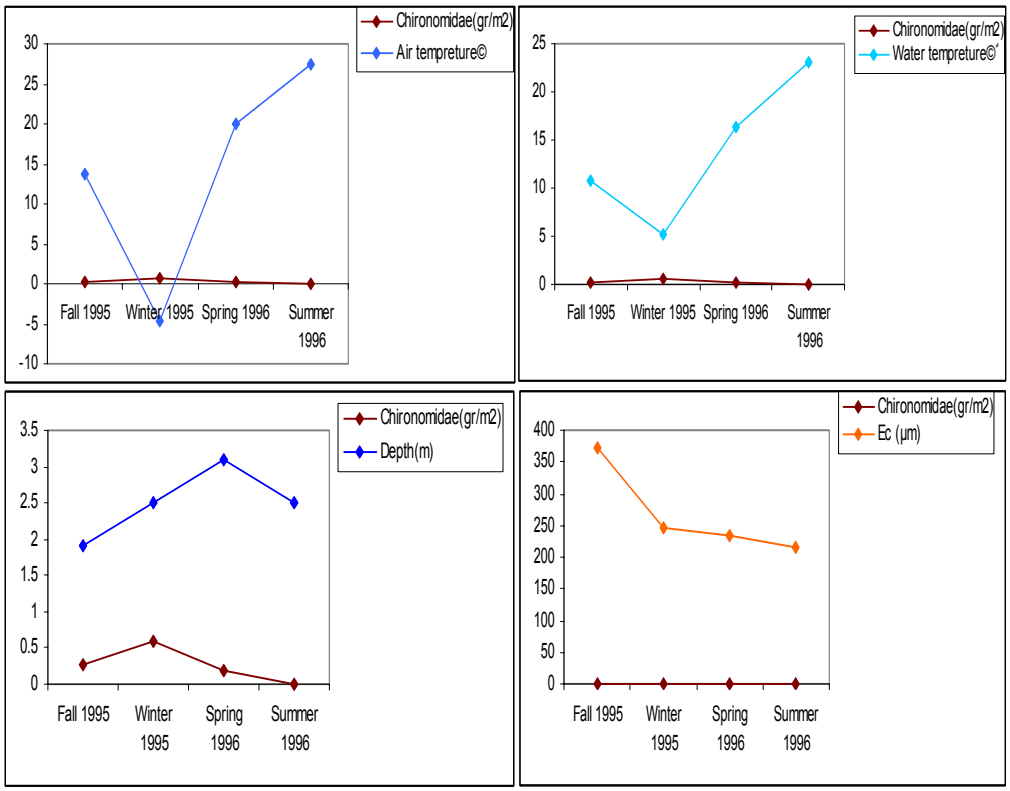

Fig. 2. Trends in Chironomidae concentration and studied physico-chemical factors.

the natural carbon cycle, both as an absorbing sink and an emitting source of CO_2 . Unfortunately, the land use changes, wetland conversion and over-utilization of these resources create an imbalance in the flow of CO_2 and the amount of carbon reserved in the living and dead plant coverage of wetland. This also alters the habitats location of some species, specially the less tolerant ones (or extinction of low-tolerant ones). Some of the most important adverse effects of dam construction on Choghakhor Wetland that this study reveals are:

- Change from wetland to lake condition (construction of a dam on the wetland causes an increase in the water height to 6 m or more in some areas of the wetland);
- Release of nutrients in the water;
- Effects on plankton and aquatic animal and plant populations (effects on aquatic biodiversity and its changes);
- Changes in downstream water physiochemistry.

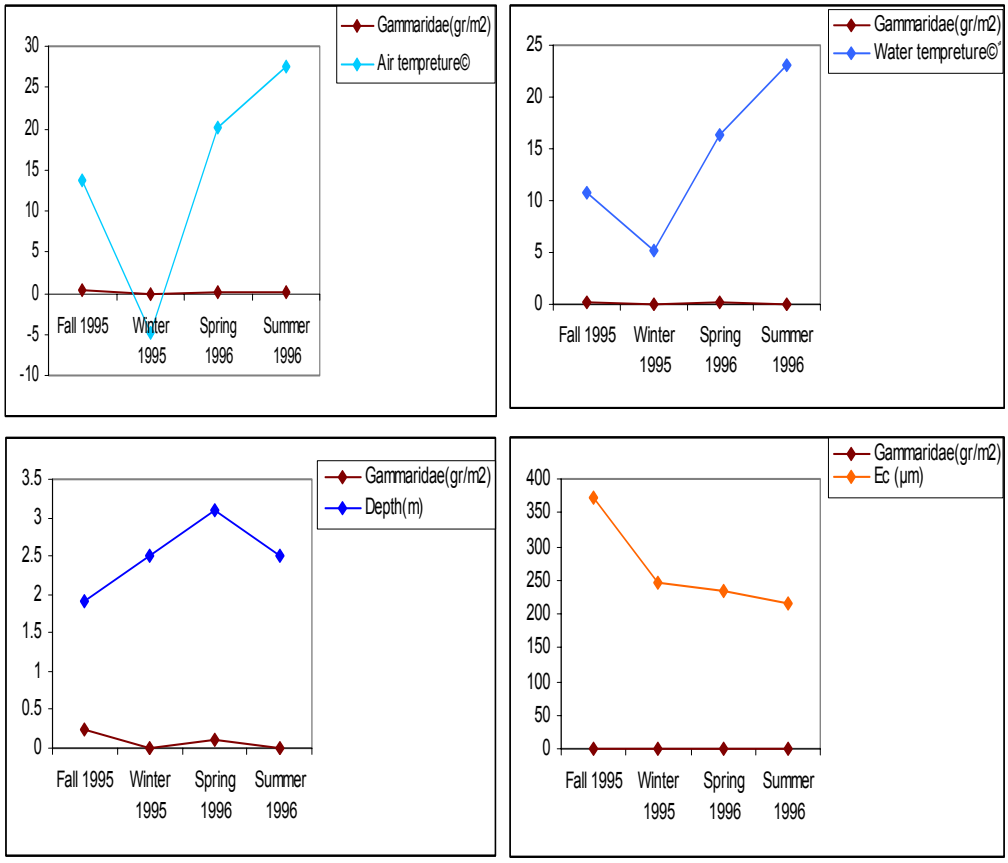

Fig. 3. Trends in Gammaridae concentration and studied physico-chemical factors.

Although since 1999 Choghakhor has been announced as a hunting-restricted zone to be better conserved and to be subject to proper management, it seems that this wetland, not being in the Ramsar Convention yet, has great problems regarding its conservation. There is no environmental management plan for Choghakhor Wetland yet. This causes not only the lack of wise operation, but also the fact that this wetland is even out of its main function as a wetland and changes to a lake now. The dam constructed on the wetland caused an increase in the water height to 6 m and more in some areas, which is the harshest factor threatening the wetlands creatures, and causes fundamental changes in macro-benthos, diminishing the habitat and changing its biodiversity.

So, as a result of this study it is strongly suggested to organize a working group consisting of environment assessor and environment manager, botanist, zoologist,

geomorphologist and other experts in order to do basic scientific research on the wetland. Also, it is suggested to assess both long-term and short-term effects of human activities on these natural water resources.

5. Conclusion

The biological condition of wetland is influenced and determined by multiple chemical, physical and biological factors, both in water and sediments. An inappropriate reliance on only physico-chemical and biological properties of the water may underestimate aquatic ecosystem impacts. In fact, the investigation and monitoring of the water may assess only point sources of pollution and not the water resource condition. The present study showed that physico-chemical and biological measurements of the water must be undertaken to evaluate all relevant stressors to the aquatic life. The approach proposed in this paper is to use the biotic index, that excludes temporary disturbances; this constitutes a useful tool to provide more detailed information about changes in aquatic life conditions.

References

Coad, B.W., 1995, *Freshwater fishes of Iran*, Acta Sci. Nat. Acad. Sc. Brno **29**, 1, 1-64.

Coad, B.W., 1996, *Biodiversity of Iranian freshwater fishes*, Research Division of Canadian Museum of Nature.

Cosslett, C., 2000, *GEF Criteria for wetland selection* (unpublished).

Department of Environment, 2001, *Expert reports on wetlands, habitat and wildlife* (unpublished).

Document p120, 1996, Fishing Research Institute of Iran.

Evans, M.I., 1994, *Important bird areas in the Middle East*, Bird Life IUCN/IWRB.

Hassanzadeh Kiabi, B., H. Majnoonian, H. Gashtasb and J. Mansoori, 2004, *Suggested criteria to evaluate the conservation status of Iran wetlands*, Journal of Environmental Studies **33**, 74-89.

Majnoonian, H., 2000, *Iran conservated areas*, Teheran, Department of Environment.

Accepted September 12, 2006

PUBLS. INST. GEOPHYS. POL. ACAD. SC., E-6 (390), 2006

Automatic Eddy Viscosity Assignment for 2-D Hydrodynamic Model of Szczecin Bay

Ryszard EWERTOWSKI[1,2]

[1] Technical University of Szczecin, Building and Architecture Dept., Water Building Faculty
Al. Piastów 50, 70-311 Szczecin, Poland
email: rewert@amu.edu.pl

[2] Maritime Research Institute in Gdańsk, Branch Szczecin
ul. Niedziałkowskiego 47, 71-403 Szczecin, Poland

Abstract

An automatic calculation of eddy viscosity fields for 2-D horizontal hydrodynamic model of Szczecin Bay is discussed. Two methods for turbulent diffusion coefficients are applied – Peclet formula and Smagorinski model. Both are used for steady flow simulations on FEM network in Szczecin Bay. The results of simulation indicate some strength of Smagorinski model over Peclet one in terms of flexibility for describing complex flow conditions. Also mixed formulation has brought interesting results concerning presence of eddy vorticity.

1. Introduction

In numerical simulations of hydrodynamic phenomena in shallow water basins, currents and tracers cannot have smaller structures than the model grid step. All the eddies whose size is smaller than grid step are treated as turbulent diffusion. This problem, called the turbulence closure, is discussed here in application for 2-D horizontal model of Szczecin Bay. The turbulence closure methods usually have their own parameters, called diffusion coefficients, that are variable in space and time. In the paper, horizontal diffusion (viscosity) is alternatively taken as constant and as a function of velocity field and element size (Peclet and Smagorinski formulation). The Peclet and Smagorinski methods allow for dynamic adjustment of eddy viscosity (EV) in computed flow, thereby they are discussed here as a promising yet cheap solution for 2-D depth-averaged flow.

2. Approach and methods

Surface water flow phenomena in shallow waters are described here using the depth-averaged version of the Reynolds-Avaraged-Navier-Stokes (RANS) method. It decomposes the total solution in two parts: an averaged solution and superimposed fluctuations. Only the effect of these fluctuations on the average solution is modeled with an eddy-viscosity model. The main role of this model is to remove energy from the resolved scales by modeling the unresolved stress so that the dissipative effect is well captured. In the momentum equations of RANS the non-linear terms $\overline{\rho}(\overline{u_i u_j} - \overline{u}_i \overline{u}_j)$ of the Subgrid Scale Stress tensor (SGS) have to be closed. The two relatively simple closing methods are discussed here and compared in application to the Szczecin Bay steady flow problem: the Peclet method and the Smagorinski model. Their main task is to model the effect of the neglected scales on the resolved ones during the whole simulation of flow in the given numerical schematization.

The Smagorinski method is based on two main premises: the isotropic part of Reynolds stresses $\overline{\rho}(\overline{u_i u_j} - \overline{u}_i \overline{u}_j)$ can be neglected due to incompressibility effects in the SGS fluctuations and the deviated part τ_{ij} is expressed by eddy viscosity concept:

$$-\overline{u_i u_j} \equiv \tau_{ij} = \mu_t \left(2\overline{S}_{ij} - \frac{1}{3}\delta_{ij} k \right) \tag{1}$$

where $\overline{S}_{ij}$ is the resolved strain rate tensor of the filtered velocity (Eq. (2)), $k = 1/2\, u_i u_i = 1/2\left(u_1^2 + u_2^2 + u_3^2\right)$ is the kinetic energy of turbulent motion per unit mass, and δ_{ij} is the Kronecker delta (= 1 for $i = j$, = 0 otherwise).

$$\overline{S}_{ij} = \frac{1}{2}\left(\frac{\partial u_i}{\partial x_j} + \frac{\partial u_j}{\partial x_i} \right) \tag{2}$$

The eddy viscosity coefficient μ_t, is obtained directly, based on assumption that small scales tend to be more homogeneous and isotropic than the large ones and modeling errors should not affect overall accuracy of the simulation, since the subgrid-scale stresses only account for a small fraction of the total stresses and turbulent transport. An algebraic model for eddy viscosity coefficient μ_t is approximated as follows:

$$\mu_t = \rho\left(C_S \theta \Delta^* \right)^2 \left\| \tilde{S} \right\| \tag{3}$$

where θ is a damping function, Δ^* is the filter width, C_s the Smagorinski constant and $\tilde{S} = \sqrt{2\overline{S}_{ij}\overline{S}_{ij}}$. To complete the definition of the SGS viscosity, it is necessary to specify the grid filter. For unstructured FEM meshes, there are no reliable criteria to define the width of the filter and the mesh element size Δ has been selected.

The disadvantage of Smagorinski model is that the C_S constant is problem dependent, usually varying in the range of $0.055<C_S<0.25$. Additionally, to avoid difficulties near solid boundaries the model needs special treatment: the sub-grid viscosity is forced to vanish there by applying in Eq. (3) a damping function (Eq. (4)), which narrows the filter width near the boundaries:

$$\theta = 1 - e^{(-d_b/A_b)} \tag{4}$$

where A_b is a constant (e.g. $A_b = 30$) and d_b is the "distance" from the nearest boundary, $d_b = d_e \frac{u_*}{\nu}$, with d_e – distance from the center of an element to the boundary, u_* – the shear velocity ($\sqrt{\tau_b / \rho}$), ν – kinematic viscosity.

The modified Smagorinski formula has been incorporated into mathematical description of 2-D hydrodynamic model RMA2 (Donnell et al. 2003) that was used for Szczecin Bay. The RMA2 code calculates horizontal flow-velocity components and water levels (water-surface elevations) for sub-critical, free-surface flow, implementing a finite-element solution of the Reynolds form of the Navier–Stokes equations for turbulent flows. The governing equations of the system can be given as follows:

$$\frac{\partial h}{\partial t} + h\left(\frac{\partial u}{\partial x} + \frac{\partial v}{\partial y}\right) + u\frac{\partial h}{\partial x} + v\frac{\partial h}{\partial y} = 0 \tag{5}$$

$$h\frac{\partial u}{\partial t} + hu\frac{\partial u}{\partial x} + hv\frac{\partial u}{\partial y} + gh\frac{\partial Z_w}{\partial x} + \frac{\tau_{bx}}{\rho} - \frac{\tau_{sx}}{\rho} - f \cdot v - hE_x = 0 \tag{6}$$

$$h\frac{\partial v}{\partial t} + hu\frac{\partial v}{\partial x} + hv\frac{\partial v}{\partial y} + gh\frac{\partial Z_w}{\partial y} + \frac{\tau_{by}}{\rho} - \frac{\tau_{sy}}{\rho} + f \cdot u - hE_y = 0 \tag{7}$$

with several variables given below:

$$\tau_{bx} = \rho C_b u|U|, \quad \tau_{sx} = \rho_a \zeta W^2 \cos\psi$$
$$\tau_{by} = \rho C_b v|U|, \quad \tau_{sy} = \rho_a \zeta W^2 \sin\psi$$

$$Z_w = Z_b + h, \quad C_b = \frac{gn^2}{h^{1/3}}, \quad |U| = \sqrt{u^2 + v^2}, \quad f = 2h\omega\sin\varphi$$

$$E_x = \frac{1}{\rho}\left(\frac{\partial \overline{\tau_{xx}}}{\partial x} + \frac{\partial \overline{\tau_{xy}}}{\partial y}\right), \quad E_y = \frac{1}{\rho}\left(\frac{\partial \overline{\tau_{yx}}}{\partial x} + \frac{\partial \overline{\tau_{yy}}}{\partial y}\right) \tag{8}$$

where: t,x,y = time and Cartesian coordinates; u,v = depth-averaged x,y = velocities; h = local depth; Z_w = water surface elevation, $\overline{\tau_{xx}}, \overline{\tau_{yy}}, \overline{\tau_{xy}}$ = components of the turbulent stress, τ_{sx}, τ_{sy} = components of wind stress at the free surface, τ_{bx}, τ_{by} = friction stresses at the bottom of water column, ρ = water density, ρ_a = air density, n = Manning's roughness coefficient, ς = wind drag coefficient, W = wind speed at 10 m above sea level, f = Coriolis parameter with φ as local latitude and ω as rate of earth's angular rotation, E_x, E_y = horizontal eddy viscosities.

Neither bed roughness nor turbulent exchange can be measured directly in the field, but they can be inferred from measurements of flow, water level, and velocity. Different zones have been defined in the Szczecin Bay to make possible different distribution of modeling parameters – bed roughness and turbulent exchange coefficients.

At first approximation, eddy viscosities were assigned directly to elements in material zones, but greater consistency and flexibility is obtained within RMA2 by assigning eddy viscosities to elements on the basis of the Peclet formula, in which the Peclet number P_e is inversely related to the eddy viscosity as:

$$E_{xx} = \frac{\rho u \Delta x}{P_e}, \quad E_{yy} = \frac{\rho v \Delta y}{P_e}, \quad E_{xy} = \frac{\rho u^2 s_V \Delta x^2 s_D}{P_e}, \quad E_{yx} = \frac{\rho v^2 s_V \Delta y^2 s_D}{P_e} \tag{9}$$

where: $s_V = 1/|u+v|$, $s_D = 1/(\Delta x + \Delta y)$, Δx, Δy – size of an element along X,Y axes.

The horizontal eddy viscosities given in general shape by Eq. (8) are now expressed in terms of mean flow quantities:

$$E_x = \frac{E_{xx}}{\rho}\frac{\partial^2 u}{\partial x^2} + \frac{E_{xy}}{\rho}\frac{\partial^2 u}{\partial y^2}, \quad E_y = \frac{E_{yx}}{\rho}\frac{\partial^2 v}{\partial x^2} + \frac{E_{yy}}{\rho}\frac{\partial^2 v}{\partial y^2} \tag{10}$$

The Peclet method allows for automatic real time adjustment of eddy viscosity based upon the computed averaged velocity field and individual size of each finite element.

In the second stage of computations for flow in Szczecin Bay, the eddy viscosities have been based on a parameterization of the Smagorinski method that also provides real time adjustments of eddy viscosities based on simulated velocities. Taking into account results given by Eqs. (1)-(4) and isotropy of the Smagorinski model, the horizontal eddy viscosities from Eq. (8) are now expressed as:

$$E_x = T\nabla^2 u, \quad E_y = T\nabla^2 v \tag{11}$$

where (for a finite cell of area A_e) the factor T is given from Smagorinski model as:

$$T = C_s A_e \sqrt{\left(\frac{\partial u}{\partial x}\right)^2 + 2\left(\frac{\partial u}{\partial y} + \frac{\partial v}{\partial x}\right) + \left(\frac{\partial v}{\partial y}\right)^2} \tag{12}$$

The strength of this method over the Peclet method is that it takes into account the gradients of velocity to determine the appropriate turbulence coefficient to meet conditions in the hydrodynamic simulation. A Smagorinski turbulence approach locally increases the fluid viscosity in regions where unresolved flow features are detected, in order to model the energy dissipation of small-scale vortices. There is certain controversy concerning application of this model on anisotropic computational meshes, but here the issue has been omitted from consideration.

3. Results of simulations

A special version of the hydrodynamic model of Szczecin Bay was developed specifically for investigation of hydrodynamic and transport phenomena near the Szczecin-Świnoujście watercourse. The Surface water Modeling System (SMS) was applied to create FEM network of Szczecin Bay including the Szczecin-Świnoujście waterway, and for post processing and displaying hydrodynamic simulation (Ewertowski 2006). Two cases were simulated in steady flow regime: the outflow from Odra river and the inflow of seawater through Piana, Świna and Dziwna straits. Wind activity has been excluded from simulation. For each case the hydrodynamic parameters have been calculated for both turbulence closure methods. Results of dynamic assignment of eddy viscosity by both methods are shown in following figures. First, Fig. 1 shows eddy viscosity field obtained from Peclet method.

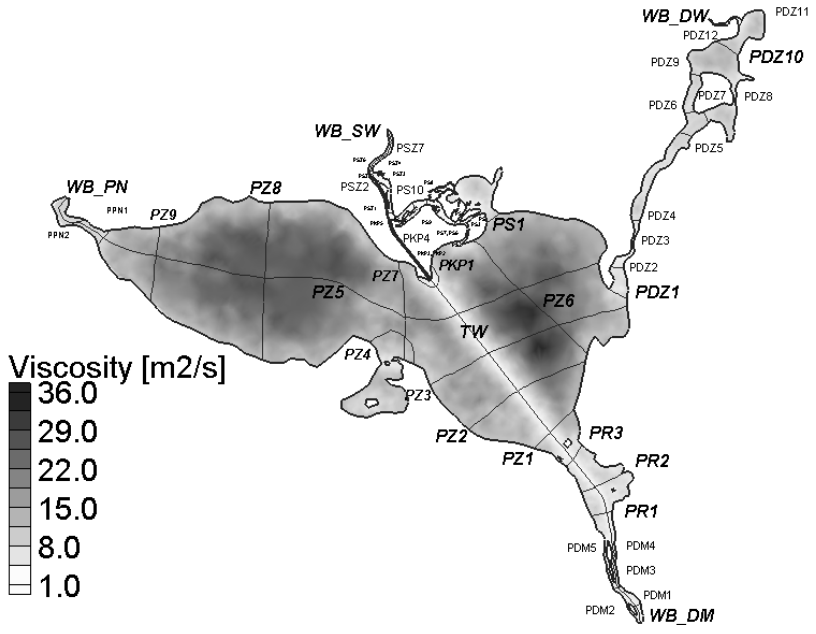

Fig. 1. Distribution of eddy viscosity from Peclet method and CGS lines.

In Fig. 1 the Continuity Lines (CGS) are marked. Along these lines one can obtain longitudinal profiles of given quantity and check the continuity of mass, flow and momentum for given solution. The next picture, Fig. 2, presents the eddy viscosity (EV) field produced by the Smagorinski method, applied for the whole Szczecin Bay.

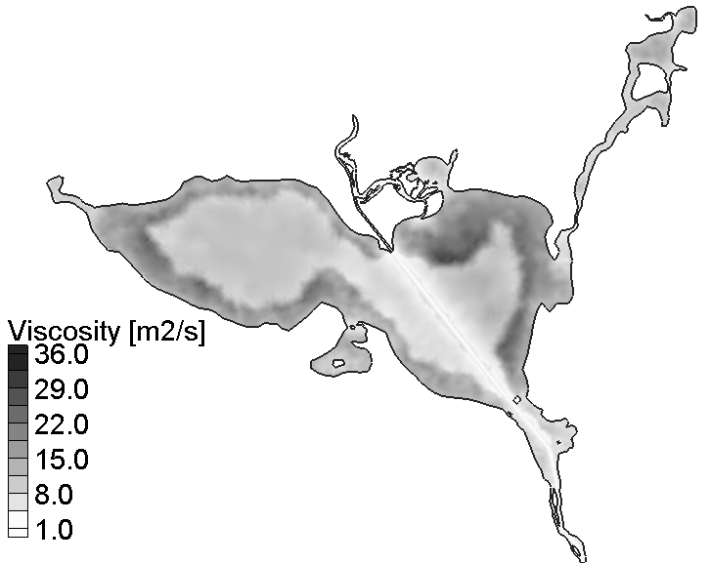

Fig. 2. Distribution of eddy viscosity from Smagorinski method.

Velocity fields presented in Fig. 3 have been calculated for two cases: on the left – for outflow of Odra River flow into the Baltic Sea, and, on the right – for inflow of water from the Baltic into Szczecin Bay. This is an enlarged part of HD solution concerning the vicinity of First Waterway Gate near the entrance of Piastowski Channel.

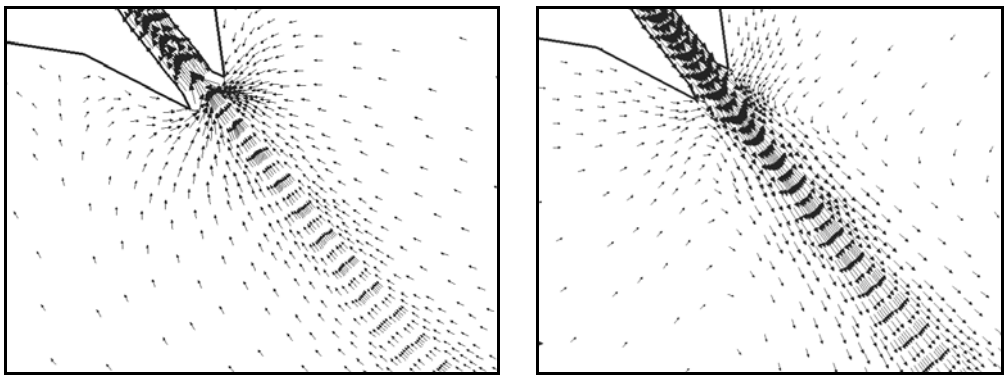

Fig. 3. Flow velocity fields (Smagorinski case) at entrance for outflow (left) and inflow (right).

The situation depicted in Fig. 4 for the same area results from using the mixed approach (Peclet + Smagorinski). Here Smagorinski model has been used for the Waterway area while the Peclet method for material zones bounding the underwater channel.

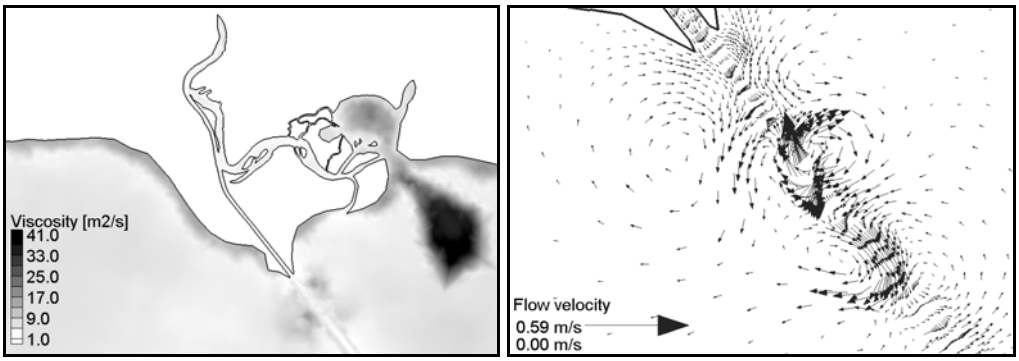

Fig. 4. Mixed mode of EV assignment and flow velocity field at entrance to Szczecin Bay.

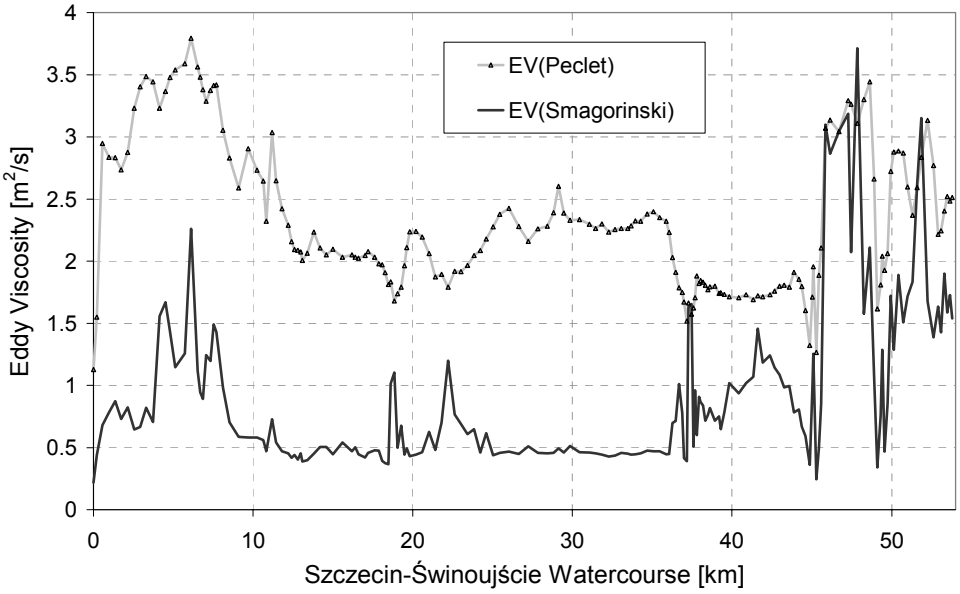

Fig. 5. Comparison of Peclet and Smagorinski EV assignments along Szczecin-Świnoujście Watercourse.

Results of simulation (EV fields, velocity magnitude, etc.) can be compared along all continuity lines (Fig.1). An example of such comparison (and significant for all further analysis) is the profile of EV along the Waterway (*TW* CGS), given in Fig. 5.

4. Discussion and conclusions

Szczecin Bay system is characterized by high flow velocities in narrow channels and straits (which may exceed 1.5 m/s), and very low flow velocities on open flat areas. These flow conditions give rise to large secondary re-circulation patterns. Both methods of turbulence closure have been carefully tested using several sets of parameters (Peclet numbers and C_s coefficients). The goal of the process was to achieve consistent and stable solutions for possible small effective eddy viscosity. Flow simulation results from Peclet method indicate that depth-averaged velocities simply parallel the curvature in the basin shoreline. In contrast, using Smagorinski model, one can obtain flow patterns accounting for complex flow structures or significant velocity variations. Longitudinal profiles of EV along Szczecin-Świnoujście Watercourse obtained by both methods (Fig. 5) differ significantly from each other, despite that velocity magnitudes along the same route are very similar. This indicates the tendency that EV calculated by Smagorinski model is much more independent of the size of element compared to Peclet method. This is especially visible when comparing EV distribution in flat areas of Szczecin Bay (Figs. 1-2). For Peclet method, EV is much higher there.

Introducing the Smagorinski model for Szczecin Bay has been done step by step for consecutive material zones. Although parameter estimation converged while simultaneously estimating the Manning's *n* coefficients and the Smagorinski-related parameters, numerical instabilities arose in the transfer of these parameters to the next material zone. Thus an iterative procedure has been implemented for achieving completely stable solution for all material zones.

The strength of the Smagorinski approach is that the model can be applied to only the smallest of the resolved scales. This results in better performance of this method, as it mimics the physics of water turbulence better than Peclet method. On the other site, the mixed approach of estimating EV by Smagorinski and Peclet method gives an opportunity to obtain very complex flow velocity field in some areas of interest. For example, in the vicinity of Piastowski Channel entrance into Szczecin Bay (First Waterway Gate) the mixed method produces a region of high horizontal vorticity (Fig. 4).

References

Donnell, B.P., J.V. Letter Jr., W.H. McAnally and W.A. Thomas, 2003, *Users guide to RMA2-WES Version 4.5*, U.S. Army Corps of Engineers Waterway Experiment Station, Vicksburg, Miss., 264 p. October 14, 2003.

Ewertowski, R., 2006, *Building of optimal FEM mesh for modelling hydrodynamic and transport processes in Szczecin Bay*, IX Konf. N-T "Problemy hydrotechniki", Wrocław (Polish, in print).

Accepted September 12, 2006

PUBLS. INST. GEOPHYS. POL. ACAD. SC., E-6 (390), 2006

Truncation Errors of Selected Finite-Difference Methods for Two-Dimensional Advection-Diffusion Equation with Mixed Derivatives

Monika B. KALINOWSKA and Pawel M. ROWIŃSKI

Institute of Geophysics, Polish Academy of Sciences
ul. Księcia Janusza 64, 01-452 Warszawa, Poland
e-mails: Monika.Kalinowska@igf.edu.pl; pawelr@igf.edu.pl

Abstract

The spread of a passive contaminant in an open-channel reach is considered with use of a two-dimensional advection-diffusion equation with the off-diagonal dispersion coefficients included. This paper presents the calculation of truncation errors, namely numerical diffusion and numerical dispersion for various finite-difference schemes. The accuracy of the considered finite-difference approximations is analysed by deriving and studying the relevant modified partial differential equation.

Key words: truncation error, numerical diffusion, numerical dispersion, Modified Equation approach, advection-diffusion equation.

Full text was published in *Acta Geophysica*, Vol. 55, No. 1, p. 104-118.

PUBLS. INST. GEOPHYS. POL. ACAD. SC., E-6(390), 2006

Estimation of Probability of Flooding in Warsaw

Adam Kiczko[a], Marzena Osuch[a] and Renata Romanowicz[b]
[a] Institute of Geophysics, Polish Academy of Sciences, Poland
[b] IENS, Lancaster University, Lancaster, UK

Abstract

This paper presents a flood risk analysis of the Warsaw reach of the Vistula river (Poland). We argue that any model of urban area has to be evaluated and calibrated using local performance as well as global measures.

In this particular flooding estimation problem, the main challenge lies in the very limited amount of available calibration data. This was overcome by an extensive survey of the river channel and floodplains geometry and application of a model with a simplified flow dynamics description, corresponding to the scarcity of data.

Calibration of the model is based on observed water levels during the flood event in July 1997. Simulations are performed for 10 different events with a specified value of probability of reoccurrence (including uncertainties) estimated by the Institute of Meteorology and Water Management in Warsaw. By combining information about model uncertainties and event occurrence probabilities, it was possible to produce a spatially distributed uncertainty of prediction of water levels along the river reach.

1 Introduction

In this paper we outline a methodology for assessment of risk from flooding for urban areas and, in particular, estimation of probability of inundation along the Warsaw reach of the Vistula River. Risk is defined here as the probability of flooding in certain areas multiplied by the cost of the possible damage due to flooding. Urban areas are characterised by a large variability in the costs of flooding. Thus it is necessary to estimate the spatial distribution of probabilities of flooding along the river reach. For example, infrastructure or buildings will show more damage than green areas along the river banks. This indicates the necessity for assessing risk on a local rather than global scale.

All flood protection measures should be related to an analysis of flood cost, which combines the estimate flood inundation probability field with an economic losses model. There are different possible approaches to the problem of the estimation of probability of flooding and the cost evaluation. One approach, presented by Dutta et al. (2003), consists in the application of a deterministic hydrologic basin model combined with a unit flood loss model.

We present here a stochastic methodology to the evaluation of river overflow risk, as a primary element of risk assessment, with a special focus on the significance of a local approach. In order to estimate the risk from flooding, we derive a probability from flooding which in turn requires application of a distributed flood routing model. As the process of flooding is non-linear, the model structure should reflect this nonlinearity. In this work we have used the 1D flood model with simplified dynamics. Model calibration and proper uncertainty analysis were performed following the Generalised Likelihood Uncertainty Estimation (GLUE) methodology introduced by Beven and Binley (1992).

2 Approach and methods

2.1 The GLUE methodology

The basic assumption of the GLUE methodology [Beven and Binley (1992)] is that in the case of over-parameterized environmental models a unique solution of the inverse problem is not possible to achieve because of the lack of data. There can be many different parameter sets which provide reasonable results. Therefore, calibration should consist of the estimation of the multidimensional distribution of model parameters. For such analysis, the Bayesian formula is used:

$$f(\theta \backslash z) = \frac{f(\theta) L(z \backslash \theta)}{L(z)} \tag{1}$$

where z is the observation vector, $f(\theta \backslash z)$ is the posterior distribution (probability density) of the parameters conditioned on the data, $f(\theta)$ is the prior probability density of the parameters, $L(z)$ is scaling factor and $L(z \backslash \theta)$ represents the likelihood measure based on the theoretical information on the relationship of z and θ. On the basis of information on the prior distribution of model parameters, which comes from the knowledge of physical structure of the modelled process, it is possible to estimate the posterior distribution of parameters. Assuming that the prior distribution of model parameters is related to an uncertainty introduced to the model, the posterior distribution will provide information on the uncertainty of the model results.

It is important to note that as equation (1) is defined over the specified parameter space, parameter interaction will be implicitly reflected in the calculated posterior distribution. This feature is especially important in the case of spatially distributed models, where parameters are very interdependent. The marginal distributions for single parameter groups can be calculated by an integration of the posterior distribution over the rest of the parameters as necessary.

The essential element of the GLUE is a practical determination of the likelihood measure $L(z \backslash \theta)$. In this paper it was assumed that it is proportional to the Gaussian distribution

function:

$$L(z\backslash\theta) \approx e^{(z-z_{sim}(\theta))^2/\delta^2}, \tag{2}$$

where z is the water level from observations, z_{sim} is a computed water level and δ^2, as the mean error variance, determines the range of distribution function. It is important to note that in the GLUE methodology a subjective control of the distribution width is allowed. On the basis of posterior likelihood values, the distribution of simulated water levels can be evaluated and subsequently used to derive spatial probability maps of risk of flooding in the area.

The model parameters space is sampled using the Monte Carlo method. It is important to note that the prior distribution ($f(\theta)$) of parameters is introduced at this stage of processing. It takes the form of the probability function used in the number generator and sampling ranges. A number of model realizations that have to be taken depend on the unimodality of the resulting distribution.

2.2 Application: Warsaw reach of the Vistula river

2.2.1 Study area

The 36 km long Warsaw reach of the Vistula river starts from the Nadwilanowka river gauge and ends before the Vistula's tributary Narew. Due to its glacial past, the upper part of this reach forms the so called "Warsaw corset", where river width decreases rapidly from 7500 m at 507 km to 600 m in Warsaw (514- 516 km). The mean annual discharge at the Nadwilanówka gauge is 573 m^3s^{-1}. This part of the river valley is highly urbanized and embankment systems are situated on both river banks along the whole reach length. The floodplains consist mainly of a diversified vegetation cover and only small parts of the left bank are protected with solid cement constructions. From the flood protection point of view, the tree rich habitats which exist along the whole right bank possibly play an important role – this is seen especially in the variation of roughness coefficients.

Low flows are regulated by a system of replying spurs, which also contributes to an increase of water levels during freshets. The character of flood-endangered city areas is diversified along the river reach. Generally, upstream parts of the reach are densely populated and downstream parts consist of a dispersed development; however each part differs significantly. On the right bank large housing complexes exist in the direct neighbourhood of embankments and such areas are considered as especially endangered.

There were just a few works published on flood modelling of the Warsaw reach of Vistula. Kuźniar (1997) estimates water surface levels for 500-year flood event and compares it with historical observations [Kuźniar (1997)]. Hydroprojekt Warszawa developed a complex program of flood prevention for the middle Vistula, in which a 1D steady-state flow model was used to assess flood inundation zones [Hydroprojekt (1999)]. Nowadays

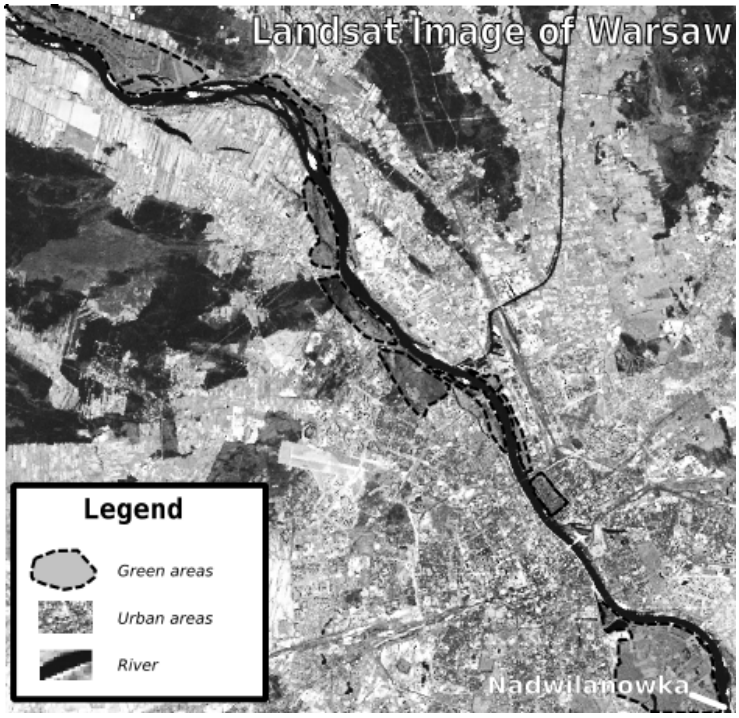

Fig 1: Landsat image of Warsaw with marked urban and green areas *(landsat.usgs.gov)*

this assessment is used in the majority of administration proceedings. Both approaches are deterministic, so the estimated flood risk zones do not reflect the uncertainty of the model parameters and its boundary conditions [(Romanowicz et al., 1996, Romanowicz and Beven, 2003)].

2.2.2 Flood routing methods

The coarse element flood inundation model developed by Romanowicz et al. (1996), was chosen for the purpose of this research. Its formulation is similar to the quasi-two-dimensional model of Cunge (1975). According to this concept, a river valley can be seen as a system of interconnected storage cells and it is assumed that there is a unique relationship between the storage of each cell and the water surface level, as well as the cross-section/water level and hydraulic radius/water level relations at the boundaries of each cell. These functions can be derived from river and floodplain geometric data in the form of look-up tables. Assuming that the flow builds up slowly on the floodplains

and hence storage and resistance terms are more important than inertial and acceleration terms in the flow equation, it is possible to describe water exchange between neighbour cells on the basis of these geometric functions applying the Manning-Strickler resistance laws. Whilst in more common flood routing models a geometric representation of the channel and the floodplain is scoped to the cross-sections, this model may incorporate more accurate spatial information about the river and floodplain geometry in the form of the storage-water level functions.

In its original version, this model gives a quasi-2D description of the flow routing process. The river is usually divided into three types of storage cells, representing different active zones: main channel, and left and right floodplains. In the present research only the flow between embankments was considered and there was no need to use such a detailed description. Therefore, a 1D version of the model based only on the cells responsible for the main channel was applied. In result of this simplification, an increased model computational performance was achieved. In this form, the model was implemented in the Matlab Simulink iconographic language.

2.2.3 Data

TIN DTM from aerial imaging and about 78 channel cross- sections constitute the basis for the representation of the river valley topography. Measurements of the channel were carried out by Wierzbicki et al. (1999). They provide very useful information for this research. The DTM on a regular grid of 20x20 [m] resolution was prepared in order to integrate the elevation data. The evaluation of model functions from elevation data of this type gives similar advantages to using a finite element model, because it is possible to include spatial diversification not only at a cross-section, but also between cross-section.

Model cells were assigned according to the location of the 78 cross-sections, which gave 77 sub-reaches. For each model cell it was necessary to evaluate the relationship between the hydraulic radius/water level and area/water level values at the closing cross-section and cell storage functions in the form of water level/volume relation. All geometric functions were written in the form of look-up tables.

The upstream end of the river reach was placed at the Nadwilanówka river gauge. This enabled the use of water level observations from this station as the upper boundary condition. It was important because it was the only cross-section in the whole reach where a discharge rating curve was available. Additionally, estimates of the probability of occurrence of flood discharges are available for this river gauge. In this study, the discharge values of probability of exceedence of 0.001 - 9960 m^3s^{-1} estimated by IMGW (2001, 40 year observation period 1921-1960), and 0.01 - 6786 m^3s^{-1} estimated by Wierzbicki (2001, 50 year observation period 1948-1997), were used.

The water surface elevation profile of the flood event of July 1997 was used for model calibration. These data themself provide a very good representation of the river system during flood events. The only important problem was that there was no unique estimate of the maximum discharge available. In 1997, IMGW estimated it as 5150 m^3s^{-1} but this value seemed to be exaggerated. Later, in 2001 Wierzbicki estimated it for just 4300 m^3s^{-1}. In this work, inflow discharges (the upper boundary condition) were considered as one source of the model uncertainty. The water surface elevation profile of the flood event of July 1934, corresponding to an estimated discharge of 5348 m^3s^{-1}, was also available. This profile refers to the 10 km river reach, from the Nadwilanówka gauge (504) to the Poniatowski Bridge. These data were used for model verification. A map of the area is shown in Fig. 1.

3 Results

Model calibration is the most important stage of the flood risk assessment. It was assumed that uncertainty introduced to the model by elevation data was much less important than uncertainty related to the estimation of roughness parameters and boundary conditions. Therefore, Monte Carlo simulations were made for two kinds of parameters. The first ones were roughness parameters at storage cells and the second one was the downstream boundary condition in the form of the water slope at the end of the river reach.

Because there was no a priori information on the parameter distribution, a uniform prior distribution was assumed [Beven (2001)]. After an initial sensitivity analysis of the model performance using different parameters sets, the following parameter ranges were chosen for the MC simulations using uniform priors: Manning roughness coefficients $0.02 - 0.16$ and water slope: $1.3192 * 10^{-4} - 8.7950 * 10^{-4}$. Wide range of roughness coefficients, which exceeds values normally observed in a river, is justified by the need of including uncertainty in other inputs like the channel geometry.

The first factor is particularly important for setting ranges of roughness parameters, as unreliable roughness values may provide unjustified model results under a different set of boundary conditions. Because the number of Monte Carlo simulations was restricted to 1000 for the sake of computation time, the parameter range had to be kept as small as possible while including the expected best values. The choice of these parameter range limits was based on the results of the preliminary exploration of the shape of the likelihood response surface and the results of sensitivity analysis.

Initial Monte Carlo runs were performed for freshet flow conditions corresponding to observations from 1997. Following the GLUE methodology, posterior likelihood values for each model run were evaluated based on the errors between the observed and simulated water levels at each cross-section. These likelihood values were used to estimate the posterior distribution of parameters used in further simulations. Main model runs were made

for 10 hypothetical flow events of known probability of occurrence.

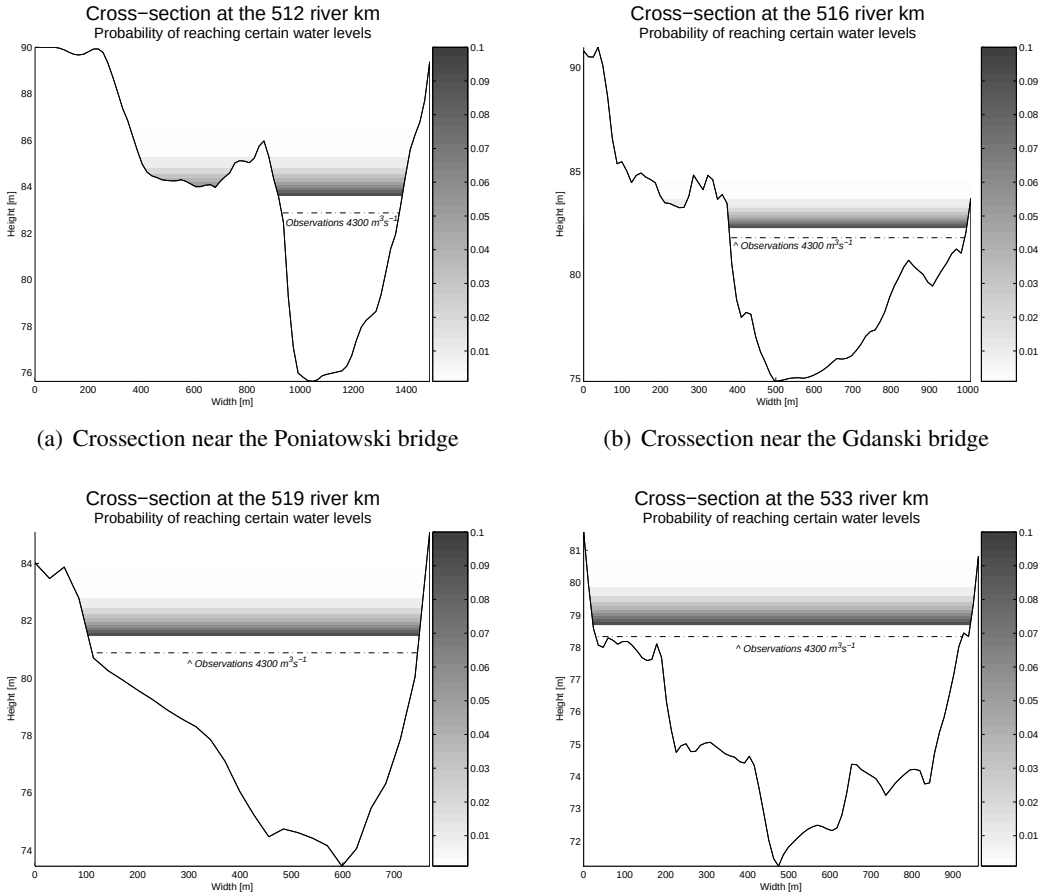

(a) Crossection near the Poniatowski bridge

(b) Crossection near the Gdanski bridge

(c) Crossection near the Grota-Roweckiego bridge

(d) Crossection near Łomianki

Fig 2: Probability of reaching certain water levels

Computational results for selected cross sections (at 505, 512, 519, 533 km) are shown in Figs. 2a-d. Figure 3 presents the estimated water surface profile for a 1 in 500 years event (Q=8833 m^3s^{-1}), together with 0.95 confidence bands shown as a shaded area. There are also shown embankments, the right marked by crosses and the left marked by circles.

4 Conclusions

This paper describes the derivation of flood inundation maps for the estimation of the risk from flooding in the Warsaw reach of the Vistula River, Poland. A Generalised Likeli-

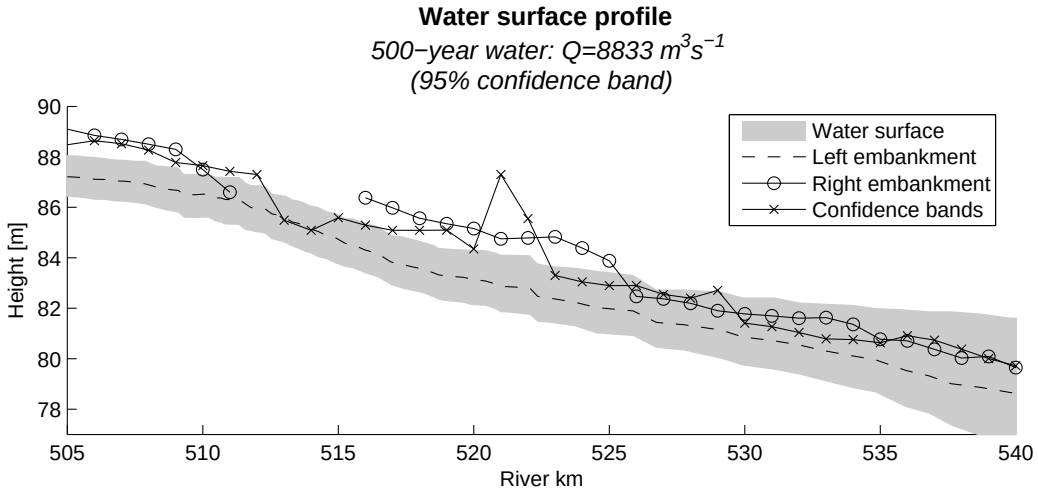

Fig 3: 500-year water surface profile, 95% confidence band

hood Uncertainty Estimation (GLUE) approach is applied together with SIMULINK based nonlinear flow routing model to derive the probability of flooding of areas along the river floodplains. The model was run for two sets of inflows, with the probability of occurrence equal to 0.001 and 0.01, respectively. The resulting longitudinal profile depicting the different probability of flooding along the river reach (Fig. 3) should be used together with the map of cost of infrastructure in the area, to build maps of risk from flooding. This can also be combined with the structural risk analysis to identify the embankment areas under the highest risk of breaching and urban area flood inundation model to develop detailed urban risk maps.

Acknowledgments

This work was supported in part by grant 2 P04D 009 29 from Ministry of Higher Education and Science.

References

Beven K. How far can we go in distributed hydrological modelling? *Hydrol. Earth Syst. Sci.*, 5(1):1–12, 2001.

Beven K. and Binley A. The future of distributed models: model calibration and uncertainty prediction. *Hydrol. Process*, 6:279–298, 1992.

Cunge J. A. Two-dimensional modelling of flood plains, in K. Mahmood & V. Yevjevich (Eds.) prediction. *Water Resources Publications*, Fort Collins, Colorado, 705–762.

Dutta D., Herath S., and Musiake K. A mathematical model for flood loss estimation. *Journal of Hydrology*, 277:24–49, 2003.

Hydroprojekt. Kompleksowy, regionalny program ochrony przeciwpowodziowej dorzecza środkowej Wisły na terenie RZGW w Warszawie. *Technical report*, 1999.

Kuźniar P. Woda 500 letnia w Warszawie w świetle materiałów historycznych i symulacji komputerowych. *Forum Naukowo-techniczne*, 1997.

Romanowicz R. and Beven K. Estimation of flood inundation probabilities as conditioned on event inundation maps. *Water Resources Research*, 39(3), 2003.

Romanowicz R. and Tawn K. B. J. Bayesian calibration of flood inundation models. *Floodplain Processes*, pages 336–360, 1996.

Wierzbicki J. Stałość pionowego układu i morfologii koryta oraz zwierciadła wód Wisły warszawskiej na odcinku położonym pomiędzy ujściem rz. Pilicy a ujściem rz. Narwi - stan 1998. *Technical report*, Politechnika Warszawska, Warszawa, 1999.

PUBLS. INST. GEOPHYS. POL. ACAD. SC., E-6 (390), 2006

Numerical Model of Selected Types of Submerged Overfalls

Apoloniusz KODURA and Piotr KUŹNIAR

Faculty of Environmental Engineering, Warsaw University of Technology
20 Nowowiejska St., 00-653 Warsaw, Poland
emails: apoloniusz.kodura@is.pw.edu.pl; piotr.kuzniar@is.pw.edu.pl

Abstract

The study presents the results of hydraulic overfall calculations regarding selected weirs. Calculations were carried out with traditional formulas using appropriate discharge coefficients. Then, they were compared with the results of numerical calculations regarding the same devices, treated as a special kind of cross section with an appropriately selected Manning's roughness coefficient. The analysis presented regards overfalls in the submersion conditions, which allows for calculation of non-uniform motion in subcritical flow conditions. Possibility of simplifying the structure of the numerical overfall model presented in the study by means of maintaining the continuity of the algorithm is of significant importance while carrying out hydraulic calculations of a developed flow section.

1. Introduction

Modelling hydraulic flow conditions in natural water-courses, containing weirs, requires introduction – into the calculation algorithm – of formulas describing dependence of the discharge on the filling. These are usually different from typical riverbed water motion equations, which disturbs and complicates functioning of the mathematical model of the entire section.

In many cases of practical submerged overfall calculations, correct results may be obtained, treated as a 'multi-arm' riverbed cross-section (the number of 'arms' corresponds with the number of spans of the weir modelled) of appropriately selected roughness coefficient. In the case of modelling of hydraulic operating conditions of existing objects, the value of the resistance coefficient may be obtained by tarring the model based on the results of water surface system levelling (Kuźniar 1996). Such an attitude allows for application of a typical hydrodynamic type of discontinuities.

The following three characteristic cases of practical calculations of weir discharges have been brought down to comparing the course of top station consumption course – calculated with formulas appropriate for a given type of overfall and water motion in open riverbeds generated with the hydrodynamic model.

2. Characteristics of calculation cases

Calculation cases presented in this study have been derived from designs of Polish hydrotechnical objects in the last few years. Selection of analysed overfalls has not been accidental. Each object serves a different purpose, has different geometric parameters and operates in different hydrological conditions.

Reservoir 'Kuźnica Warężyńska' lies in the basin of Czarna Przemsza. Its primary aim is the flood protection. It was developed with the use of the excavation bowl of a former sand mine. The outlet weir analysed herein is a three-span structure provided with flap seals 3 metres wide each (Fig. 1a). It is used to control the overfall intensity carried away from the reservoir (Matyńka et al. 2003).

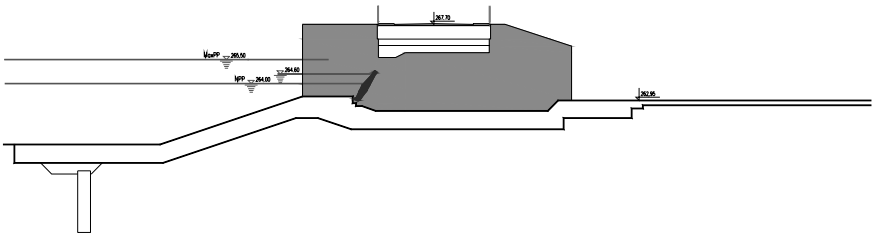

Fig. 1a. Weir 'Kuźnica Warężyńska' characteristic cross-section.

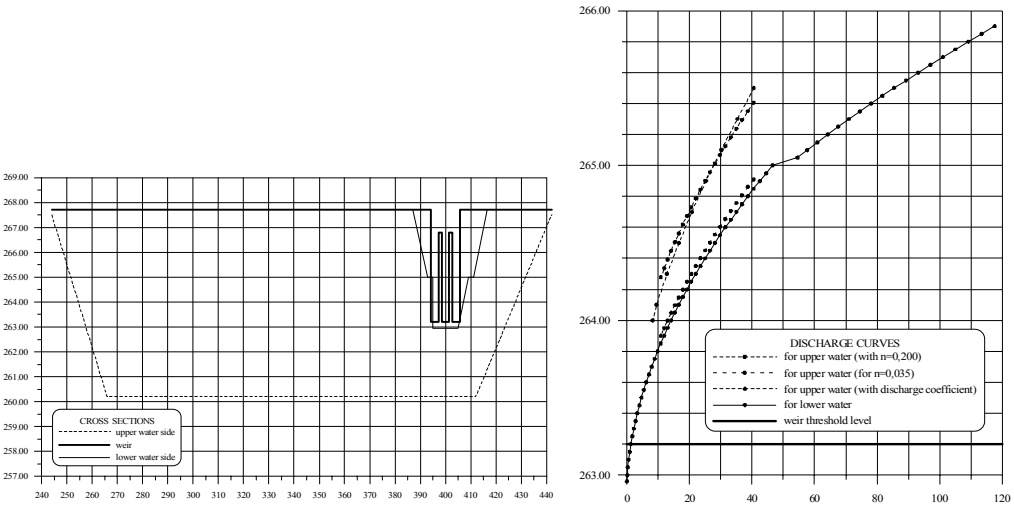

Fig. 1b. Scheme of calculation the cross-sections and results of calculations for object 'Kuźnica Warężyńska'.

Weir ‘Bukówka’, located on river Bóbr, belongs to hydrotechnical system ‘Krzywaniec-Dychów-Raduszec Stary’. The object is currently being modernised to improve operating conditions, by replacing 8 spans with two 37.20 metres wide each, provided with coating seals. The ‘Bukówka’ weir purpose is to maintain constant backwater at the small reservoir for energy-related purposes (Fig. 2a) (Matyńka et al. 2005).

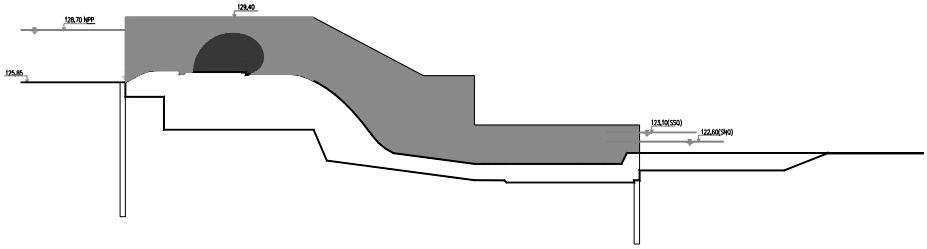

Fig. 2a. Characteristic cross-section of weir ‘Bukówka’.

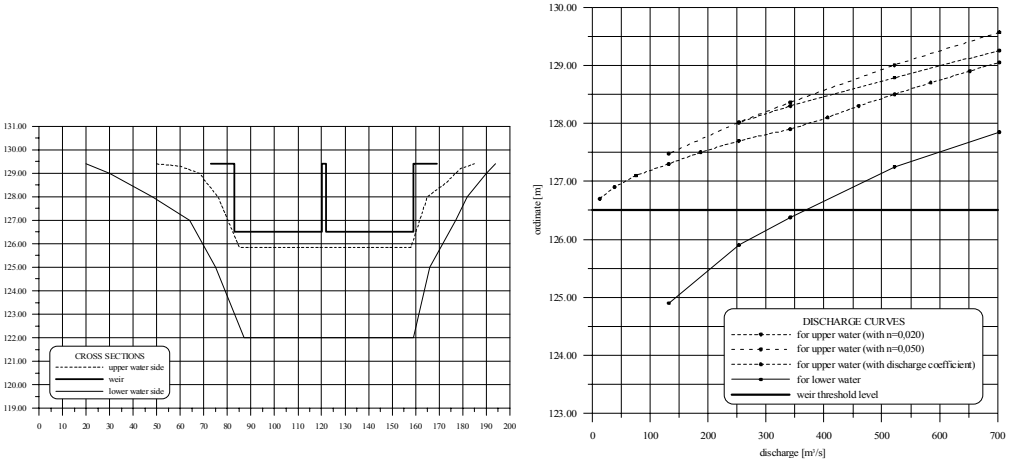

Fig. 2b. Calculation scheme of cross-sections and results of calculations for object ‘Bukówka’.

The third object considered is the designed ‘Nieszawa’ weir. Its primary function is to support the existing ‘Włocławek’ dam on the Vistula River and compensate flow deviations resulting from top and emergency operation of ‘Włocławek’ power plant. Allowing for the experience of the 30 years of operation of the ‘Włocławek’ weir, it has been deprived of the earth dam section and a sixteen-span weir and a power plant were located in the main stream section. Weir edge was designed according to the Jambor type in order to facilitate transportation of the rubble trailed. Weir spans, 20 metres wide each, have been provided with sectional seals with a flap (Fig. 3a) (Ankiersztejn et al. 2005).

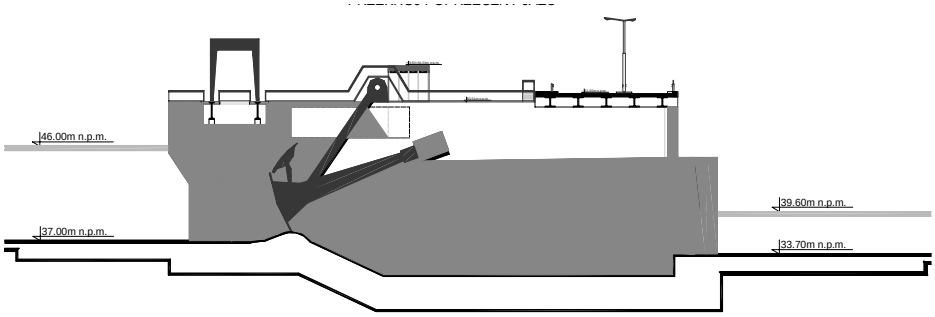

Fig. 3a. Characteristic cross-section of weir 'Nieszawa' span.

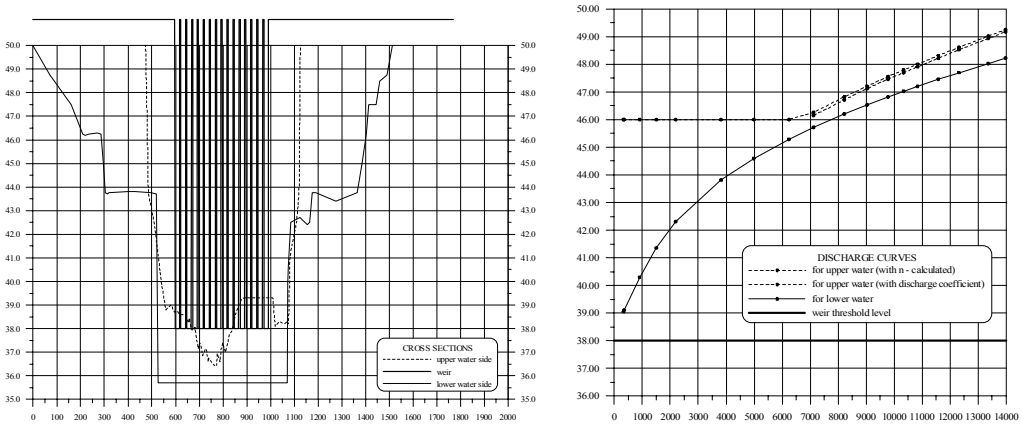

Fig. 3b. Cross-sections calculations scheme and result of calculations for the 'Nieszawa' weir.

Each of the three cases analysed represented different hydrological conditions: from wide reservoir outflow to a narrow riverbed below scheme (Kuźnica Warężyńska), scheme of comparable water levels above and below, but with different station ordinates (Bukówka) to the scheme of insignificant flow choking in the case of a wide weir with a short bar (Nieszawa).

3. Calculations based on discharge coefficient

Calculations were carried out based on traditional formulas describing the discharge of rectangular submerged overfall (Mitosek 2002):

$$Q = m \cdot \sigma \cdot b \cdot \sqrt{2 \cdot g} \cdot H_0^{3/2} \tag{1}$$

where: Q = discharge; m = discharge coefficient; σ = submersion coefficient; H_0 = overfall top ordinate and top water differences increased by velocity head.

Submersion coefficient was calculated based on the relationship:

$$\sigma = 1{,}05 \cdot \left(1 + 0{,}02 \cdot \frac{a}{p_1}\right) \cdot \sqrt[3]{\frac{z}{H}} \tag{2}$$

where: a = bottom water and overfall top ordinates difference; z = top water and bottom water ordinates differences; p_1 = overfall top and bottom below overfall ordinates difference.

Overfall discharge coefficient was calculated based on the Bazin-Hegly formula:

$$m = \left(0{,}405 + \frac{0{,}0027}{H} - 0{,}03 \cdot \frac{B-b}{B}\right) \cdot \left[1 + 0{,}55 \cdot \left(\frac{b}{B} \cdot \frac{H}{H+p}\right)^2\right] \tag{3}$$

where: B = riverbed width; b = overfall inside diameter; p = bar top and top station bottom ordinates difference.

Calculations were carried out step by step, starting with assuming zero inflow speed whose volume was added in consecutive steps.

4. Model description

To carry out calculations regarding the established water motion across the sinking devices of structures selected, a model based on motion equation in the following form was utilised:

$$\frac{Q^2}{gA}\frac{\partial(\beta / A)}{\partial x} + \frac{\partial z}{\partial x} + S_f = 0 \tag{4}$$

where: g = gravitational acceleration; x = section location on river axis; Q = discharge; z = water level ordinate; A = cross-section area; S_f = friction decrease; n = substitute resistance coefficient [s/m$^{1/3}$]; h = average depth in section; β = Boussinesque's coefficient.

Finding the solution to this equation involved iterative solution of a system of differential equations based on a 2-point scheme. Calculations were carried out in three sections: bottom station, in the weir cross-section, and at the top station. Ordinates in the remaining two sections were calculated for the motion conditions set by the flow value and water level ordinate at the bottom station. In the first approximation, the most frequently occurring value of resistance coefficient of n = 0.035 s/m$^{1/3}$ was applied. Water level ordinate values at the top station were compared with appropriate results of hydraulic calculations regarding the overfall discharge.

5. Results

Weir ‘Kuźnica Warężyńska’ calculation results have been shown in Fig. 1b. In the first calculation series, carried out for the substitute weir resistance coefficient of $n = 0.035$ s/m$^{1/3}$, the top station consumption curve was slightly over the bottom station discharge curve, whereas the average distance to the curve obtained by means of the overfall discharge calculations in the analysed flow range was approximately 0.40 m. This implied assumption of too advantageous hydraulic conditions of the modelled section operating conditions, in particular along the reservoir section of significant cross-section dimensions.

Riverbed modelling results quite compatible with the overfall calculation were only obtained for the calculation substitute resistance coefficient value of $n = 0.200$ s/m$^{1/3}$. This reflects local water overfall resistance caused by strong concentration of flow onto weir spans and choked outflow riverbed section.

Weir ‘Bukówka’ calculation results have been shown in Fig. 2b. In majority of the foreseen overfall ranges, it operates as an unsubmerged weir, which significantly reduces calculation possibilities utilising the model. Preliminary calculated consumption curve of the top station this time was above the curve obtained for the overfall, by 0.50 metre on the average. This implied overfall flow capacity greater than that of the riverbed of the same dimensions and decline resulting from calculation sections distances. The reason for the phenomenon was minor overfall submersion caused by both the significant wall height and great flow capacity of the bottom station (the outflow riverbed).

Attempts to obtain results convergent with overfall calculations with respect to the ordinates provided for in the design by reducing the substitute resistance coefficient below the value of 0.020 s/m$^{1/3}$ resulted in rushing motion.

The third analysed case was a 16-spam weir of the designed ‘Nieszawa’ dam (Fig. 3a) modelled for great overfall conditions. The weir substitute resistance coefficient value was adopted according to the Vistula River tarring conditions in the area at $n = 0.0301$ s/m$^{1/3}$. Overfall calculations results differed modelling results barely by 0.08 m on the average in the entire overfall range. This fully confirmed the thesis hereof that the hydraulic modelling of this type of object is sufficiently precise.

6. Conclusions

1. In the conditions of insignificant counteraction of the water stream flowing onto the spans of a wide weir of low bar, simplified way of presenting the weir in the riverbed, involving calculation thereof as a single, ‘multi-arm’ cross-section of the river may be applied. In particular, this condition is well-fulfilled by overfall structures while modelling great water passages.

2. In the situation of the occurrence of significant counteractions of water stream flowing onto the overfall, both lateral and bottom water, the substitute resistance coefficient required to obtain convergent results may achieve values several times greater than standard.
3. In the case of overfalls of relatively high discharge coefficients which are characterised by a high bar, a long (extended) overfall top and great flow capacity of the outflow bed, there may occur the necessity to reduce the value of the substitute resistance coefficient below the typical standard values. Still, this leads to artificial generation of rushing motion conditions and other calculation problems related thereto.

References

Ankiersztejn, I. et al., 2005, *Koncepcja Programowo-Przestrzenna – Część II, Budowa stopnia wodnego w Nieszawie-Ciechocinku*, Hydroprojekt Sp. z o.o., Warszawa.

Kuźniar, P., 1996, *Rozkład obliczeniowych współczynników szorstkości koryta Wisły (km 356-408) w różnych warunkach przepływu*, Materiały XVI Ogólnopolskiej Szkoły Hydrauliki, IBW PAN, Gdańsk 1996.

Matyńka, T. et al., 2005, *Modernizacja obiektów piętrzących przy Zespole E.W. Dychów*, Hydroprojekt Sp. z o.o., Warszawa.

Matyńka, T. et al., 2003, *Kopalnia Piasku Kuźnica Warężyńska, Adaptacja wyrobiska na cele budowy zbiornika przeciwpowodziowego*, Hydroprojekt Sp. z o.o., Warszawa.

Mitosek, M., 2001, *Mechanika płynów w inżynierii i ochronie środowiska*, Warszawa, 387 pp.

Accepted September 12, 2006

PUBLS. INST. GEOPHYS. POL. ACAD. S.C., E-6 (390), 2006

Dam-Breach Modelling of the Staw Starzycki Embankment in Tomaszów Mazowiecki

Jerzy MACHAJSKI[1] and Dorota OLEARCZYK[2]

[1] Institute of Geotechnics and Hydrotechnics, Wrocław University of Technology
Wybrzeże Wyspiańskiego 27, 50-370 Wrocław, Poland
email: Jerzy.Machajski@pwr.wroc.pl

[2] Environmental Engineering Institute, Wrocław Agricultural University
pl. Grunwaldzki 24, 50-363 Wrocław, Poland
email: dolear@iis.ar.wroc.pl

Abstract

In the paper, the analysis of possible causes of embankment failure of Staw Starzycki reservoir located on the Czarna-Bielina river in Tomaszów Mazowiecki is presented. This event happened in March 2005. The hydrological conditions generating the increase of inflow to the reservoir were analysed. On the basis of geological–engineering recognition of embankment body and foundation soil in failure cross-section, the simulation of embankment washout process with determination of final breach parameters and outcome outflow hydrograph were carried out, and compared with the real state. A summary pointing out the direct cause of embankment failure is given.

1. Introduction

On 18 March 2005 the Staw Starzycki embankment failure in Tomaszów Mazowiecki took place. The day before failure, a few people have noticed a danger of such a threat. In spite of significant increase of water levels in the Czarna-Bielina riverbed, on which the Staw Starzycki reservoir is located, all the gates of outlet works installation were still closed. It was only on the night of 17/18 March the manager of reservoir decided to open the gates, but because of their bad technical state (lack of motive efficiency) only one of the four existing gates has been opened. On 18 March, around 10 a.m., the water level increased onto the crest of embankment and the overtopping process has started. Two hours later the embankment broke. Several factors favoured the failure occurrence, from which the most significant influence had: high precipita-

tion that caused water level increase, substantial air temperature growth causing sudden snow melt, bad technical state of outlet works installation, difficult outflow as a consequence of mechanical impurities deposited on trashracks of each conduit of outlet works installation, and bad technical state of embankment. As a consequence, the embankment breach has been formed with the crest width of 25 m, the concentrated water outflow has occurred on downstream industrial area, including the transformer station.

2. Analysis of causes of Staw Starzycki embankment failure

2.1 Short characteristics of Staw Starzycki reservoir

Staw Starzycki consists of two water areas – storage reservoir and fish pond of a total area equal to 9.20 ha. Staw Starzycki was created partly by embankments and partly using natural highly elevated adjacent area. Both water areas are divided by partition embankment (Fig. 1). The main function of Staw Starzycki reservoir is the fire protection of an industrial plant situated downstream and Staw Starzycki pond was built for fish culture. The total capacity to the embankment crest is about 270000 m^3.

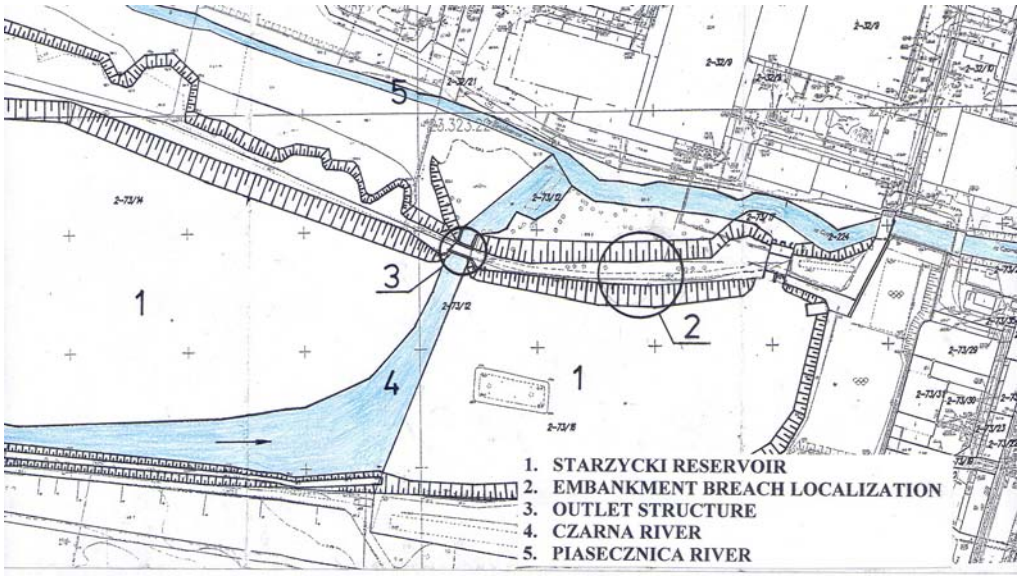

Fig. 1. Map of main objects of Starzycki reservoir.

The embankment was formed mainly with mineral soil taken from the reservoir area. The maximum height of embankment is about 3.0 m, the slope inclination ranges from 1 : 2 to 1 : 2.5, the crest width varies from 2.50 to 12.0 m. Water in

reservoir is dammed up by four inlets reinforced concrete weir, built in body embankment with wooden hand operated gates. Each of four weir inlets is 1.45 m wide and 1.89 m high. Under reservoir normal exploitation conditions the upstream water height is 1.51 m, whereas under flood freshet conditions it is 1.91 m. Characterizing the object, it has to be pointed out that it was designed, built and exploited with essential violation of requirements specified in the appropriate regulations (Regulations… 1997). The object has never been classified to hydrotechnical structures with a given class of importance. Besides, the object does not have any standard embankment elements of equipments, such as: downstream base slope drainage, upstream slope lining, drainage ditch, built-in elements of embankment body proofing and measuring-control instruments (Machajski et al. 2006).

2.2 Analysis of embankment failure causes

The analysis of embankment failure causes was carried out mainly regarding the natural factors favouring its occurrence. Because the failure was generated by inflow to the reservoir of melted water of river Czarna-Bielina catchment, firstly the hydrological conditions connected with such a situation were analysed. Simultaneously, the geotechnical conditions in the region of broken embankment were evaluated. The aims of those studies were the geological–engineering recognition of embankment body and foundation soil and the analysis of downstream slope stability, as well as the analysis of possible filtration threats. Different possible embankment failure causes were considered, such as: crest overflow, hydraulic soil base puncture and reduction of outlet works installation capacity ability. After elimination of particular possible failure causes, the simulation of embankment washout process with final breach parameters and resulting outflow hydrograph determination were carried out. The obtained results were compared with the real state.

Because a considerable area of river Czarna-Bielina catchment was covered with snow, and few days before the failure the air temperature increased causing a sudden snow melt, and additionally rain has appeared that acted as a mechanical factor enhancing the snow melting and runoff, so the authors were looking for the proper method of the maximum discharge determination that occurred in Starzycki reservoir section on the day of failure. The following methods of determination of the maximum discharge with a given probability of exceedance were considered:

- resources of snow retention,
- height of melted snow layer under the influence of rain drops heat and rainfall,
- water layer thickness raised from snow melting under the rain influence,
- melted genetic formula,
- regional relationships of maximum runoff (determined on the basis of gauging stations observations).

The most reliable results were obtained with melted genetic formula (Fal and Skorupska 1987). The maximum discharges for the Czarna-Bielina river at the reservoir cross-section are presented in Table 1.

Table 1

Maximum discharges with a given probability of exceedance for the Czarna-Bielina river at the reservoir cross-section

River	Catchment area [km^2]	Maximum discharges with a given probability p% [m^3/s]				
		1%	0.5%	0.3%	0.2%	0.1%
Czarna-Bielina	82.5	23.8	26.9	29.2	31.0	34.1

For the needs of geotechnical expert's report of the embankment failure region, four drill-holes were made to depths 5.5 ÷ 7.0 m: two holes on the embankment crest and two on the embankment slope foundation; laboratory tests of soil samples were also made (Machajski et al. 2006). Results of geotechnical studies, proved that soil foundation is built of mineral subsoil in the form of medium sand with interbedding of aggradate muds. Sand in soil base is in state from loose to medium dense which allowed to separate four geotechnical layers. The geotechnical parameters determined for them made it possible to elaborate the soil base model used for analysing the slope stability and filtration phenomena analysis in the embankment body and its foundation.

The analysis of the embankment slope stability in the place of washout was carried out for normal water level in the reservoir before flood event, for maximum water level in the reservoir during flood, for downstream slope (to fulfil the requirements of suitable regulations), as well as for unprotected upstream slope. For calculations the following embankment parameters were taken: downstream slope inclination 1 : 2.6, upstream slope inclination 1 : 2, crest embankment width of about 9 m, on the embankment crest an exploitation road of 2.50 m width at about 2 m distance from the upstream slope edge. Moreover, the following assumptions were made: the equivalent load q = 15 kPa, uniformly distributed on the whole width, exerted by truck with load, upstream slope not proofed, lack of downstream slope drainage and drainage ditch. In the embankment downstream slope calculations, the two cases of subsoil were considered:

- case I – the coherent soil layer of low load in the form of aggradate muds is present at the downstream slope base of plasticity rate of 0.45,
- case II – at downstream slope base there is only noncoherent soil in the form of medium sands with average consolidation.

The method of slope stability calculation was chosen on the basis of the analysis of computational cross-section, with the lack of determined slide surfaces. Numerical calculations for circular-cylindric slide surfaces were carried out with the help of computer programme using classical Fellenius block method that allows to obtain the safest (the lowest) estimation of stability. The results of calculations were estimated on the basis of criterions given in valid regulations. For that purpose, the coefficient of damage consequence was determined on the basis of stability index as well as real, critical, and permissible hydraulic gradients.

The stability analysis proved that for normal water level in the reservoir the downstream slope global stability fulfils the required criterions. Slightly lower stability was stated in the case of upstream slope and for local stability. For the case of flood event, the stability calculations were carried out for the maximum water level reaching the embankment crest. It was stated that both downstream and upstream slopes have sufficient global stability, so even for a water level as high as that during flood in March 2005, the reservoir embankment was stable. Due to the lack of downstream slope base drainage and drainage ditch, as a result of which the filtration curve came out on slope at the height of 0.40 m above ground level, the downstream slope in local stability conditions showed small and insufficient stability, that could create a small landslide of limited extent, but could not create the failure in the form of embankment break. After the downstream water level grew up to a height of 1.0 m above the ground level, the embankment stability state has further deteriorated. Globally, the embankment slope was stable but locally, at the downstream slope base (below the water level), the stability was not preserved.

Because the analyses described above showed that the embankment failure was caused by the water overtopping, calculations were made of the outlet works installation capacity ability. As a consequence of their unproper functioning, the water level in the reservoir reached the embankment crest. The following computational schemes were assumed (Vischer et al. 1998):

- conditions of outlet works installation normal exploitation – submerged inlet resulting from normal or maximum water level in reservoir, open outlet,
- conditions of classical free surface flow of outlet works installation – both inlet and outlet are not submerged,
- conditions of classical pressured flow of outlet works installation – both inlet and outlet are submerged; for the analysed elevation scheme of the adjacent area located downstream the structure, this situation is purely theoretical.

The results of calculations showed that independently of both the inflow and outflow conditions, and independently of computational scheme, the outlet works installation built in the embankment body will allow to pass through the calculated discharges (Machajski et al. 2006). This is especially well seen when the reservoir water level is equal to the embankment crest elevation. However, the essential requirement is that all the four gates of outlet works installation are completely open.

3. Modelling of the embankment breach

Because the calculations did not show any threat of both embankment slope stability loss and filtration, when looking for the reasons of embankment failure, only the possibility of overtopping was assumed. Such a situation could be caused by: inappropriately chosen computational discharges on the basis of which the outlet works installation was designed and the conditions of free water flow during flood were estimated; inappropriately chosen parameters of outlet works installation; the possibility of gates blocking of outlet works installation resulting in the limitation of the capacity ability. Gates blocking could be a result of mechanical impurities carried by water, neglecting of the maintenance works by servicing personnel, or damaged operation installation so there was no possibility to open the gates. Each of the above-mentioned situations causes a crest embankment overflow, resulting in its washout, which begins in the form of progressing erosion from the side of downstream slope, and relatively quickly extends to the entire embankment body cross-section (Kubrak et al. 2004).

For the needs of determination of damming water in Staw Starzycki reservoir outflow, the embankment breach modelling was caried out, on the basis of which the resulting parameters and time of final breach shape were determined. Breach parameters, the resulting outflow hydrograph, as well as the total time duration of the failure were calculated on the basis of computer simulation of washout process progression, applying computer program BOSS DAMBREACH, of the American firm BOSS International (6300 University Avenue, Madison, Wisconsin, 53562-3486 USA), that is in possession of the Institute of Geotechnics and Hydrotechnics, Wrocław University of Technology. Simulation was carried out on the basis of the adopted embankment parameters, both embankment and base soil characteristics, reservoir parameters (capacity curve) as well as on assumed catastrophic inflow to the reservoir $Q_{0,5\%} = 26.9\ m^3/s$, causing the embankment and reservoir failure by overtopping.

The embankment at the failure cross-section had the following parameters: height of about 3.0 m, upstream face slope 1 : 2, downstream face slope 1 : 2.5, unprotected dam crest width of 8.0 m, lack of elements of embankment body proofing as well as both upstream and downstream slope lining. On the basis of analysis of embankment body soil, the following parameters were taken for numerical simulation: grain size of embankment material $D_{50} = 0.50$ mm, porosity ratio 0.35, soil unit weight 15000 N/m^3, soil internal friction angle 18^o, and (because of loose soil) the cohesive strength equal to zero. For computations the reservoir volume description to the top of dam elevation was taken. Also, it was taken into account that there was a significant lowering of embankment crest at 25.0 m length in the region of existing water intake for fire protection. Calculations were carried out under the assumption of the totally blocked outlet structure.

Numerical simulation allowed to determine two significant computational values, i.e., the failure time duration and maximum outflow discharge from breach; also the resulting breach outflow hydrograph was determined (Fig. 2).

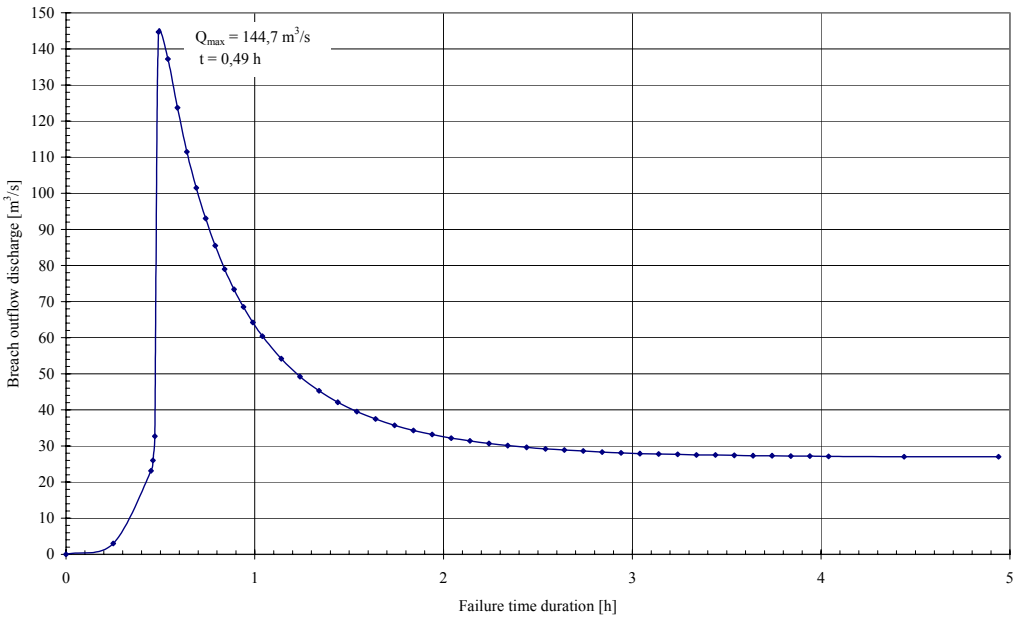

Fig. 2. Breach outflow hydrograph of Starzycki reservoir embankment.

Washout time duration from the beginning of overtopping process to the time of reservoir emptying is equal to 4.40 hour, the maximum outflow discharge through the created breach, calculated at 0.490 hour, is equal to 144.6 m^3/s. Additionally, the following breach parameters were determined: width in the bottom – 17.70 m, width in the crest – 25 m, the depth – 3.10 m, and slope inclination 1 : 1. The water outflowing from the breach together with the water from left sided tributary of the Czarna-Bielina river has inundated an adjacent industrial area with the maximum depth of 1.0 m. The results from calculations obtained from the numerical model were compared with the embankment breach parameters measured in site, and confirmed their very good consistence. This consolidated the authors' opinion that the only reason of Staw Starzycki embankment failure in Tomaszów Mazowiecki was the overtopping process.

4. Conclusions

It is difficult to determine a direct reason of failure of embankment-creating reservoir. The most probable reason may be found by eliminating, through technical analyses,

the different possible causes of such a failure. Trying to determine the failure causes of Staw Starzycki embankment in Tomaszów Mazowiecki on the basis of real situation, the authors faced some difficulties. In fact, several overlapping factors favoured the occurrence of failure. For the needs of expert's report, it is important to find the main cause. Our analysis showed that the main cause for the studied event was the overtopping – one of the most often occurring causes of dam or embankment failures, which is also pointed out in all statistical information.

References

Fal, B., and B. Skorupska, 1987, *Principles of calculation of maximum discharge with a given probability of exceedance. Melted genetic formula*, Gospodarka Wodna **5**, 124-130 (in Polish).

Kubrak, J., and M. Szydłowski, 2004, *Determination of outflow of water through breaches in dams*, Gospodarka Wodna **9**, 384-387 (in Polish).

Machajski, J., A. Batog, D. Olearczyk and O. Puła, 2006, *The causes analysis of Staw Starzycki embankment failure and flood threat in the form of Czarna and Wolbórka rivers inundation in Tomaszów Mazowiecki*, Wrocław University of Technology, Institute of Geotechnics and Hydrotechnics, Research report SPR No. 1/2006, 80 pp. (in Polish).

Regulations of Minister of Environment Protection, Natural Resources and Forestry of 20.12.1996 regarding technical conditions of hydroengineering structures and their location, 1997, Dz. U. No 17/1997, art. 111 (in Polish).

Szydłowski, M. (ed.), 2003, *Mathematical modeling of hydraulic consequences of dam failures*, Monographs of Water Management Committee of the Polish Academy of Sciences **22**, 173 pp. (in Polish).

Vischer, D.L., and W.H. Hager, 1998, *Dam Hydraulics*, John Wiley & Sons Ltd., Chichester, 360 pp.

Accepted September 12, 2006

PUBLS. INST. GEOPHYS. POL. ACAD. SC., E-6 (390), 2006

Flow in Open Channels under the Influence of Ice Cover

Wojciech MAJEWSKI

Institute of Meteorology and Water Management
ul. Podleśna 61, 01-673 Warszawa, Poland
e-mail: Wojciech_Majewski@imgw.pl

Committee of Water Resources Management,
Polish Academy of Sciences
ul. Kościerska 7, 80-328 Gdańsk, Poland;
e-mail: kgw@ibwpan.gda.pl

Abstract

During winters in Poland, lakes, ponds, rivers, channels, run-of-reservoirs, ditches and streams are covered with ice, which changes significantly the flow and thermal conditions in water bodies. The paper presents a very complicated process of ice formation on stagnant and flowing waters. Various kinds of ice are described together with their consequences for flow and thermal conditions. The possibility to define flow conditions in open channels with ice cover is described. In 1982, a significant flood on Włocławek Reservoir (Lower Vistula River) appeared, which was caused by the coincidence of unfavourable, extreme hydrological and meteorological conditions. These conditions, as well as the run and consequences of the flood, are described. Detailed field measurements of ice cover and flow were carried out. One-dimensional model for steady nonuniform flow was developed and applied to the conditions existing in 1982 on the Włocławek Reservoir.

Key words: ice formation, thermal regime, ice phenomena, ice jam flood, Włocławek Reservoir.

Full text was published in *Acta Geophysica*, Vol. 55, No. 1, p. 11-22.

PUBLS. INST. GEOPHYS. POL. ACAD. SC., E-6 (390), 2006

Bed Changes Verification of Two-Dimensional Quasi-Steady Sediment Stream Model in the Odra River

Zygmunt MEYER[1] and Adam KRUPIŃSKI[2]

Technical University of Szczecin, Department of Geotechnical Engineering,
Al. Piastów 50, 71-310 Szczecin, Poland
[1]email: meyer@ps.pl; [2]email: krupina@ps.pl

Abstract

In the present work, the authors turned special attention to bed changes in a river section below hydro-technical structures. To analyse the sediment transport, the authors used a mathematical model taking into account the two-dimensional transport. This model was constructed based upon the balance of sediment streams for an elementary volume along the river and diffusion character of the lateral sediment stream. In the paper, the authors present the verification of mathematical model for a straight section of the river. Geometry and hydraulic parameters of the river section were taken after the field measurements based on the Odra river between train and road bridges near to the town Kostrzyń.

1. Introduction

The present paper is a continuation of the research over the problem of sediment transport. In the present work, the authors pay special attention to the sediment transport and bed changes in the section of river below the bridge pillars. For the analysis of sediment transport, a mathematical model of two-dimensional sediment transport was used. The model was presented at the International School of Hydraulics in 2004 and 2005. Similar to the earlier publications, a section of the Odra river, about 350 m in length, situated between the railway bridge and the road bridge near to the town of Kostrzyń, was taken as a practical object. The verification was based upon field measurement on 05 May 2006, and the observations of the bed position were taken in April 2006. During this time, the flow changed from 300 to 500 cubic meters per second, and the bed elevation changes of about 2 meters, just below the bridge pillar, were increased to 4 meters. This situation became the basis for verifying the quasi-stable model of sediment stream.

2. Mathematical model

The mathematical model presented in the previous papers (Meyer and Krupiński 2004, 2005) was worked out for an elementary volume of the river, of dimensions *dx*, *dy* and depth *H*. For this elementary volume, the principle of balance of sediment streams was applied. On this basis, changes in the depth were defined. Taking the principle of the sediment stream balance, it was possible to describe the density changes.

The following equation of continuity of sediment stream was obtained:

$$\frac{\partial \omega_x}{\partial x} + \frac{\partial \omega_y}{\partial y} = \upsilon_x \cdot \frac{\partial \rho_r}{\partial x} \tag{1}$$

where: ω_x = total sediment stream in the *x* direction, ω_y = total sediment stream in the *y* direction (the crosswise sediment stream), υ_x = the water velocity in the *x* direction, ρ_r = depth averaged density of sediment.

The velocity of total sediment stream in Eq. (1) was calculated based upon the modified Ackers-White methods as a unit sediment stream:

$$\omega = \frac{\omega_{A-W}}{A} \quad \left[\frac{kg}{s}\frac{1}{m^2}\right] \tag{2}$$

where: $\omega_{A\text{-}W}$ = the main sediment stream (total load) based upon the Ackers-White formula, A = the area ($H \cdot dy$) for an elementary volume.

The model permitting calculation of both velocity components of water was taken as for two-dimensional steady flow and the following equations were obtained:

$$\begin{aligned} \upsilon_x \frac{\partial \upsilon_x}{\partial x} + \upsilon_y \frac{\partial \upsilon_x}{\partial y} &= D_x \frac{\partial^2 \upsilon_x}{\partial x^2} + D_y \frac{\partial^2 \upsilon_x}{\partial y^2} \\ \upsilon_x \frac{\partial \upsilon_y}{\partial x} + \upsilon_y \frac{\partial \upsilon_y}{\partial y} &= D_x \frac{\partial^2 \upsilon_y}{\partial x^2} + D_y \frac{\partial^2 \upsilon_y}{\partial y^2} \end{aligned} \tag{3}$$

where: υ_x , υ_y = the water velocity in the *x* and *y* directions and D_x, D_y = the turbulent viscosity coefficient in these directions.

In the earlier research, the authors have taken the assumption that the crosswise sediment stream has a diffusion character (Meyer and Krupiński 2005). This assumption can be written in the following form:

$$\frac{\partial \rho_r}{\partial t} + \upsilon_x \frac{\partial \rho_r}{\partial x} + \upsilon_y \frac{\partial \rho_r}{\partial y} = D_y^* \frac{\partial^2 \rho_r}{\partial y^2} \tag{4}$$

where: D^*_y = the diffusion coefficient.

For the steady flow, derivatives of density changes over time are equal to zero. Numerical simulation has shown that the value of derivatives with the lateral water velocity was considerably smaller than the derivatives with the main direction water velocity. The lateral sediment stream can be described in the following form:

$$\upsilon_x \frac{\partial \rho_r}{\partial x} = D_y^* \frac{\partial^2 \rho_r}{\partial y^2} \tag{5}$$

The above equation is a well-known formula for the diffusion phenomenon and has a closed mathematical solution.

Calculations for the assumed boundary conditions involve water velocity, the intensity of sediment stream at the main flow direction, changes of sediment density and transverse sediment streams. Then, the bed changes at each elementary volume can be written in the following form:

$$\frac{dh}{dt} = \left(\frac{\partial \omega_x}{\partial x} H \cdot dy + \frac{\partial \omega_y}{\partial y} H \cdot dx \right) \cdot \frac{1}{\rho} \tag{6}$$

where: dh = the depth changes, ρ = density of sediment.

In the earlier research the authors have taken the assumption that the changes of bed position after the sediment stream changes require 24 to 48 hours to stabilise, and that this comes from field measurements. In the present work, the calculation was made by 24 hours step. It means that the depth is changing from one step to the other according to the flow, but during each step the depth is steady. This model was called quasi-steady.

3. Calculation example

The straight section of Odra river with bed construction, about 350 m in length, between the railway bridge and the road bridge near to the Kostrzyń city, was chosen for calculations. This section of river is presented in Fig. 1. Measurements included the bed sediment composition, the river bed position and the intensity of water flow.

The method of finite differences was used for calculations of the presented equations: for the first derivatives pattern of finite differences, three-point symmetrical and the front pattern differences for second derivatives.

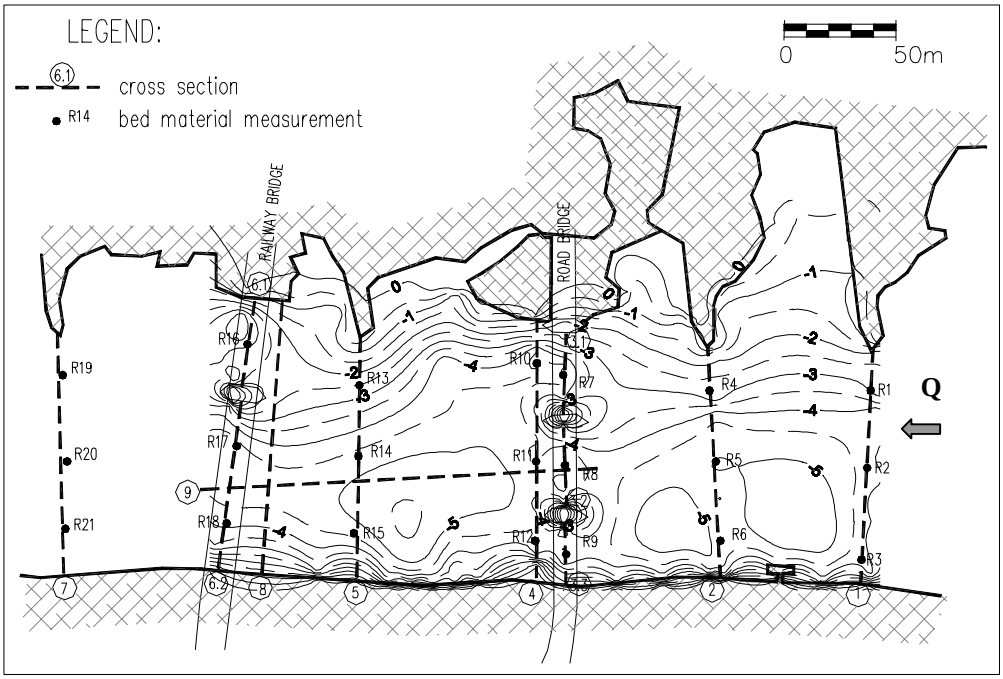

Fig. 1. Section of the Odra river map with measurement locations.

For the river section, the following initial data were taken:

- model requires the grid of nodes of about 150×300,
- the crosswise water velocity v_y at the banks and at edges of pillar are equal to zero. For $x = 0$ and $x = B$, $v_y = 0$,
- for the sediment stream calculation based upon the field measurements the representative diameter *Dz* was taken,
- in the first step of calculations, the boundary conditions were accepted from field measurements.

To define the bed level from the field measurements and the level after each step of calculations, the cross validations of the grid were made by Kriging method.

In Fig. 2 the authors present a scheme of the initial bed position, the bed position changes after 10 and 20 days, and the calculated final bed level after 30 days. A comparison to the bed position from field measurements is also presented.

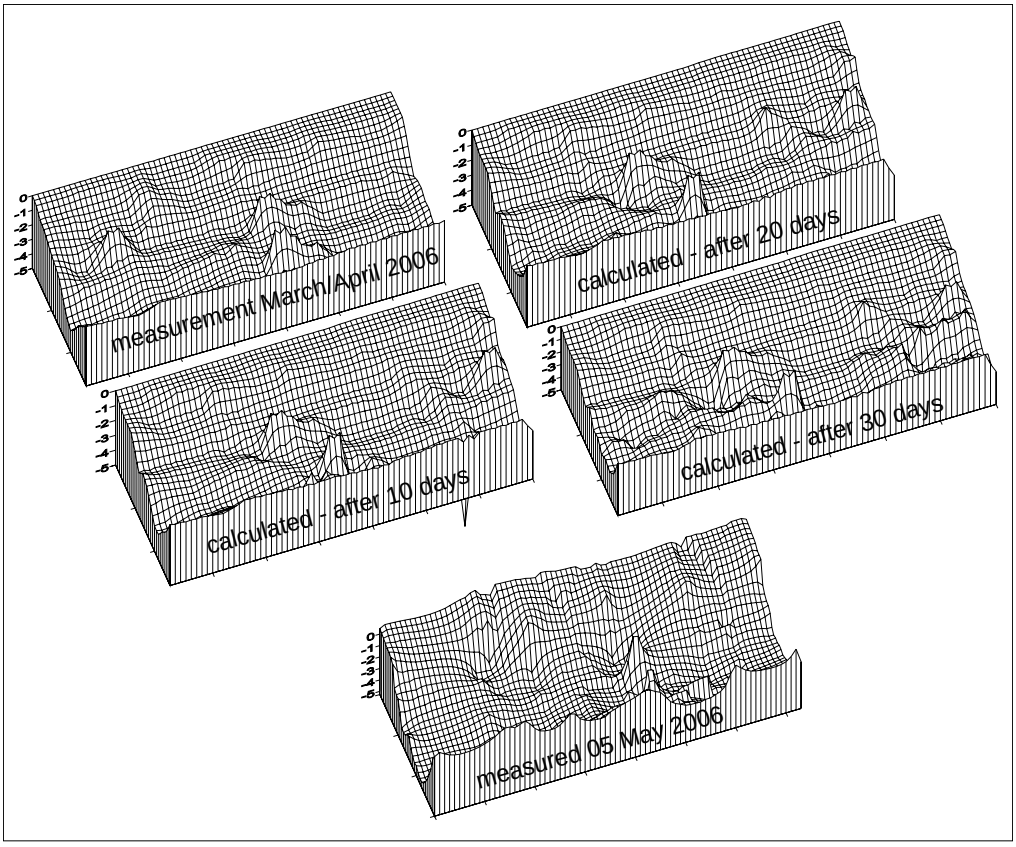

Fig. 2. Calculated and measured bed position scheme.

4. Conclusions

The paper presents the numerical quasi-steady model of two-dimensional sediment stream. As a calculation example, the result of calculation of bed position for section of the Odra river is shown.

As initial data for calculation, the bed position from observations at March/ - April 2006 was taken. For this data, the numerical calculation of bed position were made for 24-hours quasi-steady step. In the paper, the authors presented the calculated bed position after 10, 20 and, finally, 30 days. The final calculated bed position can be compared with the measurement from 05 May 2006.

The analysis of results has shown that the characteristic deepening at the end of objective section of river after 30 days agrees with measurement. The shallows from the east (upper edge of each scheme) and the shallows just behind the first bridge (railway bridge) became much deeper, and this also agrees with measurements. Ac-

cording to calculations, the bed position in the initial section tends to deepen, but some undulation appears. This difference can be compared with the initial boundary condition at the inflow in numerical calculation. As can be seen in Fig. 2, the presented model should not be used in the present form just behind the pillar. On the other hand, it gives a good agreement with field measurements in larger scale scour, as after 30 days just in the front of the second bridge. A good agreement with field measurements can also be seen from the analysis of average depth position at each cross-section. For example, at the "road bridge" cross-section, the average measured depth was 1.3 m in March and 2.1 m in May, while the calculated one was 2.0 m. An analysis of the extreme depth point at this cross-section has shown that the extreme depth measured at May was 2.9 m and calculated one was 3.1 m.

Programme of further researches:

- the analysis of numerical methods in order to choose the optimum solution,
- the analysis of the accuracy of different schemes,
- further verification of the proposed mathematical model based upon measurements on bridge area in lower Odra river.
- extension of the model for obtaining a full unsteady model.

References

Ackers, P., and W.R. White, 1975, *Sediment transport, new approach and analysis*, Journal of the Hydraulic Division ASCE **99**, No HY 11.

Meyer, Z., and A. Krupiński, 2005, *Numerical model of the lateral sediment stream in the river with bed constructions*, XXV International School of Hydraulics, 155-160.

Szymkiewicz, R., 2000, *The Mathematical Modelling of Flows in River and Open Channels*, PWN (in Polish).

Matyka, M., 2002, *Computer Simulations in Physics*, Helion (in Polish).

Accepted September 12, 2006

PUBLS. INST. GEOPHYS. POL. ACAD. SC., E-6 (390), 2006

Sub-grid Scale Parameterisation of 2D Hydrodynamic Models of Inundation in The Urban Area

Sylvain NÉELZ and Gareth PENDER

Heriot-Watt University, Riccarton, Edinburgh, EH14 4AS, UK
e-mail: s.p.f.neelz@hw.ac.uk

Abstract

This paper presents preliminary results from a study considering the parameterisation of coarse-grid 2D flood models to take into account sub-grid scale flow patterns occurring in the urban area. A simulation of a severe flood in an urbanized coastal floodplain is first run using a fine grid that can resolve the flow around and between buildings. Next, the same model is run again using the same underlying topography, although stripped from any buildings, and a set of 7 values of the roughness parameter (Manning's *n*), all larger than (or equal to) the value used in the original run. A further set of simulations is carried out using a five-fold increased grid cell size. It is found that while it may be possible to model the overall effects of the buildings using strongly increased roughness parameter values, using a coarse grid otherwise has implications related to the loss of information about the site topography that results in flood flow routes being incorrectly modelled.

Key words: urban flood modelling, roughness parameterisation, 2D hydrodynamic models.

Full text was published in *Acta Geophysica*, Vol. 55, No. 1, p. 65-72.

PUBLS. INST. GEOPHYS. POL. ACAD. SC., E-6 (390), 2006

Hydrodynamics of Aquatic Ecosystems: Spatial-Averaging Perspective

Vladimir NIKORA

Engineering Department, University of Aberdeen, King's College, Scotland, UK
e-mail: v.nikora@abdn.ac.uk

Abstract

Hydrodynamics of aquatic ecosystems is a relatively new, emerging multidisciplinary research area dealing with two key inter-connected issues: (i) physical interactions between flow and organisms (e.g., due to drag forces); and (ii) ecologically relevant mass-transfer-uptake processes (e.g., due to molecular and turbulent diffusion). Owing to physical and biological complexity of boundary conditions in aquatic systems, the conventional hydraulic methodologies are often impracticable and new approaches are required. One of such approaches, the double-averaging methodology, is discussed with particular focus on flows over biologically-modi-fied beds.

Key words: ecosystems, flow-biota interactions, rough-bed flows, mass-transfer, periphyton.

Full text was published in *Acta Geophysica*, Vol. 55, No. 1, p. 3-10.

PUBLS. INST. GEOPHYS. POL. ACAD. SC., E-6 (390), 2006

Large Eddy Simulation with Solid Particles around a Cylindrical Pier

Radosław PASIOK and Andrzej POPOW

Institute of Geotechnics and Hydroengineering, Wrocław University of Technology
radoslaw.pasiok@pwr.wroc.pl

Abstract

The paper presents results of numerical study of flow around a cylindrical pier. Flow complexity with various turbulent flow objects is described: downflow at the upstream side of a pier, horseshoe vortex and vertical wake vortices. The flow model, large-eddy simulation, is formulated on the basis of Navier-Stokes equations. Finite volume method is used for discretization. Second order finite difference schemes were used for equations approximation. A discrete particle motion model was formulated for spherical mass particles. The model allows for interaction between flow and particles. The study resulted in particle trajectories around a cylindrical pier with a developed scourhole. It indicates that some of the bed particles are caught by strong jet directed towards the surface. The jet is bounded and driven by vertical wake vortices.

1. Introduction

Numerical models are presently often used for turbulent flow investigations. The paper exemplifies the use of such models to track mass particles in a vicinity of cylindrical pier. Flow observations reveal that a complex ordered flow pattern occurs even in the case of simple-geometry hydraulic structure (Graf 2002).

Models based on Reynolds averaged Navier-Stokes (RANS) equations give as a result a statistical flow field characteristics. Thus, applying them to unsteady flow objects studies is limited (Wilcox 2000). Flow objects are coherent fluid packets that temporarily move along similar trajectories. The object size, or its scale, can be very diversified. There are many other works aimed at flow structure description (Ahmed 1998, Graf 2002). In the case of cylindrical pier, the most often specified objects are: downflow at the upstream side of a pier, horseshoe vortex and vertical wake vortices. These vortices are accompanied by considerable velocity and pressure gradients.

Many authors suggest that the objects participate in bed material transport (Breusers 1991). The paper gives a brief description of large-eddy simulation (LES) formulated for the present study. Similarly to RANS, the model is based on Navier-Stokes equations. However, degrees of freedom (number of parameters involved) of exact solution are limited by variables filtering (deVilliers 2006).

To get the exact solution, all the space and time scales of the solution must be taken into account. Then, there is no need to introduce additional assumptions concerning different turbulent scales interaction, i.e., we do not need a turbulence model. This is called a direct numerical simulation (DNS). It demands great computational power as the grid must be very fine, and accurate higher order numerical schemes must be used. The computational cost of DNS is proportional to the Reynolds number cubed (Re^3).

The computational domain was discretized by finite volume method (Ferziger 1999). Second order finite difference schemes were used for equations approximation. Finally, a discrete particle motion model was formulated for spherical mass particles.

2. Turbulent flow model

The model is based on Navier-Stokes (N-S) equations for incompressible fluid:

$$\frac{\partial \mathbf{u}}{\partial t} + \nabla \cdot (\mathbf{uu}) = -\frac{1}{\rho}\nabla p + \nabla \cdot \nu \left(\nabla \mathbf{u} + \nabla \mathbf{u}^T \right) . \tag{1}$$

Equations (1) are solved only for a certain range of turbulent object scales. To maintain influence of objects not directly included in the solution, a model of their action is introduced – this is analogous to a turbulence model in RANS. RANS, however, does not give much information about the flow objects of our interest. In LES we solve directly large-scale anisotropic turbulence objects that can be represented on a computational mesh. These are called resolved objects or scales. It is assumed that the smaller objects, which cannot be represented on a mesh, are more isotropic and much easier to model. These are subgrid scale objects. The size that separates resolved and subgrid scales is called a cut-off length and should be placed sufficiently far in the inertial subrange of turbulent energy spectrum, i.e. where the energy transfer is described by the Kolmogorov law. Considering the turbulent energy spectrum, the difference between RANS and LES can be easily depicted (Fig. 1). In RANS, practically all the spectrum is modeled. In LES, by variables filtering procedure (deVilliers 2006), an exact solution for a considerable part of the spectrum is obtained. Therefore, in LES we get much more detailed flow information than in RANS. Nevertheless, it should be noted that LES comes at much bigger computational cost. The influence of unresolved subgrid scales is expressed by the subgrid model. In this work the dynamic Smagorinsky model is used (Sagaut 1998). To obtain the effect of energy

transfer between resolved and unresolved scales, an eddy-viscosity concept is formulated and it is assumed that the subgrid stress tensor τ depends on the rate of strain tensor of resolved scales.

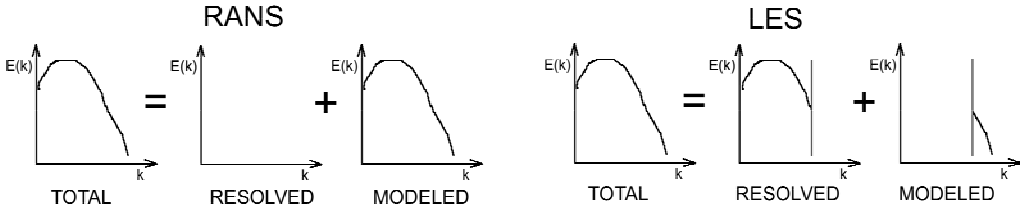

Fig. 1. Decomposition of turbulent energy spectra ($E(k)$) in RANS and LES, k is the wave number, i.e. inverse characteristic length of objects. Adopted from (Sagaut 1998).

Filtered N-S equations together with subgrid model can be written as:

$$\frac{\partial \overline{\mathbf{u}}}{\partial t} + \nabla \cdot (\overline{\mathbf{u}}\overline{\mathbf{u}}) = -\frac{1}{\rho}\nabla \overline{p} + \nabla \cdot \nu \left(\nabla \overline{\mathbf{u}} + \nabla \overline{\mathbf{u}}^T \right) + \nabla \cdot \tau \ . \tag{2}$$

The equations represent conservation law for an infinite small space-time region. To use them in finite volume method they must be integrated over the control volume and time (as LES is intrinsically unsteady):

$$\int_t^{t+\Delta t} \left[\frac{\mathrm{d}}{\mathrm{d}t} \int_V \overline{\mathbf{u}} \mathrm{d}V + \int_V \nabla \cdot (\overline{\mathbf{u}}\overline{\mathbf{u}}) \mathrm{d}V - \int_V \nabla \cdot \nu_{eff} (\nabla \overline{\mathbf{u}} + \nabla \overline{\mathbf{u}}^T) \mathrm{d}V \right] \mathrm{d}t = -\int_t^{t+\Delta t} \left[\frac{1}{\rho} \int_V \nabla \overline{p} \, \mathrm{d}V \right] \mathrm{d}t \ , \tag{3}$$

where ν_{eff} is the sum of kinematic and modeled subgrid viscosity.

Solution of the algebraic equations system for all transported quantities is obtained by iterative conjugate gradient method Bi-CGSTAB (Van der Vorst 1992). The pressure matrix is solved in PISO procedure (Issa 1986). A collocated, unstructural mesh is used.

3. Solid particle model

A discrete particle motion model is based on the equation resulting from Newton's second law. Forces acting on a particle, friction and gravity are taken into account. The friction force is computed on the basis of friction coefficient C_D in the formulation of Schiller and Nauman (Clift 1978). The equation of particle motion reads:

$$\frac{\mathrm{d}\mathbf{u}_p}{\mathrm{d}t} = -\frac{\mathbf{u}_p - \mathbf{u}}{\tau_{\mathbf{u}}} + \mathbf{g} \ , \tag{4}$$

where $\mathbf{u}_d$ and $\mathbf{u}$ are velocities of particle and surrounding fluid, respectively. $\tau_{\mathbf{u}}$ is the particle momentum relaxation time (Nordin 2000):

$$\tau_{\mathbf{u}} = \frac{8m_p}{\pi\rho C_D D^2 \left|\mathbf{u}_p - \mathbf{u}\right|} = \frac{4}{3}\frac{\rho_p D}{\rho C_D \left|\mathbf{u}_p - \mathbf{u}\right|} \ , \tag{5}$$

where subscript p applies to the discrete phase, i.e. solid particles, m is mass, ρ is density and D is particle diameter. Equation (4) is solved independently from fluid equations – fluid phase is frozen while the new particles positions are solved, then particles are frozen and their momentum is added as a source term to the momentum equation of fluid. The decoupling let us avoid stability problems in momentum calculations. Particles model includes a simple collision *hard sphere model*. When a collision between two particles occurs, the algebraic equation of momentum conservation is used. Particles velocities after collision are computed on the basis of coefficient of restitution $C_R = u_n^{ac} / u_n^{bc}$, where u_n is the relative particles velocity magnitude before (^{bc}) and after collision (^{ac}). A change of colliding particles momentum is:

$$\Delta\mathbf{p}_{cp} = m_p\left(1 + C_R\right)\left(\mathbf{u}_1^{bc} - \mathbf{u}_2^{bc}\right) \ , \qquad \text{where} \qquad m_p = \frac{m_1 m_2}{m_1 + m_2} \ . \tag{6}$$

The corrected velocities:

$$\mathbf{u}_1^{ac} = \mathbf{u}_1^{bc} - \frac{\Delta\mathbf{p}_{cp}}{m_1} \qquad \text{and} \qquad \mathbf{u}_2^{ac} = \mathbf{u}_2^{bc} - \frac{\Delta\mathbf{p}_{cp}}{m_2} \tag{7}$$

are used as an initial condition for particles motion equation (4).

4. Results

The models described above are used for studies of flow and particles motion around a cylindrical pier with a scourhole. It is not a scouring model at piers. The aim of computations is to investigate trajectories of particles already lifted from bed – particles are randomly generated slightly above the bed. Turbulent objects that develop around a pier: horseshoe vortex and wake vertical vortices (Fig. 2) are greatly affected by existence of scourhole – all the vortices are much more intense. The previous studies (Pasiok 2004) with marker-particles (i.e. with zero mass) indicated the possible mechanism of transporting particles out of the scourhole. The markers tended to concentrate in vertical vortices cores, regions of local vorticity maxima and pressure minima. Once trapped into a vortex core, markers were transported out of the scourhole.

Simulations with mass particles do not show such an effect. Some of the particles generated slightly above the bed level on downstream side of pier are lifted up as

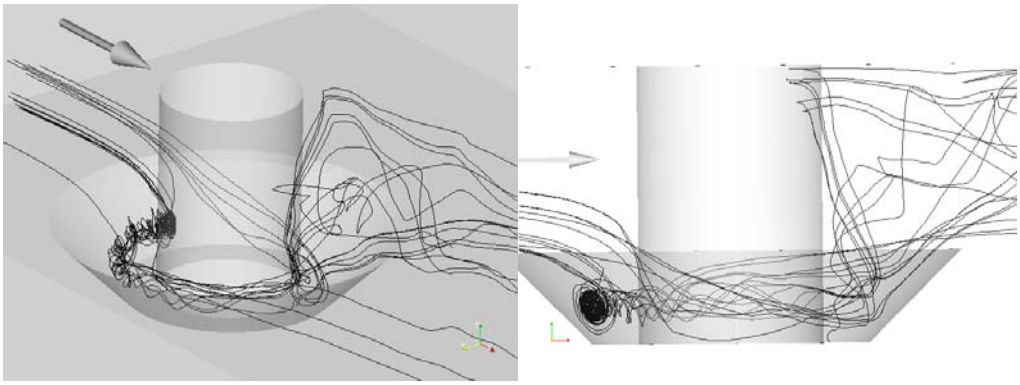

Fig. 2. Instantaneous velocity streamtraces around a cylindrical pier with a scourhole.

shown in Fig. 3. The results of simulations performed for limited range of mass particle diameters indicate that particles move mostly in a strong jet directed towards the surface. The jet is enclosed by downstream pier wall and vertical wake vortices. The vertical vortices are the main driving force for the jet. Figure 4 shows example particles positions at various levels above the bed ($z = 0.5$ is the initial bed level). Arrows show velocity vectors directions and magnitudes. Brightness corresponds with vertical velocity component value.

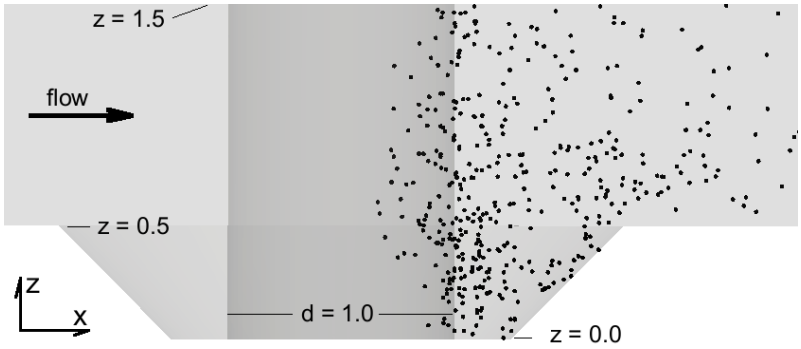

Fig. 3. Positions of particles generated close to the bed on downstream side of the scourhole (particles size not to scale).

5. Conclusions

The study was aimed at investigation of mass particles trajectories around a pier. The results obtained so far indicate that the trajectories depend on the intensity of wake vertical vortices that drive the upward jet. These strong turbulent objects are highly

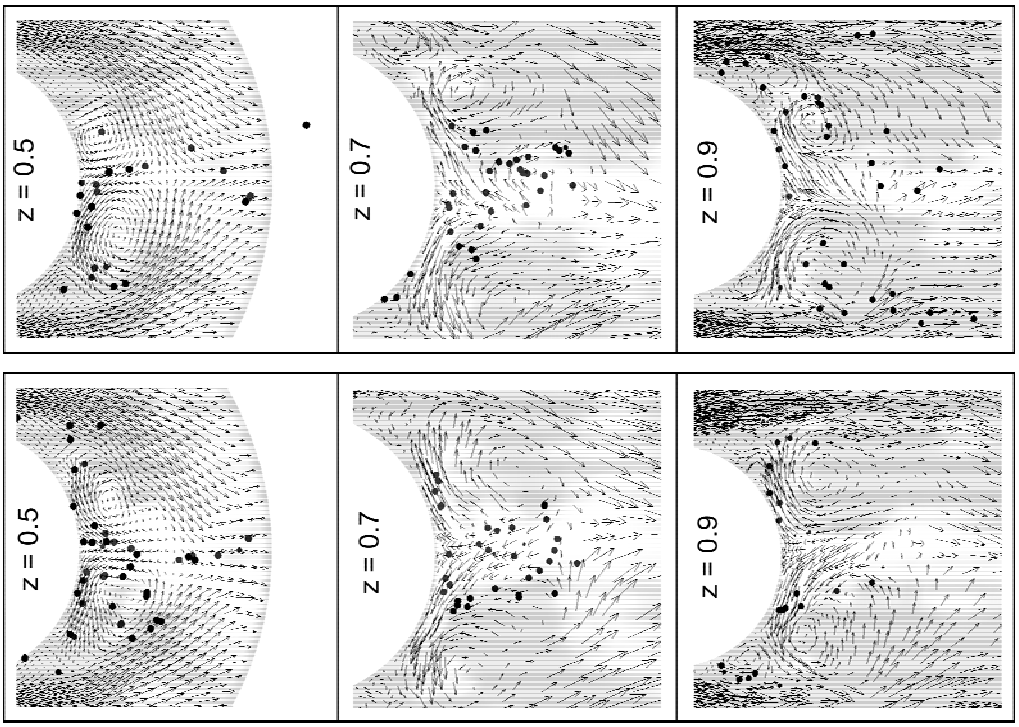

Fig. 4. Example particles positions at various levels and times. See text for details.

unsteady. It is crucial, therefore, for scouring model to use a sufficiently detailed flow description. Further simulations are planned with a wider range of particle diameters, different scourhole shapes and mean flow conditions.

Acknowledgments. The authors gratefully acknowledge that all the computations for the present work were carried out with the OpenFOAM (Open Field Operation and Manipulation) CFD Toolbox (Weller 1998; http://www.openfoam.org) released from OpenCFD under the terms of the GNU GPL 2 license (http://www.gnu.org).

References

Ahmed, F., and N. Rajaratnam, 1998, *Flow around bridge piers*, J. Hydraul. Engin. **124**, 3, p. 288.

Ashworth, P.J., S.J. Bennett, J.L. Best and S.J. McLelland, 1996, *Coherent Flow Structures in Open Channels*, John Wiley & Sons.

Breusers, H.N.C., and A.J. Raudkivi, 1991, *Scouring (Hydraulic Structures Design Manual)*, A.A. Balkema, Rotterdam.

Clift, R., J.R. Grace and M.E. Weber, 1978, *Bubbles, Drops and Particles*, Academic Press.

deVilliers, E., 2006, *The Potential of Large Eddy Simulation for the Modeling of Wall Bounded Flows*, PhD thesis, Imperial College of Science, Technology and Medicine, London (not published yet – private correspondence).

Ferziger, J.H., and M. Perič, 1999, *Computational Methods for Fluid Dynamics*, Springer.

Graf, W.H., and I. Istiarto, 2002, *Flowpattern in the scour hole around a cylinder*, J. Hydraul. Res. **40**, 1, pp. 13-20.

Issa, R.I., 1986, *Solution of the implicitly discretized fluid flow equations by operator splitting*, J. Computational Physics **62**, pp. 40-65.

Leszczyński, J.S., 2005, *Dyskretny model dynamiki zderzeń ziaren w przepływach materiałów granulowanych*, Wydawnictwa Politechniki Częstochowskiej.

Nordin, N.P.A., 2000, *Complex Chemistry Modeling of Diesel Spray Combustion*, PhD thesis, Chalmers University of Technology.

Pasiok, R., and A. Popow, 2004, *A Numerical Free Surface Flow Model in the Analysis of a Bed Stability at Piers*, Proceedings of XXIV International School of Hydraulics, Gdańsk.

Sagaut, P., 1998, *Large Eddy Simulation for Incompressible Flows*, Springer.

Van der Vorst, H.A., 1992, *Bi-CGSTAB: a fast and smoothly converging variant of Bi-CG for the solution of non-symmetric linear systems*, SIAM Journal of Scientific Computing **13**, 2, pp. 631-644.

Weller, H., G. Tabor, H. Jasak and C. Fureby, 1998, *A tensorial approach to computational continuum mechanics using object oriented techniques*, Computers in Physics 12, 6, pp. 620-631.

Wilcox, D., 2000, *Turbulence Modeling for CFD*, DCW Industries Inc.

Accepted September 12, 2006

PUBLS. INST. GEOPHYS. POL. ACAD. SC., E-6 (390), 2006

Influence of Local Streams on the Quality of Water in the Coastal Zone in Sopot

Małgorzata ROBAKIEWICZ

Institute of Hydro-Engineering, Polish Academy of Sciences
Kościerska 7, 80-328 Gdańsk, Poland
email: marob@ibwpan.gda.pl

Abstract

Sopot, one of the most renowned recreational cities in Poland, located at the Gulf of Gdańsk coast, is cut by a number of streams collecting the rain water from the moraine hill surrounding the city, and discharging it directly into the sea. The quality of water, due to passage through the urbanized area, is often below required standards, especially due to bacteria pollution. At present, the rain water is discharged directly on the sandy beaches, and in case of high pollution, causes problems for the coastal zone; sometimes it is necessary to close beaches for recreation. The local administration considers re-location of the outfalls seaward to solve the problem. To assess the consequences of the proposed investment, numerical modeling was carried out. The new situation becomes more complicated due to potential construction of the yachts harbor attached to the existing pier. Numerical tests will support the decision to be made.

1. Introduction

The city of Sopot, one of the most renowned recreational cities in Poland, is located on the moraine hills and stretches along the southern coast of the Gulf of Gdańsk. The city is cut by 11 streams discharging water directly into the Gulf. The urbanized areas suffer from different types of pollutants; the most painful from the recreational point of view is bacteria pollution. In the past, this type of pollution was the main reason of closing sandy beaches for tourism there. This problem, known in most urban areas in the world located at the coast, is still present, although less severe than in the past.

In the last decade, local administration put great effort to eliminate all potential sources of pollution. Positive results of these works are noticeable during sanitary inspections carried out regularly in the coastal zone, which resulted in opening bathing

areas for public use. However, severe EU regulations and wish to attract tourists to spend holidays in this city push local administration to invest into the infrastructure. New ideas to re-locate the coastal river outlets sea-ward and construct the yachts harbour attached to the existing wooden pier, required analysis with regard their influence on the water quality standards in the coastal zone.

2. Present situation and proposed investments

Eleven streams pass through the city of Sopot, discharging their waters into the coastal zone of the Gulf of Gdańsk (Fig. 1). In the central part of the coast, a wooden pier with a perpendicular groin (located about 350 m from the coast) is situated. At present, natural streams passing through the beach are closed in the concrete pipes and their outlets are protected from the sea-side by a palisade to protect the outlets from the sea (Robakiewicz 2005). Due to water level variations, these protecting structures are sometimes at the beach, sometimes in the sea. These concrete structures not only spoil the visual impression of the sandy beach but also create problems with the free outflow of water through the pipes due to sedimentation.

Two important investments to increase attraction of the region are considered by local administration: (1) modernization of the ground and surface water outflow system from the city, and (2) construction of the yachts harbour attached to the existing pier. Both investments will influence the coastal zone, and can have consequence with regard water quality standards of the bathing waters.

The main idea of the investments considered is to re-locate discharge of water transported by natural streams from the coast off-shore using underwater pipes. It is proposed to connect small streams into bigger ones in the following manner (Fig. 1):

outlet A – collecting water from streams 1, 2 and 3, and discharging water sea-ward at the extension of stream 2;

outlet B – collecting water from streams 5, 6, and 7, and discharging water sea-ward at the extension of stream 7;

outlet C – collecting water from streams 8, 9, 10 and 11, and discharging water sea-ward at the extension of stream 10.

For the local administration, it is most important to know the consequences of this investment on the coastal waters. In the last few years, water quality measurements carried out regularly in spring, summer and autumn by sanitary inspection indicated improvements. However, it has to be mentioned that those measurements were carried out in dry days. From the observations in various urban areas in the world it is known that the quality of water dramatically decreases in the first 15 minutes of heavy rain, as during that short period, cities are ‘cleaned’ by rain water. To assess the influence of rain water on the quality of coastal water, numerical analysis was car-

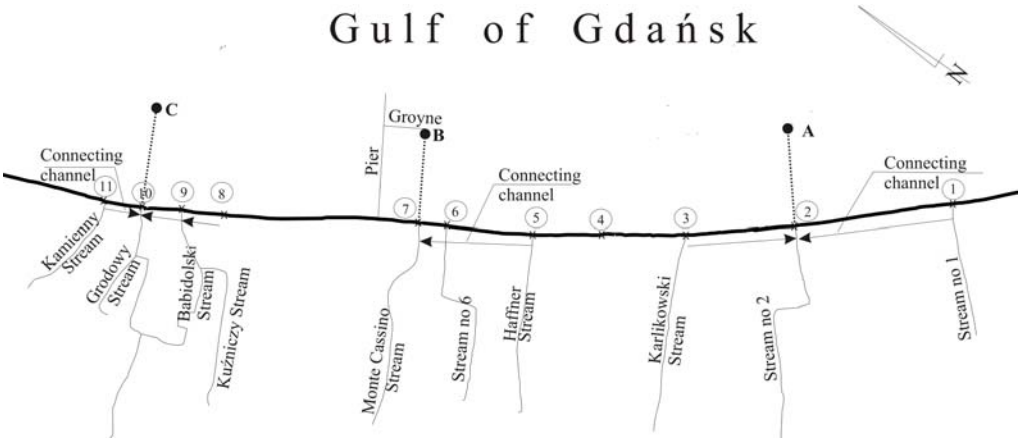

Fig. 1. Location of streams in Sopot.

ried out. To carry out such an analysis, discharge of streams during the one-year rain was estimated (Table 1).

Table 1

Discharge of streams – yearly rain (acc. Pracownia Hydrotechniki i Inżynierii Środowiska)

No.	Name	Q [m³/s]	Outlet	Q [m³/s]
1.	Stream no 1	0.533	A	2.177
2.	Stream no 2	0.689		
3.	Karlikowski stream	0.955		
4.	Stream no 4	0.134		
5.	Haffner stream	1.116	B	2.528
6.	Stream no 6	0.382		
7.	Monte Cassino stream	0.986		
8.	Kuźniczy stream	1.714	C	4.378
9.	Babidolski stream	0.670		
10.	Grodowy stream	0.148		
11.	Kamienny stream	1.846		

3. Consequences of re-location of outfalls

To assess the influence of re-location of natural outlets off-shore, numerical simulations have been done. The main idea was to analyse mixing of rain water with the marine water and trace such a ‘plume’ in its passage towards the coast. For this purpose

a local 3D hydrodynamic model based on Delft3D-FLOW software was set-up. The modelled area stretching approx. 5 km along the coast and 3 km off-shore was covered by 502×252 grid cells in horizontal plane using curvilinear orthogonal grid, and 10 layers uniformly distributed in vertical using sigma co-ordinates. In the model the presence of the pier in the shape proposed after construction of the yachts harbour was introduced (Fig. 1). Calculations were carried out for the following uniform conditions: discharge in locations A, B and C as given in Table 1; wind direction and speed as characteristic for the summer time based on long-term statistics (1951-1975) for Gdynia station (Kwiecień 1990): N – 3.9 m/s; E – 4.1 m/s, S – 3.5 m/s, W – 4.1 m/s and calm weather. According to the proposed design, the rain water will be discharged about 1.5 m below the free surface, so the modelled outfalls were located there. To trace mixing processes, water discharged into sea was 'marked' by a conservative, non-reactive substance. In all simulations it was assumed that salinity of rain water is 0 psu, while for coastal water – 7 psu. Additionally, it was assumed that there is no temperature difference between inland and coastal waters. In all calculations discussed in this paper water in locations A, B and C was discharged 15 minutes (quantities as in Table 1) to imitate short but intensive rain, while observations of behaviour of the 'plume' was carried out for the next 2 hours. An analysis for each location is presented below.

3.1 Discharge in location A

The proposed location of discharge A is approx. 400 m off-shore where local depth is about 5 m. As the estimated amount of discharged water is only 2.2 m^3/s, changes of salinity in the vicinity of the outlet are very small (not exceeding 0.01 psu), with no influence on changes in the marine environment. Analysis carried out for this location leads to the following conclusions (Fig. 2):

- in calm weather, the diluted rain water reaches the coast after 1.5 hours on the distance of approx. 200 m; rain water content at the coast can reach 0.2%;
- in case of N wind, the diluted rain water spreads along the coast, not approaching coast closer than 100 m;
- in case of E and S wind, the diluted rain water reaches the coast on the distance of about 100 m; rain water content at the coast can reach 0.2%;
- in case of W wind, the diluted water spreads quite similar as in case of N wind, but does not reach the coast.

3.2 Discharge in location B

The proposed location of discharge B is approx. 350 m off-shore where the local depth is about 3.8 m. The amount of water to be discharged during the considered rain is estimated as 2.5 m^3/s. It is proposed to locate outlet B directly attached to the groin of the pier from the coast side. Analysis carried out for location B leads to the following conclusions:

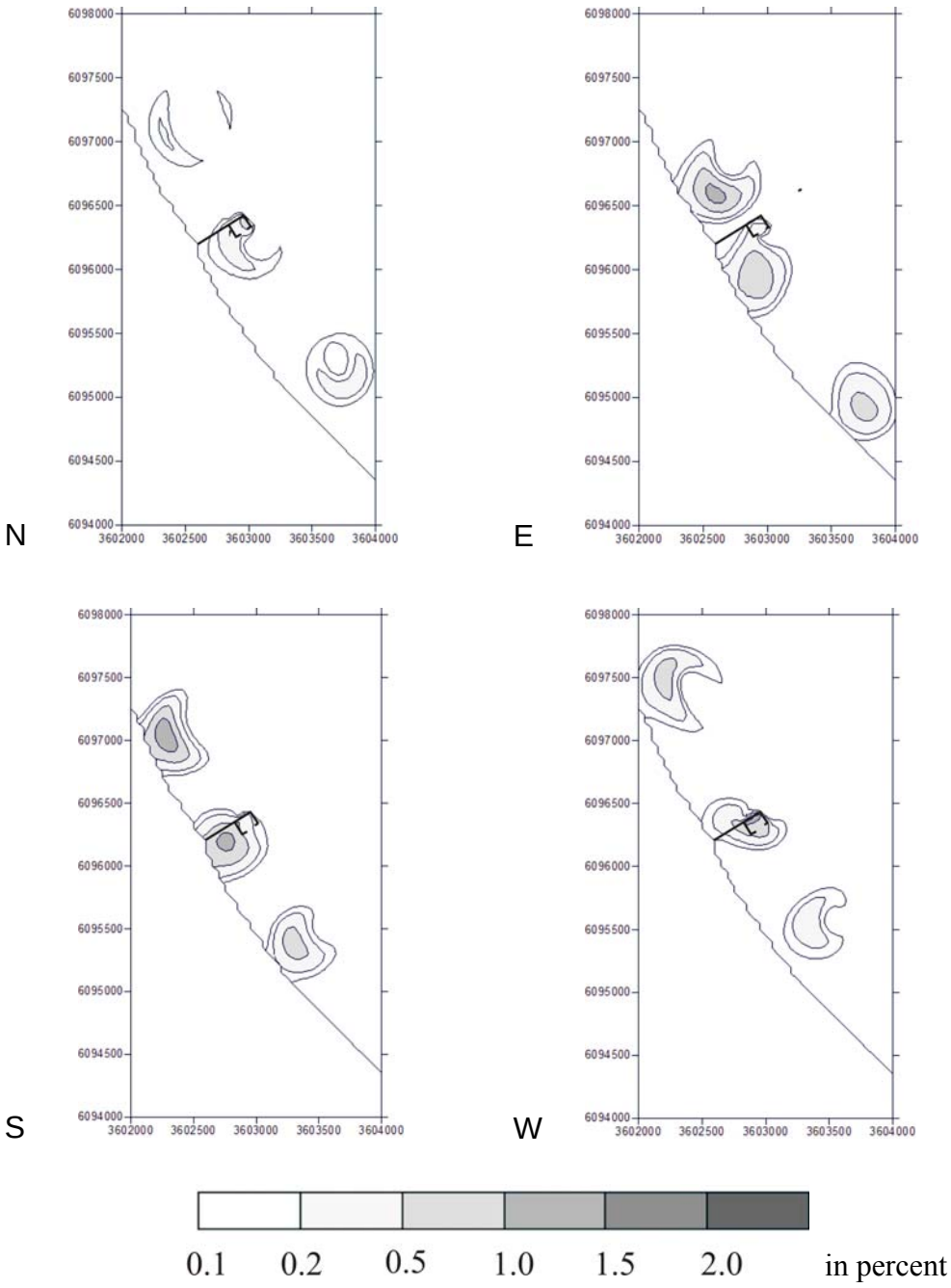

Fig. 2. Spreading of tracer in the coastal zone depending on wind direction (2 hours after rain).

- in calm weather, the diluted rain water reaches the coast on the distance of about 350 m on both sides of the wooden pier, and the rain water content is about 1%. It has to be mentioned that rain water is transported inside the planned yachts harbour;
- in case of N wind, the diluted rain water approaches coast on the distance of 100 m, and spreads inside the yachts harbour;
- in case of E wind, the diluted rain water is easily transported to the coast (400–500 m); the rain water content is about 0.5%;
- in case of S wind, the diluted rain water comes back to the coast on the distance of 500 m; the rain water content is about 1.0%;
- in case of W wind, the diluted rain water is easily transported inside the proposed yachts harbour (the rain water content is about 1.5%).

3.3 Discharge in location C

The proposed location of discharge C is approx. 400 m off-shore where local depth is about 5 m. The amount of discharged water is 4.4 m^3/s, and similarly as in previous cases changes of salinity in the vicinity of the outlet are very small. From the analysis carried out, the following conclusions can be drawn:

- in case of calm weather, the diluted rain water (content 0.5%) reaches coast on the distance of 300–350 m;
- in case of N wind, the diluted rain water spreads along the coast on a distance of 100 m;
- in case of E wind, the diluted rain water (content up to 0.5%) reaches coast on the distance of 300 m; it has to be noticed that ‘plume’ approaches similar ‘plume’ of water due to discharge B;
- in case of S wind, the diluted rain water very quickly spreads towards the coast; on the distance of about 400 m a plume reaches the coast (rain water content of 1%);
- in case of W wind, the diluted rain water reached the coast on the distance of about 250 m; the rain water content in the plume reached 0.2%.

4. Conclusions

Based on the analysis carried out for three proposed off-shore outlets it can be concluded that:

- rain water discharged through pipelines in locations A, B and C will not change salinity distribution pattern remarkably; it has to be mentioned that at present the rain water is discharged at the coast and the proposed investment only changes the location, not influencing the amount of water to be discharged;

- rain water discharged in location A, in majority of meteorological conditions intensely diluted, reaches the coast. In the area of 200 m along the coast, the rain water content can reach 0.1–0.5%. In comparison with locations B and C mixing processes close to this outlet are the best;
- taking into account location, distance from the shore and amount of water discharged, location B is not a favorable place for mixing processes. It is not only too close to the coast but also can create pollution problem in the yachts harbor;
- the amount of water discharged in location C is doubled in comparison with location A, while the distance of the outlet is similar in both cases. It is recommended to move location C some 100–200 m off-shore to support mixing processes.

According to *Directive 2006/7/EC of the European Parliament and of the Council of 15.02.2006 concerning the management of bathing water quality*, 'pollution' means the presence of microbiological contamination or other organisms or waste affecting bathing water quality and presenting risk to bathers' health. According to this Directive by the end of bathing season 2015 bathing water should be at least of 'sufficient' quality. For coastal waters and transitional waters it means, for example, that Escherichia coli (cfu/100 ml) can not exceed 500 to be 'sufficiently' clean. In case the discharged water contains 10^6 cfu/100 ml of Escherichia coli this leads to the conclusion that to reach the minimum standard dilution at the bathing water should be at least 0.5%.

From the regulations mentioned above and the results of model calculations it can be concluded that the proposed investment will be successful only in case water discharged by piped off-shore is 'clean' enough, as the proposed pipelines are relatively short. In this context, it is very important to control the quality of water in heavy rain to be absolutely aware of the possible risk, and in case of high pollution take measures to reduce it.

References

Kwiecień, K., 1990, *Climate*. **In:** A. Majewski (ed.), "The Gulf of Gdańsk", Wydawnictwa Geologiczne, Warszawa, 66-119 (in Polish).

Robakiewicz, M., 2005, *Mixing of fresh and saline waters and changes of water temperature with regard to A and C outlets based on local numerical model*, IBW PAN Internal Report (in Polish).

Accepted September 12, 2006

PUBLS. INST. GEOPHYS. POL. ACAD. SC., E-6 (390), 2006

Estimation of Novosibirsk Water Intakes Work Conditions under Daily Regulation of Ob River Flow by Novosibirsk HPP

Alexander SEMCHUKOV[1], Arkadiy ATAVIN[1] and Vladimir DEGTYAREV[2]

[1]Institute for Water and Environmental Problems of the Siberian Branch
of Russian Academy of Sciences
Morskoy ave. 2, 630055 Novosibirsk, Russia
email: iwep@ad-sbras.nsc.ru

[2]Novosibirsk State University of Architecture and Civil Engineering
Leningradskaya st. 113, 630008 Novosibirsk, Russia
email: email@sibstrin.ru

Abstract

Numerical algorithm of high accuracy was developed for simulation of rapidly changing unsteady flow in an open channel of arbitrary shape. The algorithm was applied for the estimation of daily regulation of Ob river flow by Novosibirsk Hydroelectric Power Plant on work of Novosibirsk water intakes situated downstream of it.

1. Introduction

The Novosibirsk Hydroelectric Power Plant has a lowland reservoir with relatively small operating storage. In a low-flow period of a low water year (for example, in winter) the critical water scarcity occurs in the reservoir, and the water level often falls below the dead water level. In that case, HPP has to work under policy of strict economy and spend no more water than it is necessary to cover peak demands for electricity. In other time of day, water discharge is performed according to some very low technical norm. The pronounced unsteady nature of water movement in some periods of time can lead to fall of water levels near water intakes of Novosibirsk below the values regulated by the Reservoir Water Management Rules, even under average daily discharge corresponding to sanitary norm. In that case, the inlets deepening may be not sufficient, and it may lead to air suction and thus breaking of normal work of pumps.

The situation is aggravated by gradual lowering of mean water level downstream Novosibirsk HPP during the period of its exploitation caused by stream channel degradation because of HPP effect and sand and gravel mining from the river bed (Maltcev and Bavsky 2000).

For the purpose of estimation of the influence of daily regulation of Ob river flow by Novosibirsk HPP on work of Novosibirsk water intakes, the numerical algorithm of high accuracy for simulation of rapidly changing unsteady flow in an open channel of arbitrary shape was developed (Semchukov et al. 2003).

2. Governing equations

In Novosibirsk a lot of work on numerical simulation of unsteady flow in open channels was done by the Institute for Hydrodynamics of the Siberian Branch of Russian Academy of Sciences (Vasiliev 1999).

For simulation of unsteady water movement, one-dimensional equations of Saint-Venant are used (Atavin 1975, Stoker 1957):

equation of continuity (mass conservation law)

$$\frac{\partial \omega}{\partial t} + \frac{\partial Q}{\partial x} = q \ , \tag{1}$$

dynamic equation (momentum conservation law)

$$\frac{\partial \ Q}{\partial t} + \frac{\partial}{\partial x}\left(Q \ \ v\right) + g\omega\left(\frac{\partial z}{\partial x} + \frac{Q|Q|}{K^2}\right) = 0 \ . \tag{2}$$

Here ω = cross-sectional area, m^2; Q = discharge, m^3/s; z = water level, m; q = distributed water inflow, m^2/s; g = acceleration of gravity, m/s^2; t = time, s; x = coordinate along bed axis (at the line of greatest depth), m; $v = Q/\omega$ = mean velocity, m/s; K = conveyance of a bed.

Conveyance K is defined by the Chezy formula $K = \omega C\sqrt{R}$, where $C = 1/n_r R^{1/6}$ is the Chezy factor defined by Manning equation, m$^{1/2}$/s; n_r is the roughness factor, s/m$^{1/3}$; R is the hydraulic radius, m. For a river we can assume $R = h$, where $h = \omega/B$ is the mean depth (B is a stream width, m).

It is assumed that the flow is subcritical. In this case one border condition must be given for both inflow and ouflow sections of river reach under consideration (Atavin 1975, Rozhdestvensky and Yanenko 1978).

In simulations described below, the water discharge as a function of time is given at the inflow section and a discharge rating curve (dependence of water discharge on water level) is given at the outflow section:

$$Q(x_{in},t)=Q_{in}(t)\ ,\quad Q(x_{out},t)=Q_{out}(z)\ \ . \tag{3}$$

An initial distribution of discharge and water level are given as initial conditions:

$$Q(x,t_0)=Q_{start}(x)\ ,\quad z(x,t_0)=z_{start}(x)\ . \tag{4}$$

3. Numerical algorithm

Schematization of river bed is performed in the following way: a certain number of base sections are selected at the considered reach of river bed. These sections are situated in characteristic points of the bed, i.e. in the places of biggest widening and narrowing, biggest and smallest depth and at the ends of considered reach. A few levels are selected at each section and for each level a bed width is found. Then geometric parameters are linearly interpolated along the river: first levels with certain number from the bottom are interpolated and then – bed widths at these levels. If the river has a few branches at a certain distance from the dam, a section is built to cross all branches, widths of branch beds at the same levels are summed up and then the branch beds are considered as a single bed.

To prevent negative numerical effects, associated with a sharp change of bed geometric parameters, the diffusive procedure for smoothing morphometric information was developed (Semchukov et al. 2003).

The roughness factor, defining frictional force, plays a special role among morphometric characteristics of a bed. It is defined for each area between base sections based on bed character (Agroskin et al. 1964) and then can be specified by water level measurements under steady flow. The numerical procedure basing on numerical solution of Saint-Venant equations for steady flow was developed for this purpose.

The explicit two step finite-difference scheme of Lax-Wendroff of second order of accuracy by time and space was used for flow simulation (Lax and Wendroff 1960).

The Saint-Venant equations are solved in ‘discharge–cross-sectional area’ variables ($q - \omega$), which allows to write the finite-difference scheme in almost divergent (almost conservative) form. Namely, all terms of equations (1-2), except of the term describing work of hydrostatic force, are approximated in divergent form similar to (Ostapenko 1993). Such approach allows obtaining an efficient numerical method, allowing simulation of rapidly changing flow with high precision.

The algorithm based on Saint-Venant equations written in characteristic form (Atavin 1975, Stoker 1957) was developed for numerical realization of border conditions.

The uniform grid was used and the time step was automatically chosen each time to provide stability of the finite difference scheme (the Courant number had to be not greater than 1).

4. Simulation results and conclusion

In this work the 19.4 km long Ob River reach limited by section 200 m downstream Novosibirsk HPP dam, and section of Novosibirsk river gauge situated in the central part of the city, is under consideration. The scheme of this reach is given at Fig. 1. The right-bank and left-bank river intakes situated at 1 km and 12 km distance downstream dam, respectively, were chosen for analysis. Farther they will be designated as intakes № 1 and № 2.

The only noticeable tributary at the considered reach of the Ob River is river Inya, but its discharge and distributed discharge were not taken into account in these simulations because of their relative smallness in the considered period of time.

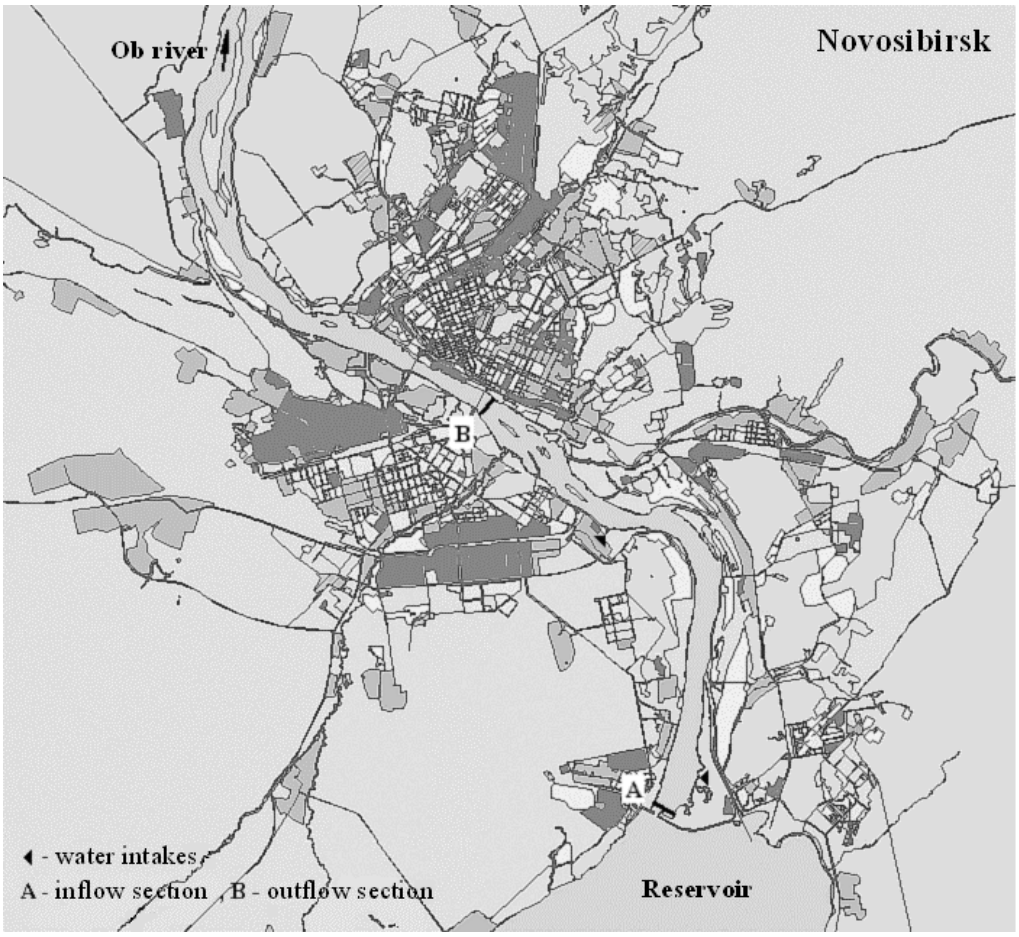

Fig. 1. Ob river reach under consideration.

The constant discharge Q, corresponding to its mean value during the period of simulation, and water level z, uniformly decreasing along the river, were given as initial conditions. Then, simulation with constant discharge at the inflow section, corresponding to its initial value, was performed until achievement of steady state (as practice showed, steady state is achieved in a few hours). Then discharge at the inflow section began to change according to its hydrograph.

In Fig. 2 the dotted line (1) displays the simulated profile of water level along river under constant discharge 1300 m^3/s under roughness factor values defined by bed character, and solid line (2) – the same profile, but obtained under specified values of roughness factor. Here daggers designate the measured values of water level. The lower solid line designates the bottom level along the line of greatest depths. This figure shows that, as a whole, the used numerical model correctly describes the stream flow under roughness factor values, defined by bed character.

In Fig. 3 the graph of real HPP discharge during March 16-17, 1988, is given. By that date the considered reach is usually free of ice, which justifies usage of the present stream flow model. During the first day of simulation time (corresponding to March 15), the discharge was constant to achieve steady state of stream flow. In

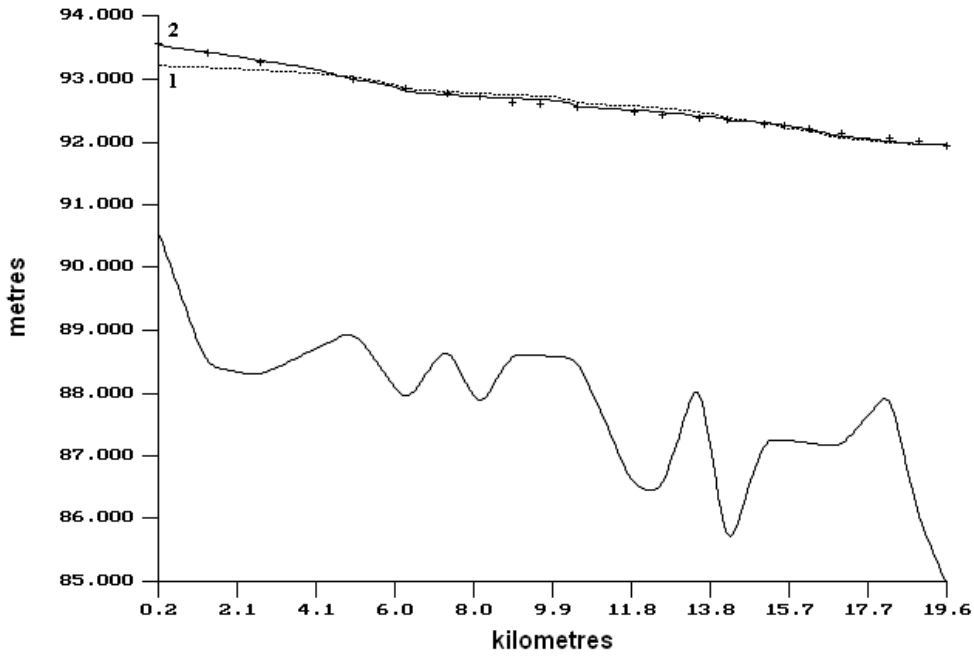

Fig. 2. Simulated water level profile under constant discharge of 1300 m^3/s under initial (1) and specified (2) values of roughness factor.

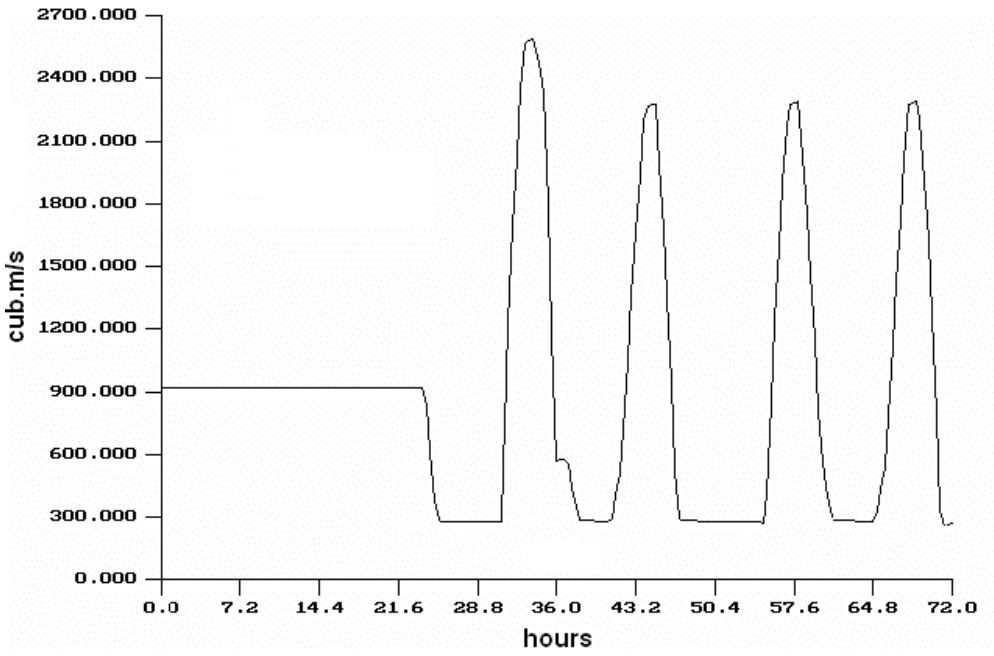

Fig. 3. HPP discharge graph at March 16-17, 1988.

Fig. 4 the graphs of water level near intakes № 1 (A) and № 2 (B) under such discharge are given. Here the dotted lines designate the inlet levels.

In this case, the normal water level condition of intake № 1 is not provided once a day during 1 hour 10 minutes – 1 hour 40 minutes and at that time the water level falls up to 13-14 cm below the necessary one. The water level at intake № 2 continues to be acceptable, but close to critical. We see that under such graph of discharge, the uninterrupted work of intake № 1 is not provided in spite of the fact that the mean discharge is 918 m^3/s, which is more than 2 times bigger than the sanitary norm, and minimum discharge is 276 m^3/s, which is also more than the value of 240 m^3/s, allowed for daily regulation (the maximum discharge is 2593 m^3/s).

The simulations with cyclically changing HPP discharge with 450 m^3/s mean value (minimal sanitary discharge for winter conditions) and 12 hours oscillation period were also undertaken. The amplitude of oscillation was 10%, 20% and 50% of the mean value. Already at the 20% discharge oscillation, the normal water level condition of intake № 1 is not provided 2 times a day during 4 hours and at that time the water level falls up to 7-8 cm below the necessary one, and at 50% discharge oscillation, the water level at intake № 2 is critical 2 times a day during 2-3 hours.

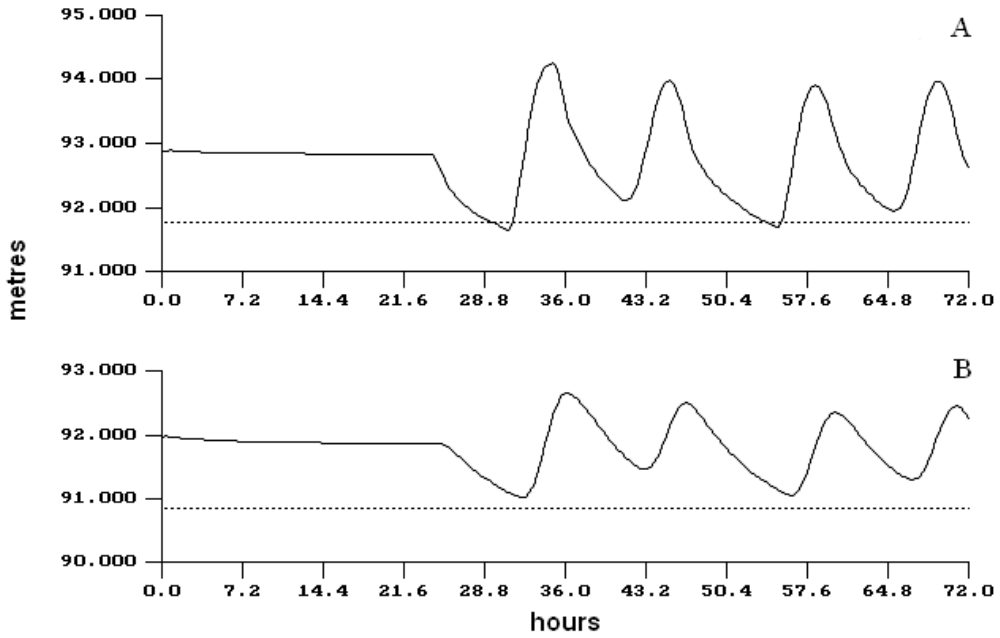

Fig. 4. Simulated water level graphs at intakes № 1 (A) and № 2 (B) during March 16-17 1988.

The given simulations show the importance of accounting for impact of daily regulation of Novosibirsk HPP discharge on water supply of Novosibirsk and the necessity of additional research on choosing allowable conditions of daily regulation of discharge during winter low-water period.

Acknowledgments. This work was supported by Russian Foundation for Basic Research (project RFFI 06-05-65076). The authors thank Prof. O.F. Vasiliev and Dr. V.V. Ostapenko for help in work on this article.

References

Agroskin, I.I., G.T. Dmitriev and F.P. Pikalov, 1964, *Hydraulics*, Moscow, 352 pp. (in Russian).

Atavin, A.A., 1975, *Simulation of unsteady water flow in branched systems of river beds or channels*, Dinamika Sploshnyh Sred **22,** 25-36 (in Russian).

Lax, P., and B. Wendroff, 1960, *Systems of conservation laws*, Comm. Pure and Appl. Math. **13**, 217-237.

Maltcev, V.S., and S.P. Bavsky, 2000, *Usage of water resources of the Novosibirsk reservoir*, Vodnoye Hozyaystvo Rossii **2**, 4, 347-356 (in Russian).

Ostapenko, V.V., 1993, *Shock-capturing method for open channels*, Zhurnal Vychislitelnoy Matematiki i Matematicheskoy Fiziki **33**, 5, 743-752 (in Russian).

Rozhdestvensky, B.L., and N.N. Yanenko, 1978, *Systems of quasi-linear equations and their application to gas dynamics*, Moscow, 687 pp. (in Russian)

Semchukov, A.N., A.A. Atavin, V.I. Kvon, V.V. Degtyarev and N.V. Alekseeva, 2003, *Estimation of work conditions of river intakes downstream HPP's under daily regulation of discharge*, Izvestiya Vuzov. Stroitelstvo **2**, 73-82 (in Russian).

Stoker, J.J., 1957, *Water Waves. The Mathematical Theory with Applications*, New York, 600 pp.

Vasiliev, O.F., 1999, *Mathematical modeling of hydraulic and hydrologic processes in water bodies and streams (review of works carried out in the Siberian Branch of Russian Academy of Sciences)*, Vodnye Resursy **5**, 600-611 (in Russian).

Accepted September 12, 2006

PUBLS. INST. GEOPHYS. POL. ACAD. SC., E-6 (390), 2006

Importance of Advective Zone in Longitudinal Mixing Experiments

James SHUCKSMITH[1], Joby BOXALL[1] and Ian GUYMER[2]

[1]Department of Civil Engineering, University of Sheffield, UK
e-mail: j.shucksmith@sheffield.ac.uk

[2]School of Engineering, University of Warwick, UK
e-mail: i.guymer@warwick.ac.uk

Abstract

One-dimensional Fickian dispersion models such as the advection diffusion equation (ADE) are commonly used to analyse and predict concentration distributions downstream of contamination events in watercourses. Such models are only valid once the tracer had entered the equilibrium zone. This paper compares previous theoretical, experimental and numerical estimates of the distance to reach the equilibrium zone with new experimental values, obtained by examining the change of skewness in a tracer profile, downstream of a cross-sectionally well mixed source. Closer agreement was found with Fischers' theoretical estimate than prior experimental and numerical studies.

Key words: environmental hydraulics, longitudinal mixing experiment, advection diffusion equation, advective zone.

Full text was published in *Acta Geophysica*, Vol. 55, No. 1, p. 95-103.

PUBLS. INST. GEOPHYS. POL. ACAD. SC., E-6 (390), 2006

Real-Time Flow Forecasting on the Basis of St. Venant Model

Tomasz SIUTA

Institute of Engineering and Water Management
Warszawska 24, 31-155 Kraków, Poland
email: tomasz.siuta@iigw.pl

Abstract

In the paper, flow routing process in a river system within the context of real-time flood forecasting is discussed. Adaptation of St. Venant model for peak flow forecasting in a river system with the presence of uncontrolled inflow was introduced. The principal idea of the presented approach is to separate forecast of the peak flow discharge from the peak occurrence time. An illustrative example based on historical flow data taken from Raba river demonstrates the efficiency of the presented method.

1. Introduction

In recent years, more and more floods are observed in the same regions of the world. These floods constitute the threat for urbanized area and for people living there. Efficient management of flood protection system and flood warning system requires efficient real-time flood forecasting in a river system. In the paper, a method of real-time peak flow forecasting in the outlet cross section is described. This approach to forecast is based on measurements at the gauging stations of the river system and application of one dimensional hydrodynamic model (St. Venant model). Within the approach proposed by the present author, attention is focused on uncontrolled lateral inflow impact.

The real-time catchment outflow forecasting is based on rainfall-flow relation or flood routing models. If meteorological rainfall forecasts are available, they may be introduced as input data for hydrological models in order to increase the lead time value; however, this kind of forecast is not so accurate (Young et al. 2000) as the ones based on direct flow measurements in the gauging stations. In the cases of lowlands and sometimes also in downstream parts of highlands catchment, flood routing data could be sufficient to achieve flow forecasting that is reliable and accurate enough.

For this purpose, we can use empirical relations between delayed flow variables measured in the inlet and outlet gauging stations or flood routing models combined with updating techniques.

Empirical models are often efficient in real-time forecasting because they allow to incorporate errors involved with unknown input variables (uncontrolled inflows) and these models usually do not require data describing river system characteristics. On the other hand, hydrodynamic models offer the whole time series forecast instead of a single time average value. This feature is especially valuable for determining the peak flow occurrence time.

2. Flow forecasting approach

The river system with inlet gauging stations located at upstream end of the main river channel and downstream ends of tributaries is considered. The assumption was made that the uncontrolled uniform lateral inflow occurs along the main river channel. The purpose is to obtain updated forecasting of peak flow at outlet cross-section. To achieve this purpose, two stages of procedure on the basis of St. Venant model application is proposed. At the beginning, time of peak flow occurrence is determined (Peak Timing Procedure) and the next stage is to determine peak discharge value (Peak Discharge Procedure).

The St. Venant model could be introduced as follows (Szymkiewicz 2000):

$$\begin{cases} \dfrac{\partial A}{\partial t} + \dfrac{\partial Q}{\partial x} = q(x,t) \\ \dfrac{\partial Q}{\partial t} + \dfrac{\partial \left(Q^2 / A\right)}{\partial x} + gA\left(\dfrac{\partial Z}{\partial x} + s_f\right) = 0 \end{cases} \tag{1}$$

where: t = time; x = longitudinal coordinate; Q = flow discharge; Z = water level; q = lateral inflow rate; A = wetted flow area; s_f = friction slope.

The following notation was introduced: T_1 = time of peak flow occurrence in the inlet cross section located at the main river channel; T_2 = time of peak flow occurrence in the outlet cross section; T_2'' = forecasted peak flow occurrence time at the moment $T_p \in (T_1, T_2)$; T_b = period of time in which $T_b > T_2$. The numerical solution of Eq. (1) is adopted for real-time flow forecasting at the outlet cross-section, according to the following procedures:

Peak Timing Procedure

1. Determination of model's actual initial state at moment T_p in the form of Eq. (3), based on the measured actual input-output flow variables and past initial state at the moment $T_p - \Delta t$.

2. Upstream boundary condition was set as a discharge time series in period of time (T_p, T_b) extrapolated from measured time series by polynomial function (for the flows from falling limb of hydrograph) or by constant flow value taken from the while T_p at inlet cross-sections with time interval Δt (at this stage, uncontrolled inflow is not included).
3. Downstream boundary condition setting as a rating curve or the Manning formula.
4. Application of St. Venant model for time series calculation in the outlet cross section in period of time (T_p, T_b) and calculation of peak flow occurrence time estimate T_2'.
5. Correction ($\Delta T_2'$) of T_2' value due to uncontrolled inflow impact. Observed values of T_2 taken from historical hydrographs are compared with calculated values T_2' to determine correction $\Delta T_2'$ and its relation to inlet or outlet peak flow discharge. Calculation of $T_2'' = T_2' + \Delta T_2'$.

Peak Discharge Procedure

1. Initial condition setting for the moment T_p in the form of Eq. (3).
2. Setting of upstream and downstream boundary condition in similar form as previously, but the lateral inflow calculated within period of time (T_p, T_2') was added (Section 2.1).
3. Application of St. Venant model for discharge series forecasting in outlet cross-section within period of time (T_p, T_2').

To estimate uncontrolled lateral inflow within the period of time (T_p, T_2'), it is necessary to introduce the error model. This model is often expressed in the form of autoregressive process (Madsen et al. 2000); it allows for prediction of future error values based on the calculated past time series.

2.1 Calculation of uncontrolled lateral inflow time series

There are several ways to achieve uncontrolled inflow estimation. It is possible to incorporate uncertainty about dynamic model and measurement which would lead to stochastic modeling (Fread et al. 1993). If dynamic model is plausible enough and intermediate gauging stations are available, there is an opportunity for inverted solution of St. Venant model equations to achieve actual vector of flow variables in the form of Eq. (3) together with uncontrolled inflow values (Szymkiewicz 2000). The easiest way for inflow estimation consists in storage equation solution. Within this approach parts of river channel between two gauging stations could be treated as a reservoir. The uncontrolled inflow could be approximated by the following equation:

$$q_i = \frac{R_{i+1} - R_i}{\Delta t} - Q_1^i + Q_m^i \tag{2}$$

where: i = index of discrete time; Q_1 = measured (calculated) discharge at upstream cross section; Q_m = measured (calculated) discharge at downstream cross section; q = uncontrolled inflow discharge; R = storage value; Δt = interval of time between succeeding measurements.

Storage R is calculated for known water level measurements and based on available channel geometric data. Inlet and outlet discharges are assumed to be constant within period Δt and could be evaluated by Manning formula or by rating curves if they are available.

2.2 Model initial state updating

For intermediate cross-sections (Fig. 1), vector of flow variables is calculated based on numerical solution of St. Venant model equations for: given (previously calculated) lateral inflow discharge, measured inlet discharge and initial condition. The vector of variables has the following notation:

$$\overline{Q}\left(T_p\right)=\left[Q_2^{T_p},Q_3^{T_p},..,Q_i^{T_p}..,Q_{m-1}^{T_p},\;\; Z_2^{T_p},Z_3^{T_p},...,Z_i^{T_p},...,Z_{m-1}^{T_p}\right] \tag{3}$$

where: m = number of cross-sections, $Q_i^{T_p}$ = discharge at cross section i at moment T_p; $Z_i^{T_p}$ = water level elevation at cross section i at while T_p.

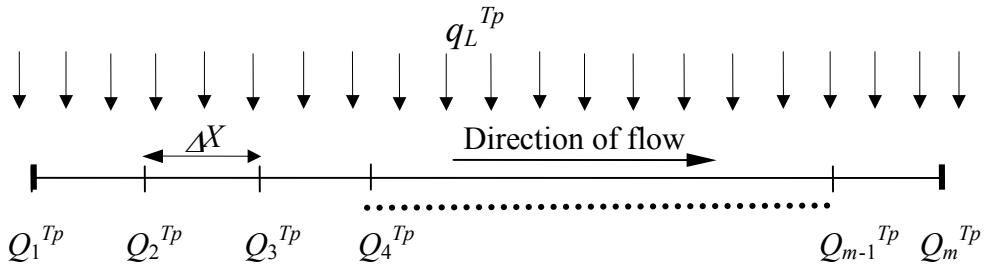

Fig. 1. Space discretization scheme.

3. Application example

The example is concerned with simulation of real-time hourly flow forecasting in the outlet cross-section of Raba subcatchment (Fig. 2). Raba is a Carpathian river which inflows to Vistula river (one of the main rivers flowing through Poland). Subcatchment of Raba taken for analysis is downstream part between Dobczyce reservoir cross-section (60.1 km) and Proszówki gauging station (21.7 km). The catchment area is equal to 702 km^2, average channel bottom slop is 0.14%. There are eight small tributaries from which Stradomka river is the biggest. At the outlet cross-section of Stradomka there is gauging station Łapanów.

Flood routing time between boundary cross sections is changing from 4 to 12 hours, depending on the peak flow value at outlet station (Proszówki). Average percentage of uncontrolled inflow determined on the basis of historical flood events is about 20% of total outflow. This uncontrolled lateral inflow is very weakly correlated with inlet 1 (Fig. 2) inflows ($R^2 = 0.39$).

Hec-Ras 3.1 program and Excel spread sheet were used for calibration and validation of forecasting model. The four-point implicit schema is applied to solve numerically Eq. (1) within Hec-Ras 3.1. The number (m) of cross-sections used in the numerical example is 405.

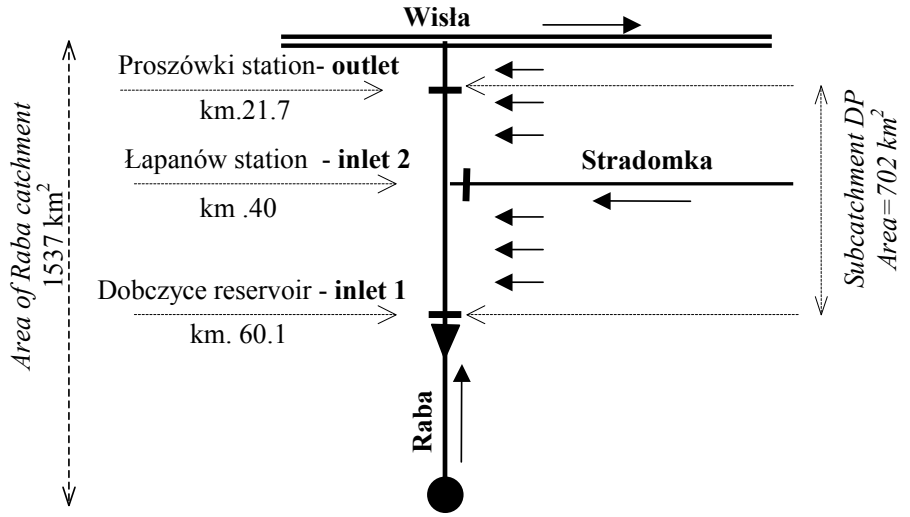

Fig. 2. Raba subcatchment scheme.

The historical data used for calibration and validation are in the form of one hour average discharge hydrographs observed at inlet and outlet cross-sections.

3.1 The model calibration

The first stage is concerned with Manning coefficient estimation on the basis of historical events from the years 1991 (peak discharge at Proszówki = 320 m^3/s) and 1996 (peak discharge at Proszówki = 580 m^3/s). In these cases, Manning coefficient calibration ($n = 0.03$) was preceded by uncontrolled inflow determination. Root mean square error (RMSE) of simulated discharge hydrograph was used as an objective function. Optimization was realized by trial and error method. The second stage is concerned with the model error identification and calibration. The first order AR model has similar RMSE value as higher order models calculated for the data, and that is why it was chosen (Eq. 4) for uncontrolled inflow prediction. Although the co-

efficient value is optimal in respect of error process explanation, it is not necessarily optimal in respect of peak flow forecast accuracy at the outlet cross section. On the basis of forecast simulations for historical flood events, a constant value of inflow-error within lead time period was found more efficient for peak flow forecast accuracy. Correction of peak timing ($\Delta T_2'$) was assumed to be one hour if peak discharge at inlet cross section (Dobczyce) was greater than 350 m^3/s, otherwise no correction was introduced.

$$q_{i+1} = 0.95 \cdot q_i \quad . \tag{4}$$

3.2 The model validation

Three historical flood events from the years 1994, 1995, and 1997 were used for model validation. Forecasts simulation was started whenever peak flow at inlet cross-section was observed. With every hour the forecast was updated and lead time value was decreased every one hour automatically.

Although the target of forecast was peak flow, dynamic modeling allows for discharge time series calculation previous to the peak (within lead time period). Results of high flow time series forecasting simulations for flood in the year 1997 are illustrated in Fig. 3. The range of lead time (3-10 hours) is changing with respect to flood events (Table 1) and its maximum value corresponds with peak flow routing time value.

The peak discharge relative error (PDE) and the right side peak time shift error values (RTS) are presented in Table 1. Results show that if lead time value is less than 67% of peak routing time, errors values are acceptable and they do not exceed

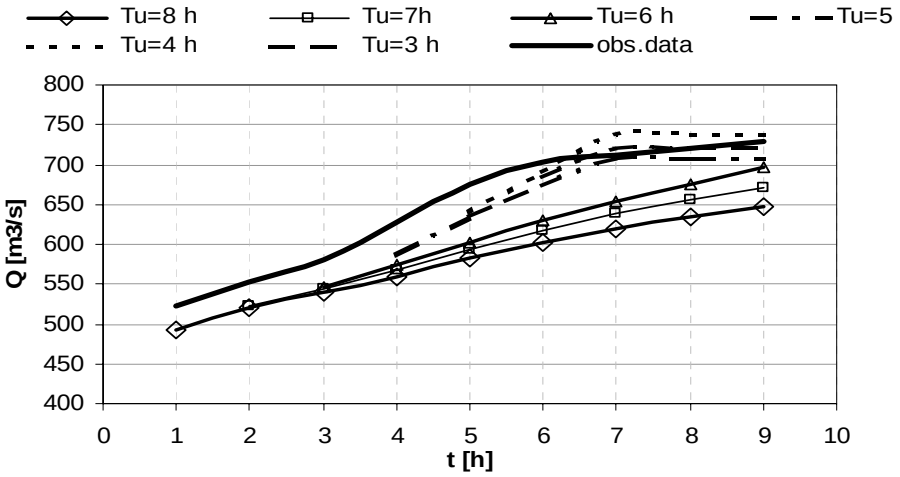

Fig. 3. Results of test flow forecasting at Proszówki cross-section for flood in the year 1997.

10.1%. Peak timing in the historical cases from the years 1996 and 1997 at Proszówki station ($Q > Q_{20\%}$) are accurate enough, although in the cases of middle peak flow (cases from the years 1991 and 1995) values, it is not possible to get peak timing properly in the described way.

Table 1

Values of forecasted peak discharge, Q_p, at Proszówki cross-section and the errors values: PDE (peak discharge error), RTS (right side time shift error)

Lead time [hours]		**10**	**9**	**8**	**7**	**6**	**5**	**4**	**3**
1997	Q_p [m^3/s]	547.26	547.26	655.91	683.35	695.86	708.23	738.56	719.97
	PDE [%]	25.0	25.0	10.1	6.4	4.7	3.0	1.2	1.4
	RTS [h]	-2	-2	2	2	1	-1	-1	-1
1996	Q_p [m^3/s]	542.69	542.69	579.13	579.16	590.07	599.65	579.23	585.09
	PDE [%]	6.6	6.6	0.3	0.3	1.6	3.2	0.3	0.7
	RTS [h]	0	0	0	0	0	0	0	0
1995	Q_p [m^3/s]	-	-	-	313.47	313.47	313.47	332.43	332.43
	PDE [%]	-	-	-	7.2	7.2	7.2	3.9	3.9
	RTS [h]	-	-	-	2	2	2	3	2
1994	Q_p [m^3/s]	-	-	-	-	-	-	-	361.1
	PDE [%]	-	-	-	-	-	-	-	0.4
	RTS [h]	-	-	-	-	-	-	-	2

4. Conclusions

The individual flood routing model makes it possible to forecast the flow effectively in parts of catchment where direct meaningful surface outflow caused by rainfall does not occur. This situation happens usually in lowlands catchments, however the results of forecasts simulations presented in the paper have shown that there is a possibility to achieve accurate enough forecast also in downstream part of some highland catchment, without any rainfall data, in spite of meaningful uncontrolled inflow occurrence.

References

Fread, D.L., and J. Ming, 1993, *Real-time dynamic flood routing with NWS FLDWAV model using Kalman filter updating*, Proceedings of the Symposium on Engineering Hydrology, Publ. by ASCE, 946-951.

Madsen, H., M.B Butts, S.T. Khu and S.Y. Liong, 2000, *Data assimilation in rainfall-runoff forecasting*, Hydroinformatics 2000, 4th International Conference on Hydroinformatics, Cedar Rapids, Iowa, USA, 23-27 July.

Madsen, H., and R. Cañizares, 1999, *Comparison of extended and ensemble Kalman filter for data assimilation in coastal area modelling*, Int. J. Numerical Meth. in Fluids **31**, 961-981.

Szymkiewicz, R., 2000, *Modelowanie Matematyczne Przepływów w Rzekach i Kanałach*, PWN, Warszawa.

Young, P.C., and C.M. Tomlin, 2000, *Data-based mechanistic modelling and adaptive flow forecasting.* **In:** M.J. Lees and P. Walsh (eds.), "Flood forecasting: what does current research offer the practitioner?", British Hydrological Society Occasional Paper **12**, 26-40.

Accepted September 12, 2006

PUBLS. INST. GEOPHYS. POL. ACAD. SC., E-6 (390), 2006

The Sensitivity Analysis of Runoff from Urban Catchment Based on the Nonlinear Reservoir Rainfall-Runoff Model

Marcin SKOTNICKI and Marek SOWIŃSKI

Institute of Environmental Engineering, Poznań University of Technology
ul. Piotrowo 3a, 60-965 Poznań
email: marcin.skotnicki@put.poznan.pl

Abstract

In the paper the results of the sensitivity analysis of the rainfall-runoff model are presented. Calculations were made on the basis of the nonlinear reservoir model. The influence of the three basic catchment parameters – roughness, length and slope on the outflow hydrograph – was investigated. It was noticed that in the assumed range of parameters the time to the peak outflow is independent of their values. The time to peak is influenced by the rainfall hyetograph shape. The peak outflow depends on a certain combination of catchment parameters called the catchment characteristic. The impact of this characteristic depends on rainfall properties. The obtained results allow to develop the formula to estimate rainfall characteristic influence on the peak outflow without a need of the rainfall-runoff model application.

1. Introduction

The use of a rainfall-runoff model requires adjusting of its parameters values in the model calibration process (Lei and Schilling 1998). This adjusting of parameters values is performed on the basis of an agreement between model output and measurement results. A calibration can be done "manually" by a trial-and-error method or using an optimisation procedure (Boyle et al. 2000). In both methods a preliminary determination of the range of parameters variability is needed. This range depends on physical interpretation of the parameter. A sensitivity analysis is often combined with calibration because it allows an estimation of parameters influence on the model output. In calibration process, only parameters with significant impact on model output should be taken into account (Lei et al. 1999).

Among all parameters of the rainfall-runoff model the ones describing impervious areas play an important role. Due to the high percentage of impervious surfaces in urban catchments these parameters dominate in runoff computation. An outflow from pervious surfaces occurs only if the rainfall intensity exceeds a retention capacity of these areas. An impervious area is characterised by roughness coefficient n, slope s, length (flow path length) L and hydrological losses connected with detention storage and wetting of the catchment surface. This kind of hydrological losses appears at the beginning of the rain event, thus their impact on the remaining part of hyetograph and the runoff hydrograph resulting from it is relatively small. The outflow hydrograph shape is influenced by the parameters describing geometry and hydraulic properties of the catchment – its roughness, slope and length.

In the paper, an alternative approach to traditional sensitivity analysis is presented. In the traditional sensitivity analysis an impact of each parameter is investigated by performing simulations of runoff for the assumed range of parameters. It was shown in the paper that in a nonlinear reservoir model the form of outflow hydrograph depends on a certain combination of parameters called the catchment characteristic C. Consequently, results of the sensitivity analysis of runoff from an urban catchment computed by the nonlinear reservoir model on the catchment characteristic C are presented. Within this analysis an influence of the catchment characteristic C on the peak outflow Q_{MAX} and the time to peak TTP is investigated. A rainfall characteristics influence parameter ε is developed to combine an influence of four main parameters of rainfall on the peak outflow. It allows to extend the sensitivity analysis of the runoff described above on rainfall events.

2. The nonlinear reservoir model

2.1 The basic equations of the model

The nonlinear reservoir model can be described as a simplified form of the kinematic wave model. In the method of runoff calculation applied to this model, a catchment is treated as a rectangular channel with bottom slope s, roughness n, width B and depth h. An outflow from a catchment is computed as an unsteady flow in a channel with a lateral inflow equal to an effective rainfall. The kinematic wave model is described by a set of two equations (Chow 1964, Szymkiewicz 2000):

- the continuity equation

$$\frac{\partial h}{\partial t} + \frac{1}{B} \cdot \frac{\partial Q}{\partial x} = q \tag{1}$$

where: B = catchment width [m]; h = runoff water layer depth [m]; q = rainfall intensity [m/s]; Q = outflow rate [m^3/s], t = time [s]; x = longitudinal coordinate [m].

- the momentum equation, according to which the bottom slope s is equivalent to the friction slope S

$$s = S \tag{2}$$

where s = catchment slope [-]; S = friction slope [-].

These relations can be treated as a specific form of de Saint-Venant equations in which the momentum equation is simplified by neglecting the inertia and the pressure forces. Consequently, this equation is reduced to the steady flow formula and can be rewritten as in the form of Manning relationship:

$$Q = B \cdot \frac{\sqrt{s}}{n} \cdot h^{\frac{5}{3}} \tag{3}$$

where n = Manning's roughness coefficient [$s/m^{1/3}$].

The continuity equation (1) describes the changes of water layer depth along a flow path (catchment length) in time. In practical applications calculations are often limited to one cross-section located at the end of a catchment. Thus, this equation can be simplified to an ordinary differential equation:

$$\frac{dh}{dt} + \frac{Q}{A} = q \tag{4}$$

where A = catchment area [m^2].

Substituting relation (2) for Q, the continuity equation can be written as:

$$\frac{dh}{dt} + \frac{\sqrt{s} \cdot h^{\frac{5}{3}}}{n \cdot L} = q \tag{5}$$

where L = catchment length (runoff path length) [m].

This equation is known as the nonlinear reservoir equation and can be solved iteratively, e.g. by means of Newton method assuming the initial condition t_O and the boundary condition h_O.

2.2 The catchment characteristic C

The three parameters describing catchment properties: roughness n, slope s and length L occur in both kinematic wave model equations (Huber and Dickinson, 1992). They can be aggregated to give an expression called the catchment characteristic C:

$$C = \frac{\sqrt{s}}{n \cdot L} \tag{6}$$

where C = catchment characteristic [$s^{-1} \cdot m^{-2/3}$].

Using the catchment characteristic defined above, the continuity and the momentum equations can be written as follows:

$$\frac{dh}{dt} + C \cdot h^{\frac{5}{3}} = q \tag{7}$$

$$Q = A \cdot C \cdot h^{\frac{5}{3}} \tag{8}$$

A change of catchment parameters values without change of the catchment characteristic value does not influence the model output. There are many sets of catchment parameters fulfilling relations (7)-(8). Determining an optimal set of catchment parameters in a calibration process requires an estimation of parameter variability limits. The range of parameters is confined by physical conditions.

3. The sensitivity analysis of runoff

3.1 The scope of analysis

The sensitivity analysis was carried out in order to determinate the influence of the catchment characteristic C value on a runoff hydrograph form. It was assumed that the runoff hydrograph is described by two parameters – the time to peak outflow (TTP) and the peak outflow Q_{MAX}.

Calculations were performed for the artificial impervious catchment of 1.0 ha area. Hydrological losses were neglected, so rainfalls can be identified with effective rainfalls. Within analysis, 104 historical rain events recorded in the city of Poznan in years 2002-2004 were used. Rainfall measurements were performed at two gauging stations equipped with tipping bucket rain gauges. The following ranges of the catchment parameters values were assumed:

- roughness n 0.010-0.030 [$s/m^{1/3}$]
- length L 50-150 [m]
- slope s 0.001-0.100 [-]

Thirty combinations of these parameters were used for the computation of the catchment characteristic C which was located in the range from 0.022 to 0.316. The next stage of analysis was performed for characteristics from these intervals.

3.2 The influence of catchment characteristic C on time to peak outflow (TTP)

The time to peak depends on a rain hyetograph representation. The nonlinear reservoir model requires rain data in a discrete form. A rainfall is represented by a set of impulses with the duration τ and the intensity q or the depth H.

It was observed that the time to peak is always equal to the time of the end of a certain rain impulse in a hyetograph. Most often this is the maximal rainfall inten-

sity (or the maximal depth). Hence the time to peak outflow is a function of the rainfall time resolution τ.

No influence of the catchment characteristic C on the time to peak outflow (TTP) was noticed in the assumed range of C values, i.e. for the majority of analysed rain events the time to peak was the same regardless of the characteristic C value. A change of TTP took place in two cases:

- If several rainfall impulses with the same or similar intensity (depth) dominated the hyetograph, the time to peak outflow was located in the range of these impulses (Fig. 1a).
- In a multi-peak hyetograph the outflow peak optionally "jumped" from one rainfall peak to another (Fig. 1b).

In both situations the time to peak was always a multiple of the rainfall time resolution τ.

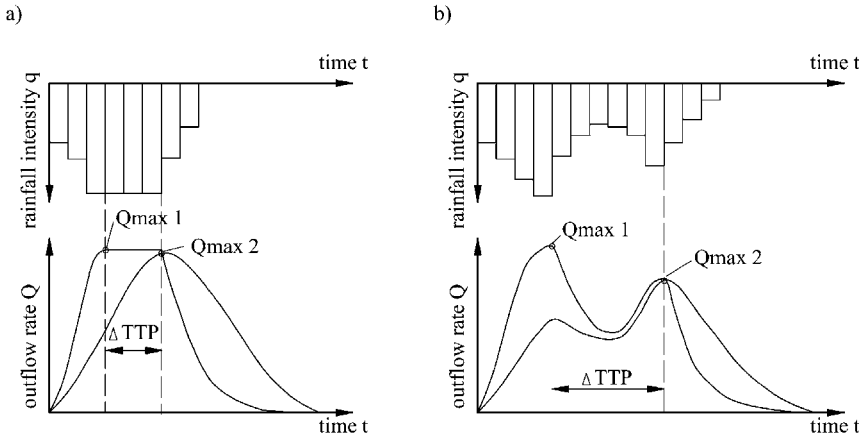

Fig. 1. The graphical interpretation of time to peak outflow (TTP) variability.

3.3 The influence of catchment characteristic C on the peak outflow Q_{MAX}

The peak outflow Q_{MAX} can be expressed as a function of the catchment characteristic C by the following power equation:

$$Q_{MAX} = \omega \cdot C^{\varepsilon} \tag{9}$$

where ε, ω are the power equation coefficients [-].

The coefficient ω is a measure of the absolute outflow value. First of all, it depends on rainfall intensity and will not be analyzed in further parts of this paper. The

exponent ε is a measure of catchment characteristic C influence on the peak outflow. If this influence is weak, the exponent value is close to zero and the whole expression C^{ε} is approaching unity. The ε value equal to unity indicates a linear relationship between the catchment characteristic C and the peak outflow.

It was observed that the influence of catchment characteristic C on peak outflow depends on individual rainfall properties, which are expressed by the exponent ε. For the considered 104 rain events, values of the exponent ε were located in range from 0.0654 to 0.7794. The mean value of ε was equal to 0.4285.

Combining the catchment characteristic (Eq. (6)) with power relation (Eq. (9)) yields the following equation (10) which enables, after some rearrangements (Eqs. (11)), to determine an impact of individual catchment parameters on the peak outflow:

$$Q_{MAX} = \omega \cdot C^{\varepsilon} = \omega \cdot \left(\frac{\sqrt{s}}{n \cdot L} \right)^{\varepsilon} \tag{10}$$

$$Q_{MAX} = \omega \cdot \left(\frac{\sqrt{s}}{n} \right)^{\varepsilon} \cdot L^{-\varepsilon} = \omega \cdot \left(\frac{\sqrt{s}}{L} \right)^{\varepsilon} \cdot n^{-\varepsilon} = \omega \cdot \left(\frac{1}{n \cdot L} \right)^{\varepsilon} \cdot s^{0.5 \cdot \varepsilon} \tag{11}$$

The influence of catchment roughness n and length L represented by the exponent ε is equal to each other but the impact of slope s is less by half. It should be noticed that in literature other parameters than the ones mentioned above are pointed as the most important for runoff modelling (Zaghloul 1981, Kowalska and Prystaj 1996, Lei et al. 1999). This can be a result of taking ranges of parameters variability different from those assumed by authors. For instance, assuming a narrow range of parameter variability can diminish its impact on the peak outflow.

The sensitivity analysis of the peak outflow Q_{MAX} on the catchment characteristic C makes it possible to estimate an influence of each parameter. It was also confirmed by an analysis performed by the author (Skotnicki 2006).

4. The relation between rainfall parameters and exponent ε of power equation

An analysis of the exponent ε calculation performed for 104 rainfalls for selected values of C allows to formulate the following conclusions:

- For rain events of long duration with small variability of intensity in time the values of the exponent ε are also small. In the extreme case of uniform rainfall intensity, the runoff is constant. Its value is equal to the product of a catchment area and a rainfall intensity.
- The largest values of exponent ε were observed for the rain events with the significant dominating peaks.

Knowledge about the impact of rainfall parameters on the peak outflow can be used in the rain event selection for model calibration. A small value of the exponent ε implies a small sensitivity of the peak outflow on changes of these parameters. Criterion of accepted accuracy of Q_{MAX} evaluation is fulfilled in this case for a broad range of catchment parameters – too wide to determine the relatively narrow range required for calibrated parameters. It refers to the statement of Schilling that the aim of calibration is to establish a set of parameters or their range, possibly narrow. Thus, rainfalls characterized by a small value of the exponent ε are not useful in the model calibration. The influence of the rainfall parameter on model output can be investigated by sensitivity analysis. Instead of traditional sensitivity analysis which requires application of special mathematical tools based on FOSM or Monte Carlo methods developed at computer models used for performing large number of simulations (e.g. in Monte Carlo method) a simple method for rain parameter influence estimation is proposed. It is based on developing relationship between rainfall parameters and the exponent ε which combines influences of a rainfall event i.e. all rainfalls parameters on the peak runoff. It allows to estimate rainfall parameters influence on the peak runoff without necessity of computation, i.e. without application of any rainfall-runoff model.

By derivation of this relationship, the following assumptions were made:

- The formula describing the relationship will be developed for performing a simplified version of the sensitivity analysis, results of which can be less accurate than results of a full sensitivity analysis based on simulation of rainfall-runoff process.
- The rainfall parameters introduced in the formula should have unique interpretation and should be easy to determine.
- The formula should be simple and easy to practical use.

Taking into account the assumptions specified above, four rainfall parameters were chosen:

- the total rainfall depth H [mm],
- the rainfall duration time T [min],
- the ratio of maximum to mean rainfall intensity q_{MAX}/q_{AV} [%],
- the relative time to peak rain intensity t_M [-]. This time is defined as ratio of initial time of peak rainfall impulse to the total rainfall duration time. In the case of a multiple peak, the first impulse is taken into consideration.

A linear function was chosen to describe the relation between the exponent ε and rainfall parameters:

$$\varepsilon = \alpha \cdot H + \beta \cdot T + \gamma \cdot q_{MAX/AV} + \delta \cdot t_M + \varphi \tag{12}$$

where α, β, γ, δ,φ are the regression equation coefficients [-],

Parameters α, β, γ, δ, φ were computed using multiple linear regression technique. It required evaluation of the exponent ε, which was performed within analysis based on the set of 104 rain events and the nonlinear reservoir model. Ranges of rain parameters used in the analysis are shown in Table 1.

Table 1

Ranges of rain parameters used in the analysis

Measurement sets		Rainfall parameter			
		H [mm]	T min	$q_{MAX/AV}$ [-]	t_M [%]
Subset A	Range	3.0-30.6	10-100	1.0-7.8	5-100
	Average	6.8	62.6	3.2	33.4
Subset B (verification)	Range	3.0-10.0	10-100	1.3-5.6	5-93
	Average	5.1	64.9	2.7	32.0

The whole set of rainfall measurements consists of two subsets. Subset A containing 54 rain events recorded at one gauging station was used for determination of regression coefficients in Eq. (12). For this purpose the Excel spreadsheet was used. The verification of the derived equation was performed using the 50 rainfalls (subset B) recorded at second gauging station. An application of the procedure described above resulted in the following form of Eq. (12):

$$\varepsilon = 0.05 \cdot q_{MAX/AV} - 0.03 \cdot (T + t_M) - 0.01 \cdot H + 0.6 \tag{13}$$

The mean relative error of exponent ε evaluation for subset B amounts to 30%. The mean absolute error is 0.10 and the mean exponent ε value is equal to 0.41. This level of exponent ε accuracy can be assumed as satisfactory keeping in mind the assumption about the simplified version of the proposed sensitivity analysis.

5. Conclusions and remarks

- The impact of the catchment characteristic C as well as individual catchment parameters on runoff hydrograph depends on rainfall characteristics.
- For an individual rainfall the influence of basic catchment parameters on Q_{MAX} depends on the type of parameter. The value of the exponent ε, which is a measure of this influence, is the same for roughness n and length L and less by half for slope s.
- The time to peak outflow depends on a rainfall hyetograph shape and its value is a multiple of rainfall time resolution τ. Hence, the precise reproduc-

tion of time, and for large catchments also spatial variation of the rainfall is required for proper modelling of runoff.

- The introduction of the catchment characteristic C reduces the number of catchment parameters from three to one without loss of model properties. Information about model sensitivity for one parameter allows to determine the sensitivity for the remaining two parameters of the catchment.
- The developed formula for exponent ε calculations (eq. 13) allows to estimate rainfall parameters influence on the peak runoff without necessity of the rainfall-runoff model application.

References

Boyle, D.P., H.V. Gupta and S. Sorooshian, 2000, *Toward improved calibration of hydrologic models: Combining the strengths of manual and automatic methods*, Water Resour. Res. **36**, 12.

Chow, V.T., 1964, *Handbook of Applied Hydrology*, McGraw-Hill, New York.

Huber, W.C., and R.E. Dickinson, 1992, *Storm Water Management Model, Version 4: User's Manual*, Environmental Research Laboratory, U.S. EPA, Athens, Georgia.

Kowalska, W., and A. Prystaj, 1996, *Simulation of Unsteady Storm Runoff in Storm Sewage System*, Monografia 206, Seria Inżynieria Sanitarna i Wodna, Wydawnictwo Politechniki Krakowskiej, Kraków (in Polish).

Lei, J., and W. Schilling, 1998, *Systems modeling revisited – verification, confirmation and the role of uncertainty analysis*, Proceedings 3rd International Conference Hydroinformatics 98, Copenhagen, 24-26 August, Balkema, Rotterdam.

Lei, J., J. Li and W. Schilling, 1999, *Stepwise hypothesis test model calibration procedure of urban runoff design model and an alternative of Monte-Carlo simulation*, Proceedings 8th International Conference Urban Storm Drainage, Sydney, Australia, 30 August – 3 September 1999.

Skotnicki, M., 2006, *Comparative analysis of sensitivity of chosen models of urban catchment runoff*, Hydraulika Tranzytowych Systemów Inżynierii Wodnej, Zeszyt Monograficzny nr 2, Gdańsk (in Polish).

Szymkiewicz, R., 2000, *Mathematical modeling of flow in rivers and channels*, Wydawnictwo Naukowe PWN, Warszawa (in Polish).

Zaghloul, N.A., 1981, *SWMM model and level of discretization*, J. Hydraulics Div. **107**, 11.

Accepted September 12, 2006

PUBLS. INST. GEOPHYS. POL. ACAD. SC., E-6 (390), 2006

Mathematical Description of Transport and Vertical Sorting of Graded Sediment in Rivers

Łukasz SOBCZAK[1] and Leszek M. KACZMAREK[1,2]

[1]Institute of Hydroengineering of the Polish Academy of Sciences
Kościerska 7, 80-328 Gdańsk, Poland
email: lukasz.sobczak@ibwpan.gda.pl

[2]University of Warmia and Mazury
Oczapowskiego 11, 10-736 Olsztyn, Poland

Abstract

Three-layer sediment transport model was originally developed for hydrodynamic conditions induced by waves and currents in coastal zones (Kaczmarek 1999). With some modifications, the model can be applied for the description of transport and vertical sorting of graded sediment in rivers. Both theoretical approach and some chosen results of the study are presented in the paper.

1. Introduction

Three-layer sediment transport model was developed for the hydrodynamic conditions of coastal zone (Kaczmarek 1999). A lot of calculations and comparisons with experimental data show that for intensive transport conditions the model gives good results (Kaczmarek et al. 2004a). Following Kaczmarek et al. (2004b) and Sobczak (2005), the model is being applied for the description of sediment transport in rivers. The paper presents details of mathematical description and some chosen results of calculations.

2. Mathematical model

2.1 Sediment transport

Knowing the concentration profile $c(z)$ and velocity profile $u(z)$ of sediment, the transport over depth h is calculated on the basis of the following equation:

$$q = \int_0^h u(z)\, c(z) dz \ , \tag{1}$$

2.2 Description of vertical sorting and transport of graded sediment in rivers

Following Kaczmarek (1999), sediment transport column is divided into three layers: bed, contact and outer layer (Fig. 1). Concentration and velocity profiles of sediment are described using different equations in each layer, due to different character of transport processes.

It is assumed that in the bed layer, because of the interaction effects between closely packed grains, finer fractions are retarded and, as a result, all fractions move as a mixture, with the same velocity and concentration. Further, upward from the bed, as a consequence of mechanisms of momentum exchange inside the contact layer, all fractions move with different transport rates. Thus, the above approach describes the situation when the most intensive sorting takes place during the pickup processes. After that, in the outer layer, it is assumed that the grain size distribution remains fairly constant.

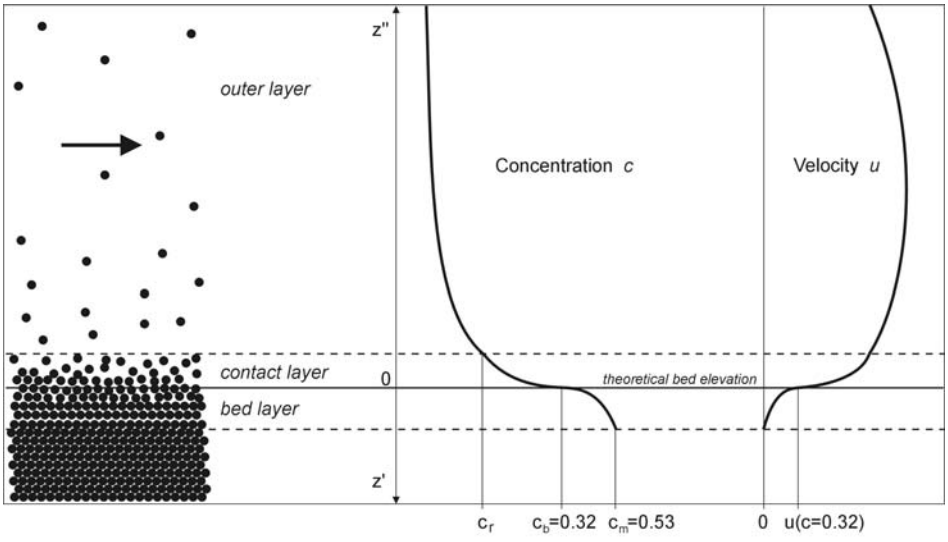

Fig. 1. Three-layer description of sediment transport.

1. Bed layer

It is assumed that the individual fractions, contained by the elementary volumes, closely interact with each other, i.e. fine grains are retarded by less mobile coarser ones. Consequently, all fractions are moving as a mixture with the same representative velocity and concentration. The profiles of representative velocity $u(z')$ and con-

centration $c(z')$ in the bed layer are proposed to be found from the set of equations (2) and (3). The hydrodynamic conditions and shear stress, being main reason of particles movement, are represented by friction velocity u_f. Original equations were derived by Kaczmarek (1999). Recently, the equations were modified by addition of gravity components acting on sediment particles, considering the bed slope inclined by angle ξ. The approach origins from theory of Sayed and Savage (1983), developed for the flow of dry granular material on the slope.

$$\alpha^0\left(\frac{c-c_0}{c_m-c}\right)\sin\varphi\sin 2\psi+\mu_1\left(\frac{\partial u}{\partial z'}\right)^2=\rho u_f^2+\left(\rho_s-\rho\right)g\sin\xi\int_0^{z'}c\,dz' \tag{2}$$

$$\alpha^0\left(\frac{c-c_0}{c_m-c}\right)\left(1-\sin\varphi\sin 2\psi\right)+\mu_{0,2}\left(\frac{\partial u}{\partial z'}\right)^2=\left(\frac{\mu_{0,2}}{\mu_1}\right)\Bigg|_{c=c_0}\rho u_f^2+\left(\rho_s-\rho\right)g\cos\xi\int_0^{z'}c\,dz' \tag{3}$$

where: z' = local vertical spatial coordinate for the bed layer; ρ = density of fluid; ρ_s = density of sediment; α^0 = constant described in (van Rijn 1993); c_m = maximum concentration of the bed sediment; c_0 = concentration of sediment at the theoretical bed elevation; φ = quasi-static angle of internal friction; ψ = angle between the major principal stress and the horizontal axis (Kaczmarek et al. 2004b); $\mu_{0,2}$, μ_1 = functions of the concentration, expressed by (Sayed and Savage 1983) and (Sobczak 2005); ξ = angle corresponding to the bed slope.

$$\psi=\frac{\pi}{4}-\frac{\varphi}{2} \tag{4}$$

$$\frac{\mu_1}{\rho_s d^2}=\frac{0.03}{(c_m-c)^{1.5}} \tag{5}$$

$$\frac{\mu_{0,2}}{\rho_s d^2}=\frac{0.02}{(c_m-c)^{1.75}} \tag{6}$$

where: d = representative diameter of sediment (d_{50} in case of graded sediment).

For the calculations the following values were assumed and tested: $\alpha^0/(\rho_s g d) = 1$, $c_m = 0.53$, $c_0 = 0.32$ and $\varphi = 24.4°$. The set of equations (2) and (3) is solved using iteration with numerical integration. Friction velocity u_f is calculated on the basis of the procedure presented by Sobczak (2005). The flow velocities can be taken directly from the measurements, like in the present study, or as a result of calculations (e.g. from de Saint-Venant equation set). The example of concentration profiles in the bed layer for the same particle diameter and flow conditions (d = 0.4 mm, u_f = 0.12 m/s) and for different river bed slopes is presented in Fig. 2. As it is seen, the differences between the calculated concentration profiles in the range of small bed

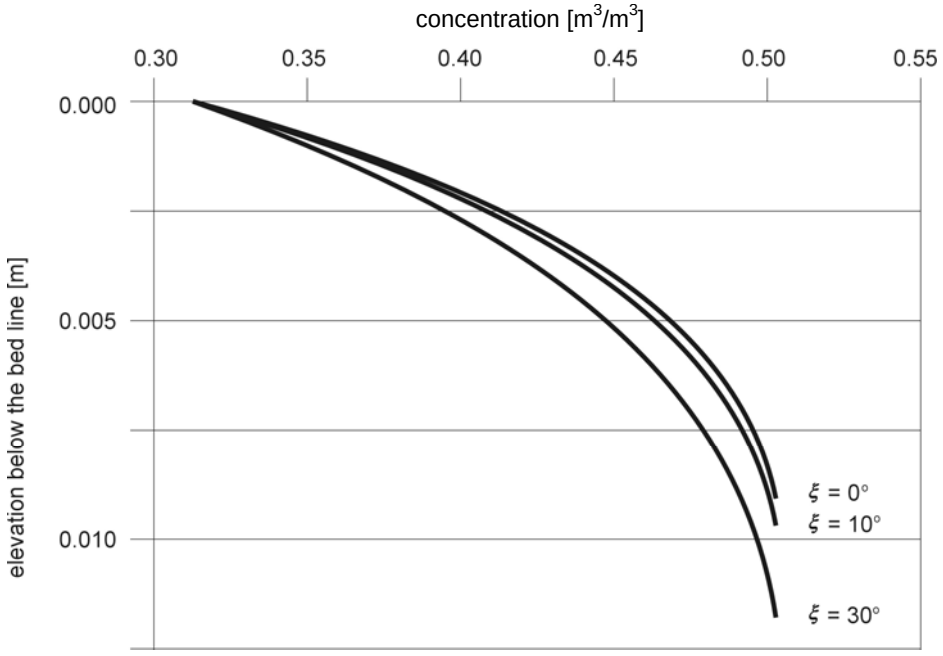

Fig. 2. Concentration profiles for different river bed slopes (d = 0.4 mm, u_f = 0.12 m/s).

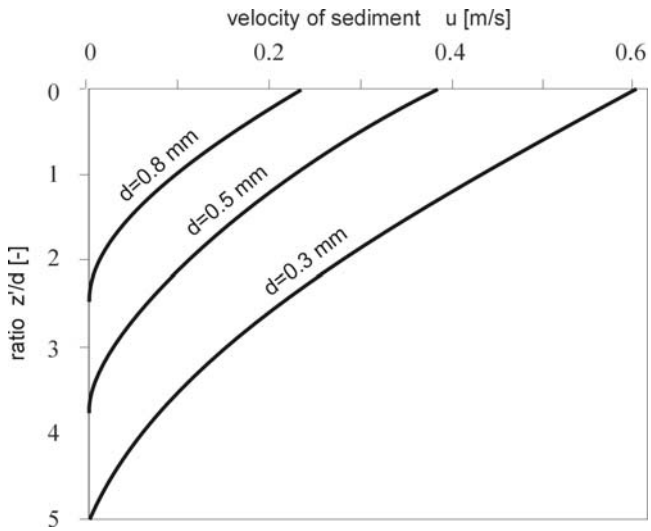

Fig. 3. Velocity profiles in bed layer for different sediment diameters under the same flow conditions (u_f = 0.12 m/s).

slopes are not too significant. However, in the case of bed forms, where slope is changing rapidly on short distances, the gravity component can be important.

The examples of velocity profiles in function of dimensionless ratio *z'/d* for different sediment size under the same hydrodynamic conditions ($u_f = 0.12$) are presented in Fig. 3. It is seen that the smaller the sediment size, the smaller the thickness of active layer. Please note that the vertical ranges of presented curves are: 5∗0.3 = 1.5 mm, 3.8∗0.5 = 1.9 mm and 2.5∗0.8 = 2.0 mm.

2. Contact layer

In the contact load layer, the *i*-th fraction velocity and concentration are modelled using the following equations, proposed by Deigaard (1993):

$$\left[\frac{3}{2}\left(\alpha_s \frac{d}{w_s}\frac{\partial u_c}{\partial z''}\frac{2}{3}\frac{s+c_M}{c_D}+\beta_s\right)^2 d^2 c_c^2 (s+c_M)+l^2\right]\left(\frac{\partial u_c}{\partial z''}\right)^2 = u_f^2 \tag{7}$$

$$\left[3\left(\alpha_s \frac{d}{w_s}\frac{du_c}{dz''}\frac{2}{3}\frac{s+c_M}{c_D}+\beta_s\right)^2 d^2 \frac{du_c}{dz''}c_c + l^2 \frac{du_c}{dz''}\right]\frac{dc_c}{dz''} = -w_s c_c \tag{8}$$

where: z'' = local vertical coordinate; $u_c(z'')$ = sediment velocity in the contact layer; $c_c(z'')$ = sediment concentration in the contact layer; α_s, β_s = coefficients according to Deigaard (1993); c_M = added mass coefficient; c_D = drag coefficient, l = mixing length $l = \kappa z'' = 0.4 z''$; κ = von Karman constant; ν = kinematic viscosity; s =relative density of sediment $s = \rho_r / \rho_w$; w_s = settling velocity.

The continuity of transport is assumed at the boundary between bed and contact layers. The values of velocity and concentration in the contact layer at the theoretical bed elevation correspond to the calculations in bed layer.

The thickness of the contact layer is found using van Rijn's formula for saltation height (van Rijn 1993):

$$\delta = 0.3 D_*^{0.7} d\, T^{0.5} \tag{9}$$

where: D_* = dimensionless diameter calculated as presented in (10); T = transport stage parameter described by (11).

$$D_* = d\left((s-1)g/\nu^2\right)^{1/3} \tag{10}$$

$$T = \left(\tau - \tau_{cr}\right)/\tau_{cr} \tag{11}$$

where: τ = shear stress; τ_{cr} = critical shear stress according to Shields.

The solution of the set of equations (7) and (8) in the form of velocity and concentration profiles is found using numerical iteration. The thickness of contact layer in calculation of sediment transport is limited to the saltation height δ.

The examples of concentration and velocity profiles for different sediment size for the same flow conditions (u_f = 0.12 m/s) are presented in Fig. 4.

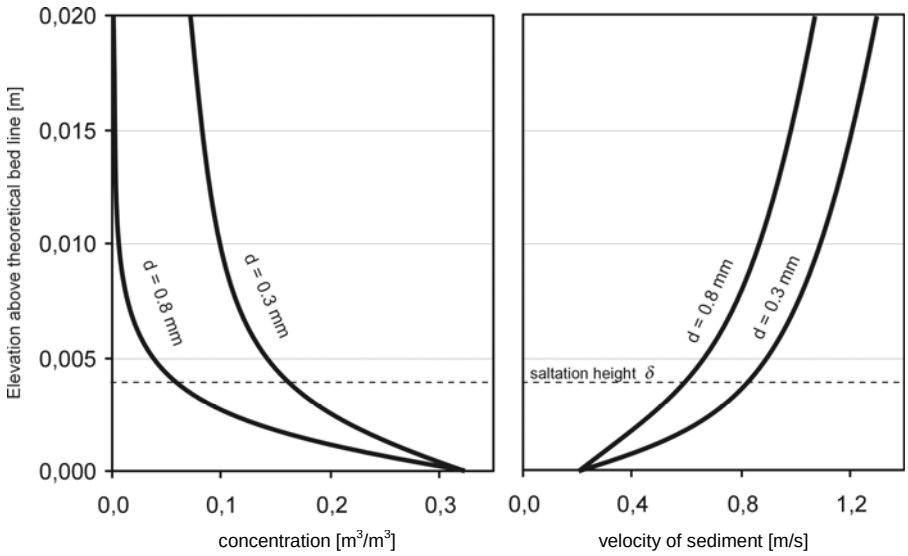

Fig. 4. Example of concentration and velocity profiles in the contact layer for different sediment diameters.

3. Outer layer

In the outer layer the *i*-th fraction concentration profile is described using Rouse formula. It is derived on the basis of advection-diffusion equation. The reference concentration is assumed to be equal to those computed at van Rijn's saltation height $c(\delta)$ in the contact layer.

The results of computations versus field data are presented in Fig. 5. Dots represent measured concentrations of suspended sediment at Lower Vistula River recorded in 2003 (km 863+000). Measurements were made using laser particle size analyser LISST-100. Concentrations of 32 size classes were recorded simultaneously by one laser shot at frequency of 1 Hz. The device was slowly pulled from the river bed to the water surface. This technique allowed us to collect vertical concentration profiles for individual fractions of graded sediment (simultaneously measured values c_i at depths h_i). Additionally, flow velocities were measured, needed as input for calculations of friction velocity u_f.

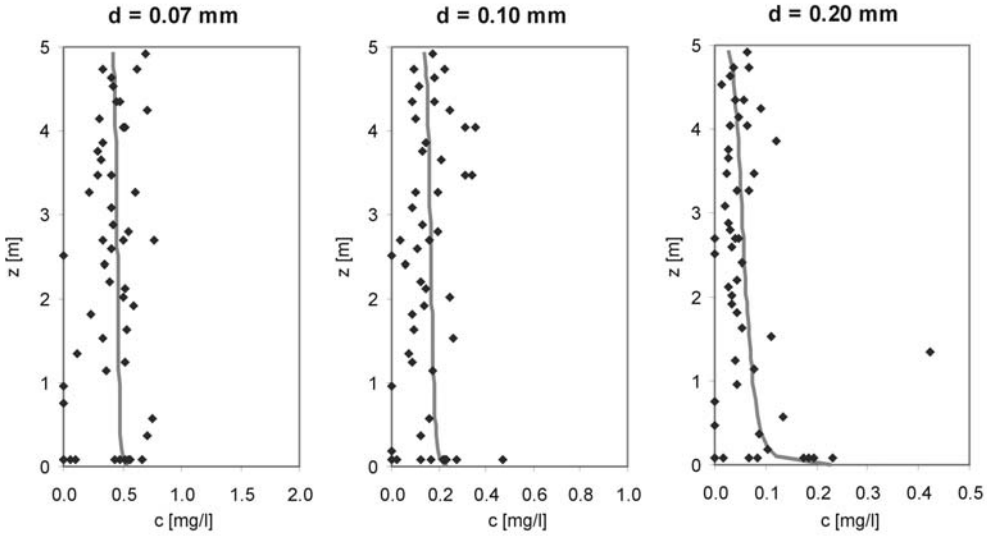

Fig. 5. Results of calculations of concentration profile in outer layer (solid lines) versus measured data (dots).

3. Summary

Sediment transport in rivers must be described with respect to the different transport character in different regions over water depth. In the present approach, sediment transport is modelled as a whole profile in three layers, starting from the elevation below theoretical bed line, where no motion of particles appears, and finishing at the water surface elevation. Description is made with respect to continuity of concentration and velocity profiles between layers.

Other important feature is the capability of vertical sorting modelling. It takes place mostly in the near vicinity of the bed, and it is crucial for the structure of suspended material. Consequently, it is very important for calculations of bed elevation changes. Except of modelling of vertical sorting, the advantage of the model is the capability of prediction of reference concentration, which is very important for calculation of suspended sediment concentration profile. In the present model, it results from the continuous vertical distributions of velocity, concentration and sediment transport. Thus, the authors believe that the proposed approach will find application in practice.

The next step will be to extend the model to make it capable of morphological change prediction, with respect to bed grain size distribution. Knowing changes of transport in time, calculations will be done using sediment transport continuity equation.

The work on verification of the model in rivers is being in progress, as well as comparisons of total transport calculations with well known empirical formulas e.g. Meyer-Peter and Müller, or Skibiński formula. Initial estimates are promising. Details of comparisons will be presented in the near future.

References

Deigaard, R., 1993, *Modelling of sheet flow: dispersion stresses vs. the diffusion concept*, Prog. Rep. 74, Inst. Hydrodyn. and Hydr. Eng., Tech. Univ. Denmark, 65-81.

Kaczmarek, L.M., 1999, *Moveable Sea Bed Boundary Layer and Mechanics of Sediment Transport*, Institute of Hydroengineering PAS, Gdańsk, 209 pp.

Kaczmarek, L.M., J. Biegowski and R. Ostrowski, 2004a, *Modelling cross-shore intensive sand transport and changes of bed grain size distribution versus field data*, Elsevier Coastal Engineering **51**, 501-529.

Kaczmarek, L.M., M. Robakiewicz, Ł. Sobczak and J. Biegowski, 2004b, *Theoretical and experimental investigations on vertical mixing and sorting of sand in rivers and coastal zones*, Ninth International Symposium on River Sedimentation, October 18–21, 2004, Yichang, China, 1363-1370.

Sayed, M., and S.B. Savage, 1983, *Rapid gravity flow of cohesionless granular materials down inclined chutes*, J. Applied Mathematics and Physics ZAMP **34**, 84-100.

Sobczak, Ł., 2005, *A procedure for calculating of sand transport in rivers*, XXV International School of Hydraulics, 251-257.

van Rijn, L.C., 1993, *Principles of sediment transport in rivers, estuaries and coastal seas*, Aqua Publications.

Accepted September 12, 2006

PUBLS. INST. GEOPHYS. POL. ACAD. SC., E-6 (390), 2006

Initial Study of Two-Shape-Parameter Flood Frequency Distributions

Witold G. STRUPCZEWSKI and Iwona MARKIEWICZ

Institute of Geophysics, Polish Academy of Sciences
Ks. Janusza 64, 01-452 Warsaw, Poland
emails: wgs@igf.edu.pl, iwonamar@igf.edu.pl

Abstract

The primary objective of flood frequency analysis (FFA) is the estimation of upper quantiles of probability distribution. Because of the fact that many natural events, river flows in particular, have a physical lower bound at zero, one can doubt whether the lower bound is the best third parameter for flood frequency models. Maybe, assuming the lower bound as zero and introducing a second shape parameter for getting greater flexibility is more adequate? In this paper the background and arguments for using two shape parameters instead of the lower bound parameter are presented. Three ways of introducing the second shape parameter are considered in respect to the commonly used FF models, and Gamma distribution serves as an example. Besides, one outlines the selection procedure of the best fitted probability distribution model for the two competing models, i.e. the three-parameter distribution with lower bound parameter and its counterpart, the two-shape-parameter distribution lower bounded at zero.

1. Introduction

Flood frequency analysis (FFA) entails estimation of the upper tail of a probability density function (PDF) of peak flows obtained from either the annual duration series or partial duration series. However, the true underlying distributional form cannot be identified either at a single-site or on a regional basis, so the view on the competitiveness or goodness of various parameter estimation methods in FFA had changed. Even if the true distribution would be known, in all probability, it contains too many parameters. These parameters cannot possibly be estimated reliably and efficiently from a hydrological sample which usually is of relatively small size, meaning that strictly such a PDF cannot be applied. Since no simple model can reproduce the data set in its entire range of variability and the interest in FFA is in the estimation of upper quan-

tiles, a statistical approach, based on the assumption of the known true frequency distribution function, falls short of accuracy of high floods. Then the interest is in the assessment of the ability of various parsimonious models together with estimation methods for reproduction of the upper tail of hypothetical parent distributions for hydrological sample sizes.

In order to reflect perennial river flow regime as well as to increase flexibility of models in respect to variety of data sets, the lower bound parameter is routinely added. It transforms Gamma distribution to Pearson III distribution, Log-logistic distribution to Generalized Log-logistic distribution, Log-Gumbel to Generalized Extreme Value distribution, and so on. On the other hand, one can observe that many natural phenomena have a physical lower bound at zero. Taking into account that an interest in FFA is in the estimation of the upper tail of distribution and that the assumed underlying distribution is not correctly specified, one can doubt whether the lower bound is the best third parameter for flood frequency models. So, going along this line, an introduction of the second shape parameter instead of the lower bound parameter (assumed as zero) is suggested in the paper.

In flood frequency analysis a probability density function (PDF) is selected more or less subjectively from among asymmetric PDFs of continuous type. The most commonly used in FFA distributions are considered here, namely: Gamma, Weibull, Inverse Gaussian (Linear Diffusion), Log-normal, Log-Gumbel, Log-logistic and Pareto. The last three of them are 'heavy-tailed' distributions, which presently are believed to be proper probability functions of extreme floods (e.g. Katz et al. 2002).

1.1 Literature review

There are only few publications recommending the use of two-shape-parameter models for extreme events. Rozdestvenskij and Chebotarev (1974), considering Pearson type III distribution, recommended replacement of the location parameter by the second shape parameter. The same function was used by Polish hydrologist Strupczewski (1964) for the approximation of floods wave shapes. Moreover, French statistician Halphen proposed in 1941 a family of Halphen distributions which have a lower bound at zero and contain two shape parameters. Because of their complex form involving Bessel functions and exponential factorial functions, Halphen's distribution system (Morlat 1956) has remained in obliviation for several years. Recently Perreault et al. (1999) revisited the three types of Halphen distributions, finding that their flexible shapes and tail properties make them excellent candidates for frequency analysis of extremes. Mielke and Johnson (1974) proposed the use of the beta-κ and beta-*P* distributions in hydrology and meteorology. Perhaps due to the computational problems the two-shape-parameter models did not come into practice of FFA. However nowadays, the progress achieved in numerical methods and computers accessibility, all these make applications of such models in FFA possible.

2. Arguments for using two-shape-parameter flood frequency distributions

In the statistical modeling of natural events, river flows in particular, a distribution should have a lower bound at zero, because many natural phenomena have a physical lower bound at zero and moreover the estimation of a parameter that defines the support of the random variable often represents technical difficulties. However, to obtain greater flexibility to fit a large variety of data sets, adding a second shape parameter becomes desirable.

For any lower bounded at zero two-parameter distributions, in the range where the three first moments exist, the skewness (C_S) is an increasing function of the variation coefficient (C_V), i.e., for variability range $0 \le x \le \infty$ the relations $C_S = \varphi(C_V)$ hold and $\partial C_S / \partial C_V > 0$. The same holds for linear moments $\tau_3 = \phi(\tau)$ and $\partial \tau_3 / \partial \tau > 0$. If for a given sample and an assumed PDF the $\hat{C}_S$ and $\hat{C}_V$ values are such that $\hat{C}_S < \varphi(\hat{C}_V)$, then the moment estimate of the lower bound parameter will get a negative value $(\hat{\varepsilon} < 0)$ as well as the estimates of the lower quantiles of the distribution. Similarly, applying the *L*-moments technique, if $\tau_3 < \phi(\tau)$ then $\hat{\varepsilon} < 0$ as well as the lower quantile estimates. A large negative value of the lower bound estimate $(\hat{\varepsilon} << 0)$ had been considered (e.g. Rozdestvenskij and Chebotarev, 1974) as an evidence of an improper choice of the flood frequency model. Obviously, the true at-site PDF must not be negatively bounded. Figure 1 shows the relation $C_S = \varphi(C_V)$ for various lower bounded two-parameter distributions. Similar relations can be shown for *L*-moment ratios.

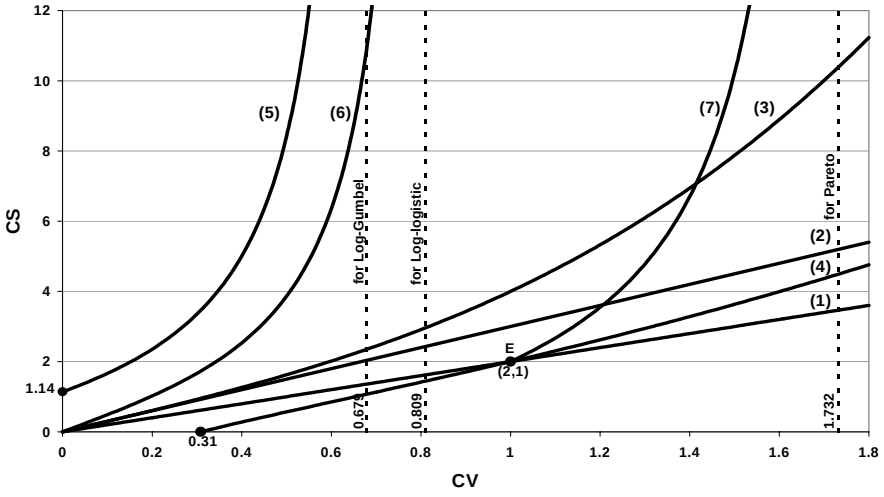

Fig. 1. Relation C_s vs. C_v for: (1) Gamma; (2) Inverse Gaussian (Linear Diffusion); (3) Log-normal; (4) Weibull; (5) Log-Gumbel; (6) Log-logistic; (7) Pareto; E Exponential.

3. Three ways of introducing the second shape parameter

Let $f(x, \alpha, \beta)$ be the PDF of lower bounded at zero distribution, where α and β are the scale and shape parameters. There are three ways, Tx, Tf, TF, for adding the second shape parameter. Each of them does not change the variability range, i.e. $0 \le x \le \infty$.

Tx. Transformation of the variable by putting $x = y^n$. Then the PDF of y is

$$g(y;\alpha,\beta,n) = |n| y^{n-1} f(x;\alpha,\beta) \tag{1}$$

and the quantiles are related by $y(F) = [x(F)]^{1/n}$.

Tf. Density transformation by raising $f(x, \alpha, \beta)$ to the power:

$$g(x;\alpha,\beta,n) = [f(x;\alpha,\beta)]^n \Big/ \int_0^\infty [f(x;\alpha,\beta)]^n \, dx \ . \tag{2}$$

TF. Power transformation of the cumulative distribution function $F(x;\alpha,\beta)$:

$$G(x;\alpha,\beta,n) = [F(x;\alpha,\beta)]^n \tag{3}$$

to have $G(x=0;\alpha,\beta,n) = 0$ and $G(x=\infty;\alpha,\beta,n) = 1$, the exponent n should be a positive real value. Then the PDF is:

$$g(x;\alpha,\beta,n) = n[F(x;\alpha,\beta)]^{n-1} f(x;\alpha,\beta) \ ; \quad n > 0 \ . \tag{4}$$

Note that the PDF [Eq. (5)] will be explicitly defined if $F(x)$ has a closed form.

Table 1

Feasibility of second shape parameter addition

Distribution function	Tx	Tf	TF
Gamma	+	–	+ –
Weibull	–	+	+ –
Inverse Gaussian	+	+	+ –
Log-Normal	–	+	+ –
Log-Logistic	–	+	+
Log-Gumbel	–	+	–
Pareto	+	+	+

None of the ways of introducing the second shape parameter is feasible for every distribution (Table 1). In some cases, the transformation does not give the second shape parameter, i.e. after conversion of the transformed PDF one gets the initial

distribution function (marked by "–"); in other cases, the transformation is inefficient (marked by "+ –").

4. Gamma distributions with two shape parameters

As an example, the result of the transformation Tx of the Gamma distribution is given below:

$$g(y;\alpha,m,n)=\frac{|n|\alpha^{(m+1)/n}}{\Gamma\left((m+1)/n\right)}y^{m}\exp[-\alpha\cdot y^{n}]\ , \tag{5}$$

where $\alpha>0$, $m\cdot n>0$ and $m<-1$ for $n<0$. It was used by Strupczewski (1964) for approximation of flood hydrographs. For $m, n>0$ all moments exist and for $n=1$ one gets from (5) the Gamma distribution.

Note that for $m, n<0$ one gets (5) as PDF of the heavy tailed distribution. The mean exists for $m<-2$, the variance for $m<-3$ and so on. For (5) the following moments ratios are valid:

$$\mu=\frac{\alpha^{-\frac{1}{n}}}{G_1}G_2\ ;\ Cv=\sqrt{\frac{G_1G_3}{G_2^2}-1}\ ;\ Cs=\frac{2G_2^3-3G_1G_2G_3+G_1^2G_4}{\left(-G_2^2+G_1G_3\right)^{3/2}}\ ; \tag{6}$$

where $G_i=\Gamma\left(\frac{i+m}{n}\right)$ and $\Gamma(a)=\int_0^\infty x^{a-1}\exp(-x)\,dx$ is the gamma function. For $n=1$ and $m=\lambda-1$, the moments amount to $\frac{\lambda}{\alpha},\frac{1}{\sqrt{\lambda}},\frac{2}{\sqrt{\lambda}}$, respectively.

Referring to Fig. 1 where the relation between the skewness and variability coefficients for Gamma distribution (i.e. (5) for $n=1$) is presented, the respective relation for various n values is shown in Fig. 2. Note that having $\hat{\mu}, \hat{C}_V, \hat{C}_S$ for a given sample, one can determine from Fig. 2 the n value and then, using Eq. (6), define m and α values. Obviously, applying L-moments instead of ordinary moments would be advisable, because the sampling L-moment ratios in contrary to ordinary moments ratios are not algebraically bounded and are much less biased, but so far L-moments for Tx Gamma are not determinate.

The case of $n=-1$ calls for special attention. It defines computationally easy two-parameter distribution being less heavy tailed than Log-Gumbel and Log-logistic and may be highly competitive in FFA to other heavy tailed distributions, at the same time reconciling advocates and opponents of heavy tailed distributions.

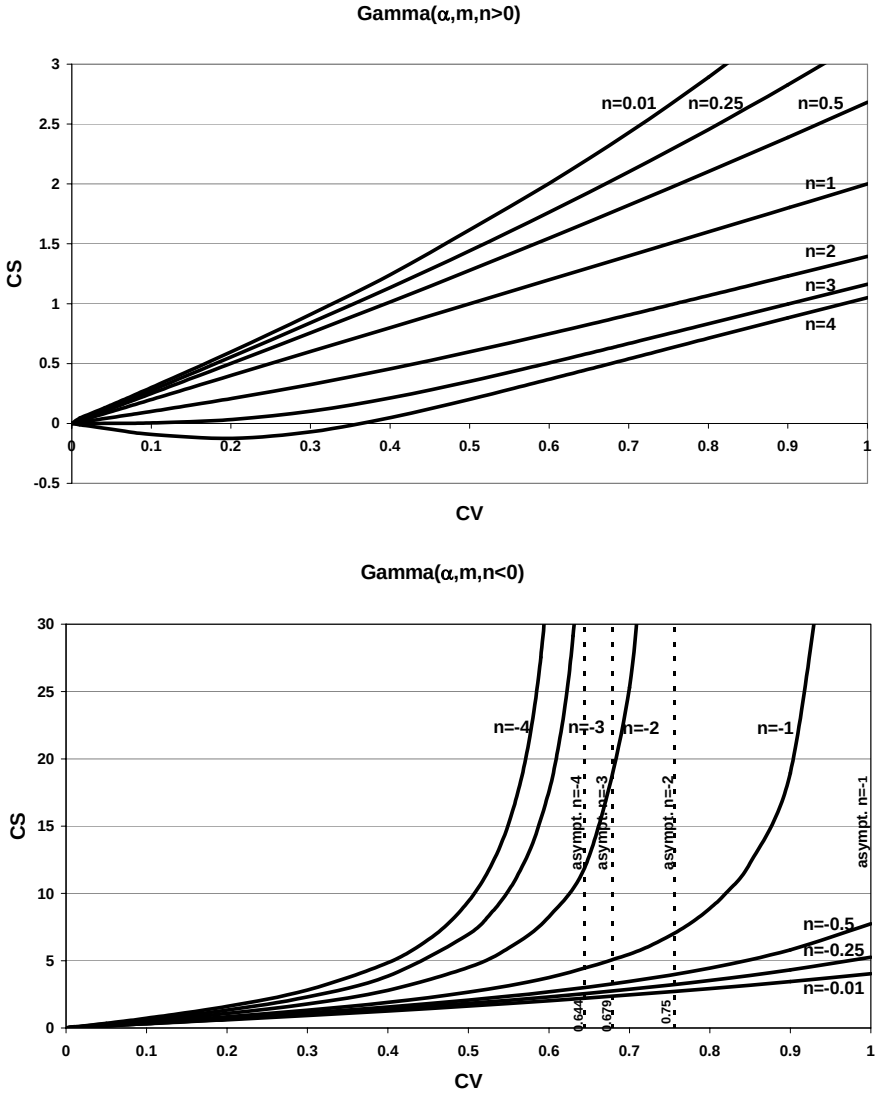

Fig. 2. Relation C_s vs. C_v for various shape parameter values for the Gamma distribution transformed by Tx.

5. Model selection

For a given sample $(x_1, x_2, ..., x_N)$, the problem considered is one of choosing between the two three-parameter models, i.e. one with the lower bound parameter and its counterpart – the two shape parameter model. The likelihood ratio and the moment ratios can be used for selection.

5.1 The likelihood ratio applied for model selection

The *L*-ratio procedure is commonly used in FFA for model discrimination. However, before using this approach for the purpose, its efficiency should be tested for each pair of distributions, different values of their parameters and sample sizes, as shown by Strupczewski et al. (2005) and Mitosek et al. (2006). In order to unify the distributions with respect to parameters, it is convenient to replace the original parameters by moments or *L*-moments, i.e. by the mean, the coefficient of variation (C_V) and asymmetry (C_S), or alternatively by the first *L*-moment (λ_1), the coefficient of *L*-variation (τ) and the coefficient of *L*-skewness (τ_3). A real drawback of discrimination procedures is that they usually tend to favor one of two alternative distributions, when the sample size is small to moderate large.

5.2 The moment ratio applied for model selection

For a three-parameter distribution with lower bound parameter, the kurtosis (C_K) can be expressed as the unique function of skewness, and the *L*-kurtosis (τ_4) as the unique function of *L*-skewness. The $C_S - C_K$ moment ratio diagrams (and the $\tau_3 - \tau_4$ diagrams) are used to identify appropriate distribution for a set of data (e.g. Rao and Hamed 2000). The location of the sample estimate with respect to the distributions gives an indication of the suitability of the distribution to the data, i.e. $\Delta = \hat{C}_K - C_K(\hat{C}_S)$ or $\Delta_L = \hat{\tau}_4 - \tau_4(\hat{\tau}_3)$.

For a three-parameter distribution with two shape parameters, the kurtosis is the unique function of both the skewness and the variation coefficient. Hence the fitness of the model to the data is measured as $\Delta = \hat{C}_K - C_K(\hat{C}_S, \hat{C}_V)$ or $\Delta_L = \hat{\tau}_4 - \tau_4(\hat{\tau}_3, \hat{\tau}_2)$ and compared with the Δ or Δ_L of the respective one-shape-parameter model.

Obviously, the probability plots can be also used to evaluate the agreement between these two distributions and observed data.

6. Conclusions

Taking into account natural and statistical aspects of flood frequency modelling, an introduction of the second shape parameter instead of the lower bound parameter assumed as zero seems to be advisable. However, this paper is only preliminaries to development and implementation in flood frequency modeling of the distributions with two shape parameters. Elaborating various estimation methods with their accuracy assessment is recommended. Comparing the fit of the two models to the data by the likelihood ratio and the moment ratio one should realize that the superior criterion is the performance of Distribution/Estimation procedures in respect to upper quantiles, measured by the bias and the Mean Square Error. Obviously, in each case the outcome would depend on the river flood regime.

Acknowledgments. This work was supported by the Polish Ministry of Science and Higher Education under the Grant 2 P04D 057 29 entitled "Enhancement of statistical methods and techniques of flood events modeling".

References

Hosking, J.R.M., and J.R Wallis, 1997, *Regional Frequency Analysis. An Approach Based on L-moment*, Cambridge University Press.

Katz, R.W., M.B. Parlangeand and P. Naveau, 2002, *Statistics of extremes in hydrology*, Adv. Water Resour. **25**, 1287-1304.

Mielke, P.W. Jr., and E.S. Johnson, 1974, *Some generalized beta distributions of the second kind having desirable application features in hydrology and meteorology*, Water Resour. Res. **10**, 2, 223-226.

Mitosek, H.T., W.G. Strupczewski and V.P. Singh, 2006, *Three procedures for selection of annual flood peak distributions*, Journal of Hydrology **323**, 57-73.

Morlat, G., 1956, *Les lois de probabilite de Halphen*, Revue de Statistique Appliquee, **3**, 21-43.

Perreault, L., B. Bobee and P.F. Rasmussen, 1999, *Halphen distribution system. I: Mathematical and statistical properties and II: Parameter and quantile estimation*, J. Hydrologic Eng. ASCE **4**, 3, 189-199, 200-208.

Rao, A.R., and K.H. Hamed, 2000, *Flood Frequency Analysis*, CRC Press, Boca Raton.

Rozdestvensij, A.W., and A.I. Chebotarev, 1974, *Statistical methods in hydrology*, Gidrometeoizdat, Leningrad (in Russian).

Strupczewski, W.G., H.T. Mitosek, K. Kochanek, V.P. Singh and S. Węglarczyk, 2005, *Probability of correct selection from Lognormal and Convective Diffusion models based on the likelihood ratio*, SERRA 10.1007/s00477-004-0210-8, 11 pp.

Strupczewski, W.G., 1964, *Równanie fali powodziowej*, Wiad. Sl. Hydrol. and Meteorol. **57,** 2, 35-58.

Accepted September 12, 2006

PUBLS. INST. GEOPHYS. POL. ACAD. SC., E-6 (390), 2006

Tracer Tests in Constructed Wetlands: Application of One-Dimensional Convective-Dispersive Equation for Modelling

Przemysław WACHNIEW

Faculty of Physics and Applied Computer Science
AGH – University of Science and Technology
Mickiewicza 30, 30-059 Kraków, Poland
email: wachniew@agh.edu.pl

Abstract

An appropriate application of the one-dimensional convective-dispersive equation for modelling of tracer breakthrough curves depends on the understanding of physical phenomena related to solute behaviour at the inlet and outlet boundaries and at the discontinuities of the system. Questions of the correct mathematical representation of the boundary conditions and of the relevant tracer injection and detection modes are discussed within the context of tracer tests in constructed wetlands. The discussed issues are illustrated by examples of tracer tests performed in two constructed wetlands of different types: a subsurface flow system and a pond. The appropriateness of the semi-infinite solution of the CDE for the pulse injection and detection of the tracer in the flux is discussed and some questions that require more elaboration are outlined.

1. Introduction

One-dimensional convective-diffusive equation (CDE) constitutes a commonly used model of conservative solute transport with numerous applications to environmental and industrial problems:

$$\frac{\partial C(x,t)}{\partial t} = D\frac{\partial C^2(x,t)}{\partial x^2} - v\frac{\partial C(x,t)}{\partial x}, \tag{1}$$

where C is solute concentration, v is fluid velocity and D is hydrodynamic dispersion coefficient. The right hand side of equation (1) represents two processes by which solutes are transported in the moving fluid: Fickian-like dispersion and advection with the flow. The adequacy of this model for describing solute transport in porous media

and in open channels is disputed (e.g. Kennedy and Lennox 2001). Particularly the dispersion of solute is non-Fickian in some conditions (cf. Peters and Smith 2001). Nevertheless, the CDE seems to be a satisfactory approximation for many practical uses. An advantage of this model is the availability, at least for some boundary conditions, of the closed-form analytical solutions which are easy to implement and are computationally efficient comparing to numerical schemes. There are, however, many misconceptions regarding the application of the CDE model, especially within the context of tracer tests performed to derive hydraulic properties of the natural and engineered systems. Many articles do not elaborate on the selection among available analytical solutions of the CDE and sometimes the presumed solutions correspond to the boundary conditions which are not consistent with particular physical settings. Such misconceptions are repeated despite the expansive body of literature published over the last 30 years which provides answers to some of these controversies.

One of the fields where the one-dimensional CDE is often used for modelling of solute transport are investigations of the hydraulic performance of constructed wetlands. This world-widely used technology is an alternative, cost-effective and environmently friendly solution for wastewater treatment (IAWQ 2000). Two basic types of constructed wetlands are: the subsurface flow systems with wastewater permeating through gravel or sand beds overgrown with vegetation, and free water surface systems (ponds). A crucial factor for the removal of dissolved pollutants in a constructed wetland are the hydraulic properties of the object, i.e., (i) the extent of contact between wastewater and the reactive surfaces (substratum, vegetation, detritus) on which purification occurs, and (ii) mixing phenomena which influence redistribution of heat and of the substrates and products of purification reactions. Tracer tests provide Tracer Breakthrough Curves (TBCs) from which the relevant hydraulic characteristics of the constructed wetland can be inferred. The methodology frequently used to define and quantify flow patterns within the constructed wetlands from the TBCs (e.g. Nameche and Vassel 1996, King et al. 1997, Bhattarai and Griffin 1999, Werner and Kadlec 2000) is based on concepts developed in chemical engineering (Levenspiel 1972). One of these models, called in chemical engineering terminology “plug-flow with axial dispersion”, corresponds essentially to the CDE. Mean water transit times and dispersion coefficients are in this approach estimated from the moments of the TBC by the ready-to-use formulae which relate the appropriate moments to the mean water transit time and to the Peclet number. These formulae are derived for the presumed boundary conditions. Thus, in this approach the CDE is used in an implicit way.

Investigations of the hydraulic characteristics of constructed wetlands have a pragmatic importance. Constructed wetlands are often small to medium objects serving small municipalities so their functioning is usually not supervised in a very rigorous way. Moreover, hydraulic performance of the wetland may change with time in an uncontrolled manner due to clogging, deposition of plant detritus and action of

vegetation. There is a need for the unsophisticated and cost-effective procedures for estimation of the actual hydraulic properties of such objects because they can, with time, become quite different from the designed properties. A necessary part of such procedures are user-friendly computer programs for analysis of the TBCs in which the appropriate analytical solutions of the CDE can be easily implemented. This work reviews the relevant literature and provides some guidance for the design and interpretation of tracer tests in constructed wetlands with respect to tracer injection and sampling modes and the appropriate formulation of the boundary conditions for the CDE. Ideas presented here might be applicable also to tracer tests performed in any porous media and in open channels.

2. Two modes of tracer injection and detection

An important but sometimes overlooked aspect of tracer tests are two possible ways by which the tracer can be injected or detected and the two respective definitions (Kreft and Zuber 1978) of the solute concentration both of which satisfy equation (1). Resident concentration C_R is a mass of tracer per unit volume of fluid at a given time instant, while flux concentration C_F is a mass of tracer per unit volume of fluid passing through a cross section. A useful definition of C_F is a ratio of the solute flux to the volumetric fluid flux. Equation (2) relates both concentrations (Kreft and Zuber, 1978):

$$vC_F(x,t) = vC_R(x,t) - D\frac{\partial C_R(x,t)}{\partial x} \quad . \tag{2}$$

Equation (2) is valid only for the uniform initial conditions (Toride et al. 1993).

A pulse type (instantaneous) resident injection could be realised by a homogeneous introduction of the tracer into a volume of fluid between two cross-sectional planes in the conduit. This is difficult to achieve and could be done, for example, by means of a dedicated apparatus or, in case of radioactive tracers, by neutron activation of the passing fluid. Resident detection could be performed by a direct measurement of tracer concentration through walls of the conduit using on-line detectors sensitive to some physical properties of the applied tracer. The pulse resident injection and detection are difficult to perform for the routine tracer tests in constructed wetlands. A condition for flux injection is that the tracer is introduced proportionally to flow velocities so that tracer fluxes are proportional to volumetric fluid fluxes for all possible flow paths. Practical realisations of flux injections and detections for such tests as well as their appropriate representation in the CDE model are discussed below. It must be noted that rates of pollutants removal are, for the reaction orders higher than one, functions of C_R (Kreft 1983) so introduction of the reaction term into the transport equation must be done in a consistent way. On the other hand, only C_F represents mass flux of the solute and integration of C_R in the time domain does not give the

mass of injected tracer. Problems related to the proper usage of the CDE and the resulting necessity of two definitions of concentration can be seen as stemming from "the gap between the Lagrangian physical process and the Eulerian representation of that process" (Holley 1996). The mechanical dispersion is Lagrangian in nature and evolves with heterogeneity of the flow while the molecular diffusion is Eulerian in nature (Gimmi and Flühler 1998) and is driven by concentration gradients.

3. Initial and boundary conditions for tracer tests in constructed wetlands

Uniqueness of the CDE solution requires that the initial and boundary conditions are imposed. Initial conditions are generally defined by the experimentator. Mathematical formulations of the initial conditions depend on the applied concentration definition and are presented for the pulse and step injections by Kreft and Zuber (1978). The boundary conditions must be formulated for tracer injection and sampling sites. Selection of injection and sampling sites in constructed wetlands is restricted by the structures built to distribute wastewater and to collect effluent from the wetland. The gravel bed or the pond where purification occurs are connected to other parts of the treatment system or to the final receiver by pipes or plumes conveying wastewater. Usually they facilitate conducting tracer tests with flux injection and detection because they concentrate the entire wastewater flow but one has to be aware of the physical constraints that these structures imply for the experiment. The tracer test is actually performed for an object which consists of the wetland and its auxiliary structures. The boundary conditions can be therefore defined not only for the injection and sampling cross-sections but also for the interfaces at which solute passes between the conveying structures and the porous volume or the pond. Such interfaces are represented by pipe openings, perforated pipes or weirs.

Surprisingly little attention has been paid in the literature to these issues. Gimmi and Flühler (1998) discuss different mathematical representations of solute transport through the interface between the inlet mixing cell and the convective-dispersive domain. Injection and sampling of the tracer are sometimes conducted through wells or tanks which can be represented as ideally mixed cells that transform the input and output signals. The approach presented by Gimmi and Flühler (1998) could be applied in a wider sense to the situations where tracer is transported in pipes and plumes in which intense turbulent mixing occurs. It is noteworthy that inflow of tracer from the mixing cell in a close contact with the porous medium is best described as a resident injection because at such conditions dispersive transport through the interface is significant. Schwartz et al. (1999) showed experimentally the importance of the correct mathematical representation of the inlet and outlet apparatus and of the boundary conditions for soil columns. Peters and Smith (2001) proposed the Transition Region model to describe the inlet and outlet as well as inner boundaries in the porous medium.

For the inlet to the porous medium the third type boundary condition:

$$vC_R(0^+,t) - D\left.\frac{\partial C_R(x,t)}{\partial x}\right|_{x=0^+} = vg(t) \ , \tag{3}$$

where $g(t)$ is solute input concentration, or alternatively the first type boundary conditions are used in the literature to describe the resident concentration. The former corresponds to the continuity of solute flux through the boundary while the latter to the continuity of solute concentration.

Several theoretical (e.g. van Genuchten and Parker 1984) and, more recently, experimental studies (e.g. Schwartz et al. 1999) have shown that for the resident concentration the third type condition (3) is the appropriate boundary condition between the reservoir and the porous medium. Applying equation (2) one can easily show that (3) is equivalent to the first type boundary condition for flux concentration.

Selection of the outlet boundary condition appears to be a more controversial question. The third type exit condition is given by:

$$vC_R(L^-,t) - D\left.\frac{\partial C_R(x,t)}{\partial x}\right|_{L^-} = vC_E(t) \ , \tag{4}$$

where L is the length of the transport domain and C_E is the exit concentration. Controversies about the formulation of the exit boundary condition stem in fact from inability to determine the exit concentration C_E. This difficulty can be overcome by assuming continuity of concentration at the exit boundary which substituted to equation (4) gives the second type boundary condition. This approach (Danckwerts 1953), popularised by the chemical engineering textbooks (Levenspiel 1972), is commonly applied for the interpretation of the results of tracer tests in constructed wetlands (examples cited in the Introduction). Again, it has been shown by Kreft and Zuber (1979) and others that such boundary condition is physically unrealistic and leads to the solution that does not fit the experimental TBCs. Surprisingly, the semi-infinite solutions predict the outlet solute concentrations better than the finite solutions with the second type exit boundary condition (e.g. Schwartz et al. 1999). Peters and Smith (2001) explain this paradox by referring to the essence of the mechanical dispersion which unlike the molecular diffusion does not result from concentration gradients so the downstream boundary conditions should not affect the solution of the CDE within the transport domain. Peters and Smith (2001) claim also that the second type boundary condition is theoretically correct for the outlet boundary and they relate the failure of the respective finite solution of the ADE to the general inadequacy of this approach to describe non-Fickian mechanical dispersion. Golz and Dorroh (2001) and Golz (2003) note that the conservation of mass requires the third type boundary conditions at both ends of the finite system and that only the solution that obeys such boundary conditions is consistent with the physical meaning of the CDE and with mathematical

logic. Golz and Dorroh (2001) and Golz (2003) propose also that the semi-infinite solution for the flux concentration is used to yield an expression for the exit concentration C_E in equation (4).

4. Two concluding examples

Tracer tests with bromide (KBr) and tritium were conducted in two constructed wetlands in Poland: gravel cells overgrown with common reed in Nowa Słupia and a duckweed pond in Mniów. Detailed descriptions of the wetlands, results of the test and their interpretation are presented elsewhere (Małoszewski et al. 2006a,b). The model chosen for the interpretation of both tests was the semi-infinite solution of the CDE derived for injection and detection in the flux (Kreft and Zuber 1978). The approach applied to model the TBCs appeared to be successful in the sense that it allowed to identify in both wetlands several flow components whose occurrence and quantitative characteristics are consistent with the physical settings. The differences between different solutions of the CDE are significant when dispersion is considerable, i.e. at Peclet numbers < 10 (Kreft 1983, Schwartz et al. 1999). Such values of Peclet numbers are not uncommon in constructed wetlands and occurred also in both considered tests.

Injections to the subsurface system were performed via the inlet of the pipe which further conveys pre-treated sewage across the upstream ends of the gravel cells of the wetland. Sewage is distributed within the cells via the perforated pipes. Realisation of strictly instantaneous injections was difficult in this case due to the relatively large volumes of tracer solutions. Injection was performed in small portions over 10 minutes what at the wastewater travel times of the order of days could be considered as the pulse injection. Tracer injection to the fast flowing fluid was without a doubt conducted to the flux as at such conditions dispersion across the boundary and backmixing were restricted. The flow and mixing conditions in the 24 m long distribution pipes are however unknown and the same applies to the perforated collection pipes which convey the effluent to the collection wells from where the tracer was sampled. The actual boundary conditions between these reservoirs and the porous medium are unknown. It is unclear if these reservoirs are well mixed so that the approach of Gimmi and Flühler (1998) could be used to represent the boundary conditions. Insights into the mixing characteristics of the reservoirs could be gained by modelling of their velocity fields or by direct sampling of solute from them.

Injection to the pond was performed through a coagulation chamber from which wastewater is conveyed through a short pipe to the bottom part of the pond. Wastewater in the chamber is strongly agitated by the inflowing stream so it can be considered well mixed and because the chamber is connected to the pond via the pipe, the injection to the pond can be considered as performed in the flux. Mixing in the chamber resulted in smoothing out the pulse injection but the tracer needed about 30

minutes to be washed out from the chamber what at the transit time of waste water through the pond found to be about 20 days assures practically the pulse injection. The effluent was sampled below the wire that dams the pond which undoubtly represents the flux detection, as convection is the dominant transport process at the weir overflow. Both tests were meant to provide responses of the studied systems to pulse injections, which imposes the initial conditions in the form of Dirac's delta in the time domain. As was discussed above, in both cases the presumably pulse injections were smoothed out before reaching the actual wetland. This could be in fact an advantage because as noted by Golz (2003), derivation of the CDE from the mass balance considerations hinges on the assumption of not very sharp input signals.

The semi-infinite solution of the CDE for flux injection and detection has a simple analytical form which facilitates its use for modelling of tracer test results. It seems to be applicable for many constructed wetlands but in some cases the auxiliary reservoirs might influence the boundary conditions. This question requires further theoretical and experimental investigations.

Acknowledgments. This work was supported through the statutory fund of the AGH – University of Science and Technology (11.11.220.01).

References

Bhattarai, R.R., and D.M. Griffin Jr., 1999, *Results of tracer tests in rock-plant filters*, J. Environ. Eng. **125**, 117-125.

Danckwerts, P.V., 1953, *Continuous flow systems*, Chem. Eng. Sci. **2**, 1-13.

Gimmi, T., and H. Flühler, 1998, *Mixing-cell boundary conditions and apparent mass balance errors for advective-dispersive solute transport*, J. Contam. Hydrol. **33**, 101-131.

Golz, W.J., 2003, *Solute transport in a porous medium: a mass-conserving solution for the convection-dispersion equation in a finite domain*, PhD Thesis, Louisiana State University, Louisiana, 2003, 96 pp.

Golz, W.J., and J.R. Dorroh, 2001, *The convection-diffusion equation for a finite domain with time varying boundaries*, Appl. Math. Lett. **14**, 8, 983-988.

Holley, E.R., 1996, *Diffusion and dispersion*. **In:** V.P. Singh, W.H. Hager (eds.), "Environmental Hydraulics", Kluwer, 111-151.

IAWQ, 2000, *Constructed wetlands for pollution*, Scientific and Technical Report – IAWQ **8**, IWA Publishing.

Kennedy, C.A., and W.C. Lennox, 2001, *A stochastic interpretation of the tailing effect in solute transport*, Stoch. Env. Res. Risk A. **15**, 325-340.

King, A.C., C.A. Mitchell and T. Howes, 1997, *Hydraulic tracer studies in a pilot scale subsurface flow constructed wetland*, Water Sci. Tech. **35**, 189-196.

Kreft, A., 1983, *Problems of the mathematical modeling the hydrodynamic dispersion*, Z. Nauk. AGH **958,** Matematyka-Fizyka-Chemia **61**, 1-84 (in Polish).

Kreft, A., and A. Zuber, 1978, *On the physical meaning of the dispersion equation and its solution for different initial and boundary conditions*, Chem. Eng. Sci. **33**, 1471-1480.

Kreft, A., and A. Zuber, 1979, *On the use of dispersion model of fluid flow*, Int. J. App. Radiat. Isotopes **30**, 705-708.

Levenspiel, O., 1972, *Chemical Reaction Engineering*, John Wiley & Sons, 2nd ed., 578 pp.

Małoszewski, P., P. Wachniew and P. Czupryński, 2006a, *Hydraulic characteristics of a wastewater treatment pond evaluated through tracer test and multi-flow mathematical approach*, Pol. J. Env. Studies **15**, 1, 105-110.

Małoszewski, P., P. Wachniew and P. Czupryński, 2006b, *Study of hydraulic parameters in heterogeneous gravel beds: constructed wetland in Nowa Słupia (Poland)*, J. Hydrol. **331**, 630-642.

Nameche, TH., and J.L. Vassel, 1998, *Hydrodynamic studies and modelization for aerated lagoons and waste stabilization ponds*, Water Res. **32**, 3039-3045.

Peters, G.P., and D.W. Smith, 2001, *Numerical study of boundary conditions for solute transport through a porous medium*, Int. J. Numer. Anal. Meth. Geomech. **25**, 7, 629-650.

Schwartz, R.C., K.J. McInnes, A.S.R. Juo, L.P. Wilding and D.L. Reddell, 1999, *Boundary effects on solute transport in finite soil columns*, Water Resour. Res. **35**, 3, 671-681.

Toride, N., F.J. Leij and M.T. van Genuchten, 1993, *Flux-averaged concentrations for transport in soils having nonuniform initial solute distributions*, Soil Sci. Soc. Am. **57**, 1406-1409.

Werner, R.M., and R.H. Kadlec, 2000, *Wetland residence time distribution modeling*, Ecol. Eng. **15**, 77-90.

Accepted September 12, 2006

PUBLS. INST. GEOPHYS. POL. ACAD. SC., E-6 (390), 2006

The Numerical Solution of the Advection-Dispersion Equation: A Review of Some Basic Principles

Steve WALLIS

Heriot-Watt University, Riccarton, Edinburgh, EH14 4AS, UK
e-mail: s.g.wallis@ hw.ac.uk

Abstract

The simulation of solute transport in rivers is frequently based on numerical models of the Advection-Dispersion Equation. The construction of reliable computational schemes, however, is not necessarily easy. The paper reviews some of the most important issues in this regard, taking the finite volume method as the basis of the simulation, and compares the performance of several types of scheme for a simple case of the transport of a patch of solute along a uniform river. The results illustrate some typical (and well known) deficiencies of explicit schemes and compare the contrasting performance of implicit and semi-Lagrangian versions of the same schemes. It is concluded that the latter have several benefits over the other types of scheme.

Key words: solute transport, numerical modelling, finite volume method, advection, reference frame, time marching.

Full text was published in *Acta Geophysica*, Vol. 55, No. 1, p. 85-94.

PUBLS. INST. GEOPHYS. POL. ACAD. SC., E-6 (390), 2006

Impact of Repository Depth on Residence Times for Leaking Radionuclides in Land-Based Surface Water

Anders WÖRMAN[1], Lars MARKLUND[1], Shulan XU[2] and Björn DVERSTORP[2]

[1]Environmental Physics Group,
Swedish University of Agricultural Sciences,
Uppsala, Sweden; e-mail: worman@kth.se

[2]Swedish Radiation Protection Authority

Abstract

The multiple scales of landscape topography produce a wide distribution of groundwater circulation cells that control the hydro-geological environments surrounding geological repositories for nuclear waste. The largest circulation cells tend to discharge water into major river reaches, large freshwater systems or the nearby Baltic Sea. We investigated numerically the release of radionuclides from repositories placed in bedrock with depths between 100 to 2000 meters in a Swedish coastal area and found that leakage from the deeper positions emerges primarily in the major aquatic systems. In effect, radionuclides from the deeper repositories are more rapidly transported towards the Sea by the stream system compared to leakage from more shallow repositories. The release from the shallower repositories is significantly retained in the initial stage of the transport in the (superficial) landscape because the discharge occurs in or near low-order streams with high retention characteristics. This retention and residence time for radioactivity in the landscape control radiological doses to biota and can, thus, be expected to constitute an essential part of an associated risk evaluation.

Key words: hydrology, radio nuclide migration, surface water-groundwater interaction.

Full text was published in *Acta Geophysica*, Vol. 55, No. 1, p. 73-84.

PUBLS. INST. GEOPHYS. POL. ACAD. SC., E-6 (390), 2006

CONTENTS

PUBLICATIONS OF THE INSTITUTE OF GEOPHYSICS POLISH ACADEMY OF SCIENCES

E. WATER RESOURCES

ISBN-83-88765-62-0